

# Study of running-in of spiral bevel gears

MINOO NAKHJIRI



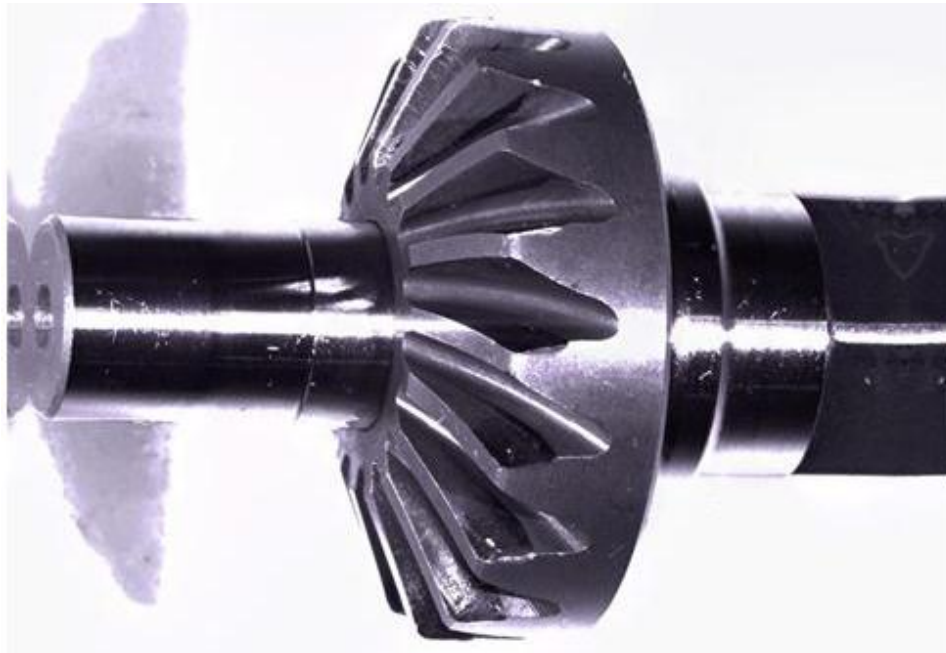
**KTH Industrial Engineering  
and Management**

Master of Science Thesis  
Stockholm, Sweden 2012



# Study of running-in of spiral bevel gears

Minoo Nakhjiri



Master of Science Thesis MMK 2012:36 MKN 058  
KTH Industrial Engineering and Management  
Machine Design  
SE-100 44 STOCKHOLM





KTH Industriell teknik  
och management

Examensarbete MMK 2012: 36 MKN 058

## Inkörning av spiralskurna koniska kuggjul

Minoo Nakhjiri

Godkänt 2012-10-25	Examinator Ulf Sellgren	Handledare Ellen Bergseth
	Uppdragsgivare Atlas Copco Tools AB	Kontaktperson Per Forsberg

### **Sammanfattning**

Handhållna eldrivna verktyg har under många år bidragit till att öka produktiviteten inom industrin. Atlas Copco Tools utvecklar sådana verktyg med fokus på produktivitet, ergonomi och kvalitet. En produktmodul som de arbetat med att förbättra är vinkelväxeln som sitter i deras elektriska mutterdragare eftersom livslängdvariationer, beroende på hur de är använda och när service är gjord, noterats.

För att få ner variationerna har Atlas Copco Tools börjat undersöka om inkörning av vinkelväxlarna kan förlänga livslängden. Inkörning kan göra ytorna jämnare och därmed förbättra smörjförhållandena i kuggkontakten. Effekten av inkörning kan mätas genom att studera nötning och effektförluster.

I detta examensarbete analyseras olika inkörningsförlopp stegvis med avseende på kontaktbild, ytfinhet och effektförluster. Minsta smörjfilmstjocklek beräknades analytiskt och med hjälp av ett kommersiellt datorprogram kunde kuggkontaktbilden för statiskt belastade perfekta kuggväxlar studeras och jämföras med den verkliga kontakten.

Av de testade inkörningsförfarandena presenteras en optimal inkörningsmetod som kunde kopplas till en förlängd livslängd. Vidare så bedömdes smörjningen vara otillräcklig. Arbetet visar också att en omkonstruktion av kuggeometrin är nödvändig för att ytterligare förlänga livslängden.





**KTH Industrial Engineering  
and Management**

**Master of Science Thesis MMK 2012: 36 MKN 058**

## **Study of running-in of spiral bevel gears**

**Minoo Nakhjiri**

Approved 2012-10-25	Examiner Ulf Sellgren	Supervisor Ellen Bergseth
	Commissioner Atlas Copco Tools AB	Contact person Per Forsberg

### ***Abstract***

Hand held power tools have enabled craftsmen and skilled workers in general to increase their productivity while cutting, assembling, and grinding. Atlas Copco Tools has been at the vanguard of ever increasing product performance in hand held power tools. One product module which has been thoroughly studied is the bevel gear transmissions present in Atlas Copco angle head nut runners. For these gears a large variation of service life has been observed due to difference in the running procedures and different service intervals.

To extend the service life of nut runners, Atlas Copco Tools has started to investigate the effects from running-in of gears. Running-in is a procedure of reducing the surface roughness which can help to enhance the contact conditions. The impact of running-in can be measured either by the steady state of wear or steady state of friction.

In this master thesis, different procedures of running-in have been investigated. The changes in contact pattern, surface roughness values and efficiency losses were measured step-vice during the different running-in setups. In addition, the minimum lubricant film thickness has been calculated analytically and a commercially available gear software provided the contact pattern for perfectly smooth gears which was compared with the real contact situation.

The different running-in procedures resulted in one optimized running-in procedure where an increase in gear life was found. The biggest change in surface roughness happens at the very first running-in step. Hence, running the gears for one longer period of time, with low torque and specific speed range, gives the best running-in effects. Moreover, starved lubrication conditions were found which are most likely linked to the present gear design. A redesign is suggested to further increase the gear life.





## FOREWORD

---

First of all I would like to thank Atlas Copco Tools for providing me with the opportunity to perform this master thesis and their extensive support throughout the thesis and also for the friendly environment that they have provided.

I would like to thank my dear supervisors Ellen Bergseth and Per Forsberg for their continuous support, guidance and help during the thesis tenure. I would also like to thank our dear teachers, Ulf Sellgren and Stefan Björklund for their motivation and guidance. I express my sincere gratitude to Ulf Viklund for his patience and guidance with lab instruments.

I would further like to thank Sandeep Vijayakar for answering my questions regarding ANSOL software. I would like to mention and thank all the colloquies from Atlas Copco Tools for being helpful and making me feel as a part of the team.

Special thanks to Athul, Mario and all my dear friends in Machine Design who supported me throughout the Masters degree studies.

Last, but not the least, I would like to thank my Parents, my aunt Kimi and my Siblings for their love, continuous motivation and moral support throughout our Master program.

Minoo Nakhjiri

Stockholm, October 2012



# NOMENCLATURE

---

## Notations

Symbol	Description
$E$	Young modulus [GPa]
$E'$	Effective elastic module [Gpa]
$G$	Dimensionless materials parameter
$H$	Dimensionless film thickness
$h$	Minimum film thickness [ $\mu\text{m}$ ]
$k$	Ellipticity parameter
$L_{10}$	Life that 10% of the specimens will fail
$L_{50}$	Life that 50% of the specimens will fail
$R$	Equivalent pitch radius [mm]
$R$	Mid-plane pitch radius of the spiral bevel gear [mm]
$R_a$	Arithmetic average [ $\mu\text{m}$ ]
$R_p$	Maximum profile peak height [ $\mu\text{m}$ ]
$R_q$	Root mean square (RMS) [ $\mu\text{m}$ ]
$R_x$	Effective radius in <b>x</b> direction [mm]
$R_v$	Maximum profile valley depth [ $\mu\text{m}$ ]
$R_y$	Effective radius in <b>y</b> direction [mm]
$R_z$	Average maximum height of the profile [ $\mu\text{m}$ ]
$U$	Dimensionless speed factor
$\bar{u}$	Rolling velocity [m/s]
$\bar{v}$	Sliding velocity [m/s]
$V$	Linear velocity [m/s]
$W$	Dimensionless load factor
$A$	Pressure viscosity factor of the lubricant [ $\text{GPa}^{-1}$ ]
$\beta$	Mid spiral angle [deg]
$\Gamma$	Mid cone angle [deg]
$\Lambda$	Dimensionless film parameter
$N$	Poisson ratio

$\sigma_{Ra}$	Standard deviation of surface roughness
$\Phi$	Pressure angle [deg]
$\Omega$	Angular velocity [rpm]

## ***Abbreviations***

---

AC Tools	Atlas Copco Tools
ANSOL	Advanced Numerical Solution
EffL	Efficiency increase due the Life test
EffR	Efficiency increase due to Running-in procedure
EffS	Efficiency Slop due life test
FE-BE Method	Finite Element- Boundary Element Method
LR	Life Ratio
PoL	Percent of Life
RMS	Root Mean Square
2D	2D surface measurements
3D	3D surface measurements

---

# TABLE OF CONTENTS

---

1	INTRODUCTION .....	1
1.1	Background .....	1
1.2	Purpose.....	1
2	FRAME OF REFERENCE.....	3
2.1	Gears .....	3
2.2	Lubrication.....	6
2.3	Surface topography .....	9
2.4	Running-in .....	10
2.5	Available test results .....	10
3	METHOD .....	13
3.1	Instruments.....	13
3.1.1	Test rig .....	13
3.1.2	Surface measurement .....	15
3.2	Test procedure.....	16
3.2.1	Following the same gear tooth.....	16
3.2.2	Measuring the gears during running-in procedure.....	17
3.2.3	Step by step measurements .....	17
3.3	Pretest.....	19
3.4	Design of experiment.....	19
3.4.1	Design parameters.....	21
3.4.2	Responses.....	22
3.5	Analytical method .....	24
3.6	Simulation and finite element method .....	27
4	RESULTS .....	29
4.1	Pretests .....	29
4.1.1	Pretest I .....	30
4.1.2	Pretest II.....	33
4.2	Main tests .....	36
4.2.1	Results of 1st repetitions.....	37

4.2.2	Results of 2nd repetitions.....	44
4.2.3	Optimization of design parameters versus life ratio .....	47
4.2.5	Study the effect of efficiency increase on life ratio .....	48
4.2.6	Speed factor and contact region.....	49
4.3	Calculation .....	50
4.4	Modeling.....	52
5	DISCUSSION AND CONCLUSIONS .....	55
5.1	Discussion .....	55
5.2	Conclusions.....	57
6	RECOMMENDATIONS AND FUTURE WORK .....	59
6.1	Future work .....	59
6.2	Recommendations.....	59
7	REFERENCES .....	61
APPENDIX A		
	Hamrock-Dawson equation .....	A.1
APPENDIX B		
	Constants used in calculations .....	B.1
APPENDIX C		
C.1	2D measurement results of pretest I.....	C.1
C.2	2D measurement results of pretest II.....	C.2
C.3	3D measurement results of main tests.....	C.3
APPENDIX D		
D.1	Efficiency and torque deviation diagrams; 1st repetitions.....	D.1
D.2	Efficiency and torque deviation diagrams; 2nd repetitions .....	D.5

# 1 INTRODUCTION

---

*Gears are one of the transmission elements used to transfer power and control the rotational speed. They have been used for more than thousand years; the oldest evidence is the Greek Antikythera mechanism from 100 BC. At present gears are widely used in power transmissions and they are made out of many different materials, e.g. plastic or metal. Gears have been studied for many years, but even today research on friction, wear, and lubrication in gears are of great importance for further improvements, even though a gear pair already can have an efficiency above 99 %. In this master thesis, the running-in (i.e. early wear) behavior is studied on a spiral bevel gear used in nut runners with the purpose to give insight for further improvements of service life.*

## 1.1 Background

Hand held power tools have enabled craftsmen and skilled workers to increase their productivity while cutting, assembling and grinding. These power tools have special requirements compared to other machines; they must be light weight, power dense, reliable, and they should be safe to use. Moreover, they should have a long service life. These tools are working with different forms of power conversion, from electrical to pneumatic and mechanical, but there is something similar in all of them; gears.

Atlas Copco Tools (AC Tools) has been at the vanguard of ever increasing product performance in hand held power tools. One product module which has been thoroughly studied is the bevel gear transmissions present in AC Tools angle head nut runners. For these gears a variation of service life has been observed due to different running procedures and different service intervals.

## 1.2 Purpose

In every AC Tools 90° nut runners, a spiral or straight bevel gear pair is used. These gears are subjected to a large spectrum of load and speed conditions, depending on operating conditions (i.e. customer needs). The angle head nut runner series ETV ST61-50-10 (Figure 1) is designed to be used for maximum 55 Nm. The nut runners can be programmed and used for different types of joints for a range of speed (30 to 600 rpm). According to a series of tests done by AC Tools, a running-in procedure can extend the service life of these gears.



Figure 1. Tensor ST handheld nut runner (Atlas Copco, 2012)

The purpose of this master thesis is to study and optimize the running-in procedure on slow rotating spiral bevel gears of AC Tools nut runner series ETV ST61-50-10 to extend the gear life.





## 2 FRAME OF REFERENCE

---

*In this chapter a general discussion about different types of gears, gear parameters, lubrication and running-in of gears is presented. Moreover, the sought knowledge regarding running-in on these specific spiral bevel gears are presented.*

### 2.1 Gears

Gears are components used to transfer motion and torque between two shafts. It is not only about transferring the torque and a uniform motion, but they can also control the speed and torque magnitude by different ratios. Spur gears are the most common gear configuration in terms of geometry, with the teeth parallel to the shaft as shown in Figure 2.

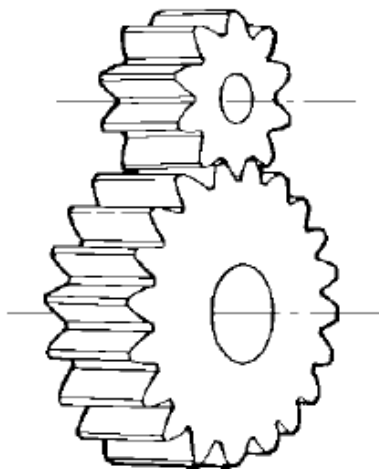


Figure 2. Spur gear (SPD/SI, 2012)

In Figure 3 the main geometrical parameters and nomenclatures of a gear set, driving gear (pinion) and driven gear (gear), are shown. Each tooth is divided by two main parts, addendum and dedendum which are separated by the pitch circle/diameter where a pure rolling occurs. If the gear contact is on any other point of the tooth rather than the pitch point, a combination of rolling and sliding motion takes part. For spur gears, the contact pattern is a line parallel to the center axis of the shaft, shown in Figure 2.

Bevel gears are commonly used to transmit power and motion between intersecting shafts (Figure 4). There are different types of teeth for bevel gears, tapered and uniform. The tapered teeth have less tooth depth, closer to the cone vertex, while the uniform teeth keep the same tooth depth along the gear cone (Figure 5). The main geometrical parameters of bevel gears are shown in Figure 6.

A further classification of bevel gears can be done according to their tooth shape, which can be straight, hypoid, or hypoid zerol, or spiral as shown in Figure 7. Figure 7 also shows that the tooth curvature of spiral bevel gears is part of a circle, and therefore it has a convex and a concave flank which is shown in Figure 8.

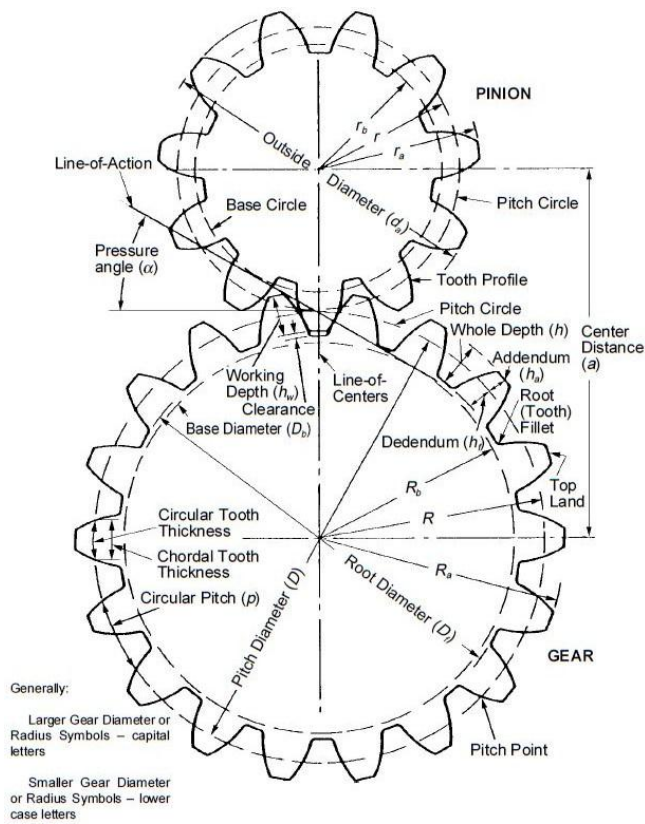


Figure 3. Basic gear geometry parameters and nomenclature (SPD/SI, 2012)

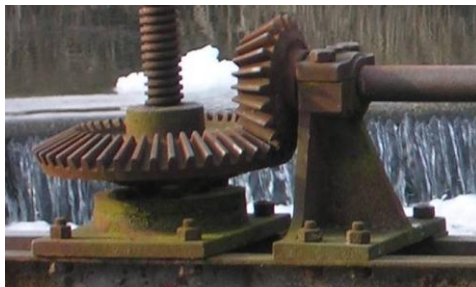


Figure 4. A pair of straight bevel gears used in flood gate, by means of power screws (Brena Clemente, 2012)

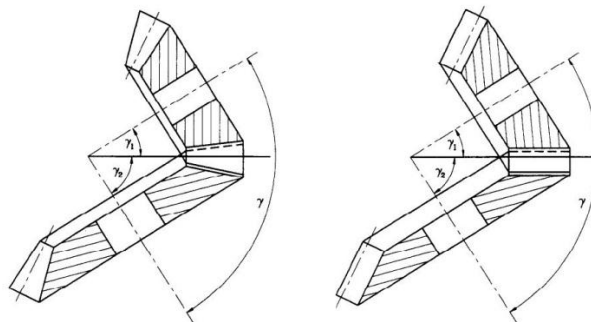


Figure 5. Bevel gears with tapered teeth on the left and with uniform teeth on the right, (F.L. Litvin 1997)

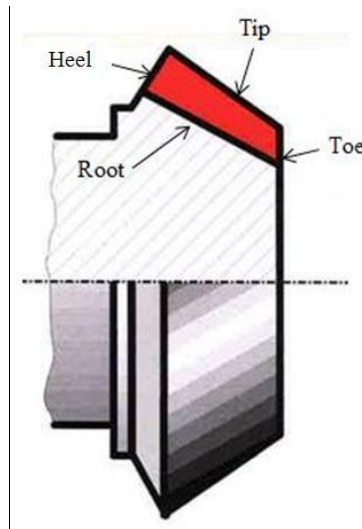
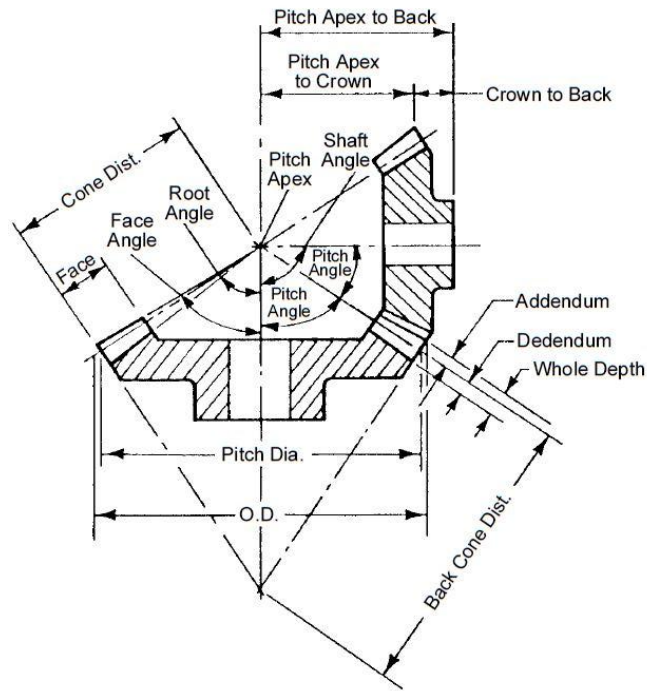


Figure 6. The main geometrical parameters of bevel gears (SPD/SI, 2012 and Klingelnberg, 2008)

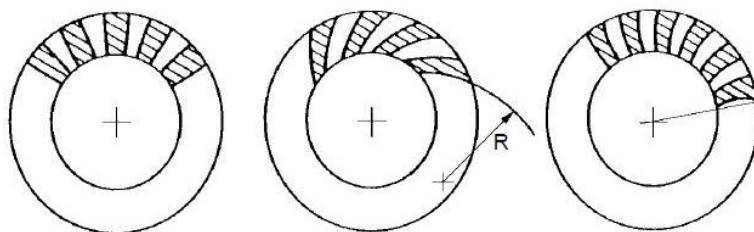


Figure 7. Respectively from left; straight, spiral, and hypoid zero bevel gears (SPD/SI, 2012)

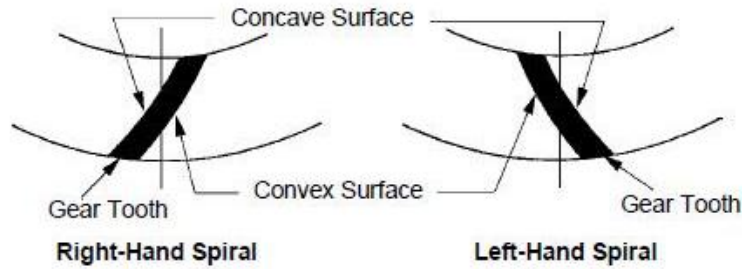


Figure 8. Convex and concave spiral flank surface for right and left hand spiral gears (SPD/SI, 2012)

The contacting pattern in spiral bevel gears is more complicated compared to spur gears. As shown in Figure 9, the contact pattern for the driven, gear, starts on the tip in the heel region and ends on the root in the toe region, therefore on the driver, i.e., the pinion, the contact starts on the root in the heel region and ends on the tip in the toe region.

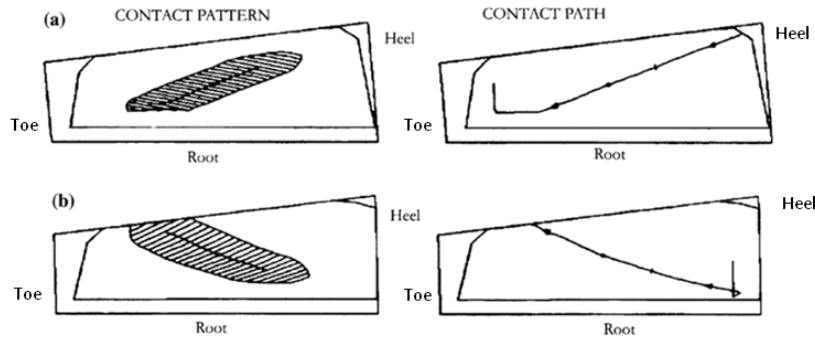


Figure 9. Contact pattern of spiral bevel gears, (a) gear tooth and (b) pinion tooth (F.L. Litvin, 2006)

## 2.2 Lubrication

Most gears are lubricated to reduce friction and wear, cooling the contact and transfer the wear particles away from the contact zone. Lubricants can be liquid or solid, solid lubrication or grease is used when there is a risk for leakage as for the studied gears. Depending on the operating condition and the lubricant properties, the lubricant will act differently in the contact. As a general discussion the following information is presented.

Hydrodynamic (HD) lubrication was understood by classic experiments of Tower (1885) where the existence of a film was detected from measuring the pressure within the lubricant, and of Petrov (1883), who reached the same conclusion from friction measurements (BJ Hamrock, 2004). Later in 1922, the opposite extreme lubrication regime, boundary lubrication (BL), was introduced by Hardy and Doubleday, where the contact is carried by the surface and the lubricant bulk has no effect. They came up with the conclusion that in the lubrication region which Reynolds referred to as boundary condition, the friction is not only dependent on the lubricant, but also on the properties of the contacting surfaces (W. Hardy, 1922).

These lubrication regimes were the first two to be detected. Later on, elastohydrodynamic (EHD) lubrication regime and mixed lubrication (ML) regimes were introduced. In both HD regime and EHD regime, surfaces are separated by a lubricant film and it is referred to as full-film

lubrication.

In ML the lubricant film is not thick enough so the opposing asperities are coming to contact and the transmitted load will be supported both by the lubricant and the asperities. As the fluid film gets thinner and the asperities have to support the most of the load, the BL regime occur. In the BL regime, only the lubricant chemical properties and the nature of the contacting surfaces (i.e. the surface topography) are important. In the BL regime of gears, the amount of boundary contact varies with the sliding velocity and the sliding velocity is more effective in the BL regime compared to the full-film lubrication regime (T. A. Stolariski, 2000).

Studying friction in journal bearings, Stribeck presented the coefficient of friction as a function of viscosity, sliding velocity, and applied normal load, see Figure 10 (F.L. Litvin 1997).

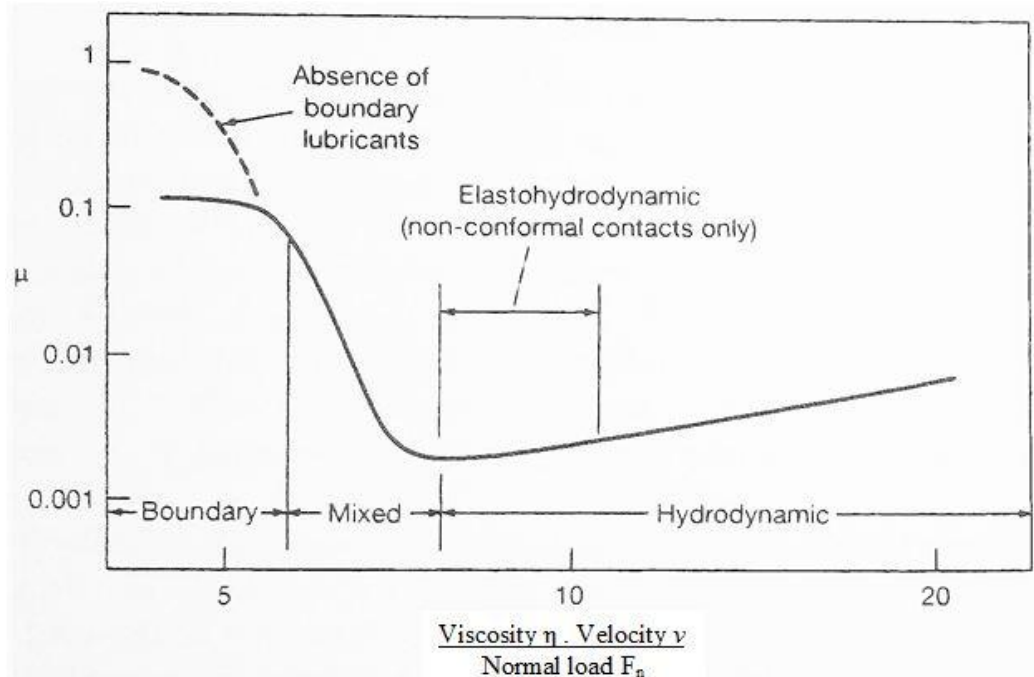


Figure 10. Stribeck curve, coefficient of friction (y axes) as function of Steinbeck number (x axes) (F.L. Litvin 1997)

In Reynolds classical hydrodynamic theory, there are assumptions taken such as that the viscosity is constant under different pressure and the solid surface is ideally rigid. Later on some investigations showed that for heavily loaded contacts, viscosity is increasing with pressure and indeed the surfaces are not ideally rigid. This led to a better prediction of the fluid film thickness (T. A. Stolariski, 2000).

The analyzed gears are lubricated with grease which contains mineral oil and lithium soap, solid lubricants, extreme pressure (EP) additives and corrosion inhibitors. Calculation of lubricant film thickness in case of grease is not accurate due to the existence of solid particles in the grease and the soap interaction with the base oil. On the other hand, in case of grease, as the shear rate increases viscosity decreases and at high shear rates grease behaves like a fluid lubricant (D. Pirro, 2001).

To estimate the lubrication regime the Lambda ratio ( $\Lambda$ ) can be used. This value is the ratio

between minimum lubricant film thickness in the contact and the root sum square (RSS) of contacting surfaces RMS roughness as shown in following equation.

$$\Lambda = \frac{h}{(R_{q,1}^2 + R_{q,2}^2)^{1/2}} \quad (1)$$

where  $h$  is presenting the minimum film thickness and  $R_{q,1}$  and  $R_{q,2}$  are the RMS roughness value of the two surfaces in contact. Calculation of  $h$  is done by standard Hamrock-Dawson equation and is presented in Appendix A.

Depending on the  $\Lambda$  value, it is possible to predict the lubrication region to some extends. The value can give indications on the dominating lubrication regime in the contact.

In the hydrodynamic lubrication regime,  $5 < \Lambda < 100$ , and in the elastohydrodynamic lubrication regime,  $3 < \Lambda < 10$ . In the boundary lubrication regime,  $\Lambda < 1$ , where there is imminent asperity contact, and also in the mixed lubrication region,  $1 < \Lambda < 3$ , asperity contacts are possible, but to a less extent than in the boundary lubrication regime. These numbers are calculated for perfectly smooth surfaces or for surfaces with  $R_a < 0.2 \mu\text{m}$  (A. Beek 2009). Figure 11 is predicting the lubrication regime from the minimum EHD film thickness and the surface roughness value of the gears (D. Townsend, 1992).

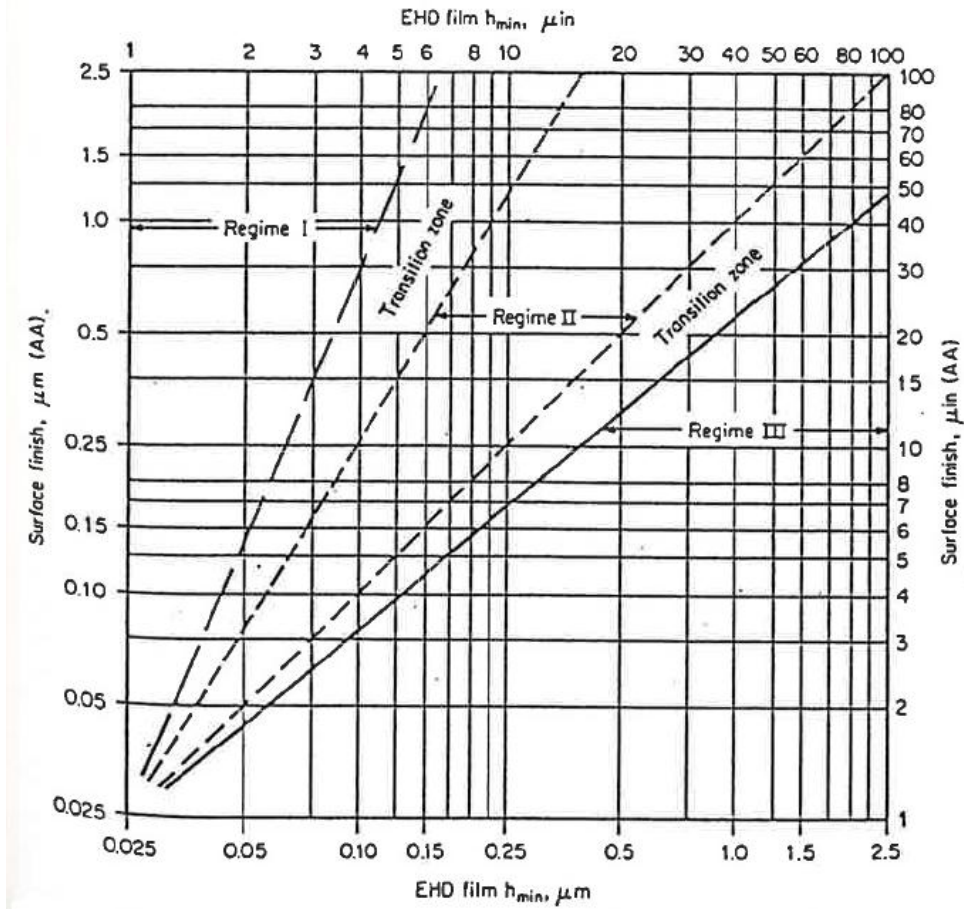


Figure 11. Guidance to predict the state of lubrication from minimum EHD film thickness and surface finish, regime I as boundary, regime II as mixed and regime III as hydrodynamic lubrication (D. Townsend, 1992).

## 2.3 Surface topography

The variation in surface roughness can be very large due to different manufacturing and finishing methods. Surface topography can somewhat be captured by surface roughness parameters in 2D defined by standards. The parameters used in this study are the arithmetic average parameter ( $R_a$ ) and the standard deviation of  $R_a$  ( $\sigma_{Ra}$ ), the square root of the arithmetic mean of the square of the vertical deviation of the profile from the center line (R.M.S. or  $R_q$ ), the maximum valley depth ( $R_v$ ), the maximum peak height ( $R_p$ ), and the maximum peak to valley distance ( $R_z$ ), shown in Figure 12 and equations bellow.

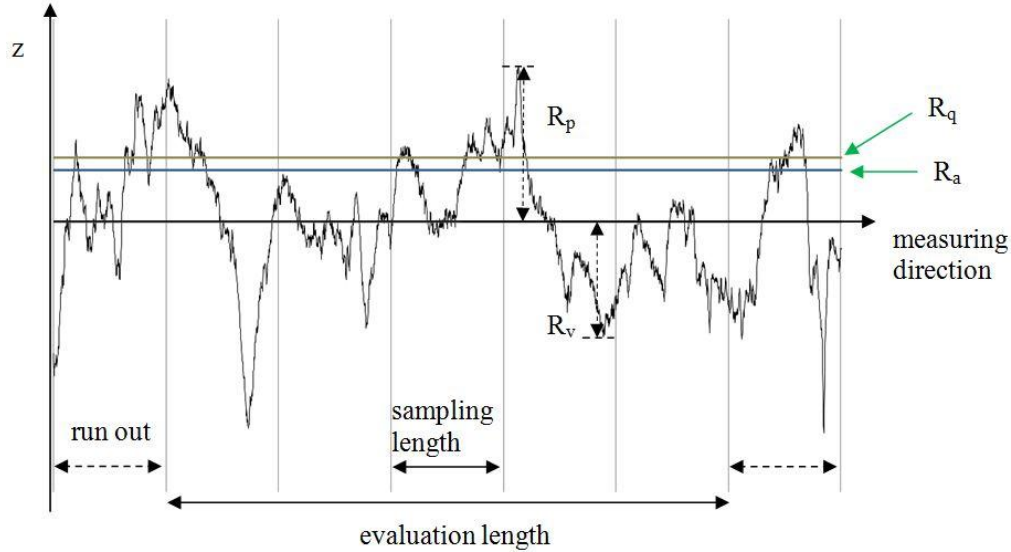


Figure 12. A measured surface roughness profile and some roughness parameters

$$R_a = \frac{1}{N} \sum_{i=1}^N |z_i| \quad (2)$$

$$R_q = \left( \frac{1}{N} \sum_{i=1}^N z_i^2 \right)^{\frac{1}{2}} \quad (3)$$

$$R_p = \max_i z_i \quad (4)$$

$$R_v = \min_i z_i \quad (5)$$

where  $N$  is the number of measured points and  $z$  is the height of each measured point along the profile (B.J. Hamrock, 2004).

As it can be seen in Figure 12, the evaluation length ( $L$ ) is five times the sampling length or cut off ( $\lambda_c$ ) but the profile length that is measured has two extra sampling lengths, one in the beginning and one at the end, which is called run out. Having a run out in the measurements or not depends on conditions and users, but the sampling length is defined by standards and varies for different surface roughness values.

In this study, since the tooth flank was shorter than the evaluation length defined by standards, the maximum possible length was measured and a specific run out was considered which has been kept the same through the study.

## **2.4 Running-in**

Running-in is practically smoothing the gear meshing during a certain period of loading time. During this process abrasive wear on the active gear flank and additionally plastic and elastic deformation on sharp asperities occur. As time goes by, the two contacting surfaces reach a better contact situation, due to smoothing of the surfaces (peaks of asperities are removed) and thus an increase in the contact area. Generally, the harder the material the longer is the running-in procedure (T.A. Stolariski, 2000).

Having new gears with intact surface asperities, the risk of scuffing is higher but over all, it can be said that an appropriate running-in can increase gear life by enlarging the real (i.e. effective) contact area and reducing the contact pressure over the asperities. If the gears pass a proper running-in procedure, the risk of scuffing will be reduced (T.A. Stolariski, 2000).

When the surfaces of the components experience the first contact usually the asperities deform plastically, and if the boundary layers (formed by the additives and oxide) fail to separate the two surfaces in contact, asperities will have direct metal to metal contact (B. J. Hamrock, 2004). A contact exposed to this will have an increased wear rate, not just because of the metal to metal contact, but also due to the creation of wear particles leading to an abrasive wear mechanism (S. Sjöberg, 2010).

One way to control a running-in procedure, is to control the surface roughness. It has been said that with smoother surfaces a better running-in procedure can be achieved. In some situations it can be said that surface asperities are helping to give a better lubrication region as it does to ski boards. In these cases the contact is said to work in the micro EHD lubrication regime (T.A. Stolariski, 2000).

After all it should be mentioned that there is no standard running-in method, it is dependent on experience. In fact the running-in procedure can vary with the contact situation, the contacting surfaces, the material properties of the components, and the chemical properties of lubricants and coatings. And finally it should be known that there is need for more studies on boundary lubrication and running-in procedures.

## **2.5 Available test results**

To increase the performance of AC Tools, Atlas Copco has performed tests on its products. The Tensor ST angle tool series is one of these tools that have been tested at several occasions. The results and relevant information from these tests have been studied and discussed to enable development of a high-quality test plan in this project.

In all AC Tools tests, the applied torque has been the main test parameter and the speed has always been constant. Comparing the results from different loads shows that after a certain number of cycles all the gear sets are reaching a steady state efficiency (Figure 13). Figure 13 shows the mean efficiency of 15 test specimens loaded by a 50 Nm torque. Generally, the specimens shows the same efficiency curve behavior even at lower loads, the only difference is the fact that specimens subjected to a lower torque have a longer life.

Moreover, a Wöhler curve (Figure 15) has been generated for the studied gears, which is used for calculations in this report. Further details of the tests are not reported here due to confidentiality reasons. It should be noted that the Wöhler curve that is calculated is the average life of the



gears, i.e.  $L_{50}$  (the minimum life that 50% of specimens will reach), and not  $L_{10}$  (the minimum life that 90% of specimens will reach). Life for these gears is calculated for the noticeable surface damage of the gear tooth. To define and calculate the life, the transmission error of the system is calculated and plotted. Life is defined as the number of cycles in which the average of the transmission error for “ $n$ ” number of cycles is exceeding the maximum transmission error in the early life of the specimen (Figure 14).

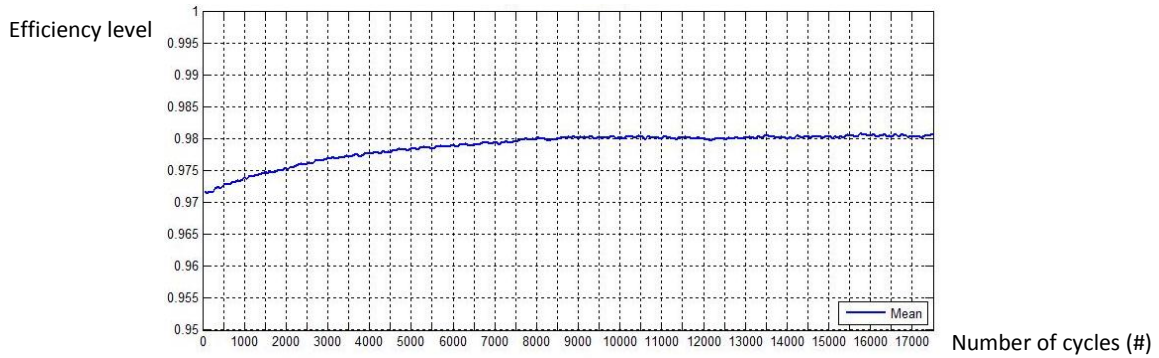


Figure 13. Mean efficiency of 15 specimens during the first 17000 cycles, tested at 50 Nm and 60 rpm

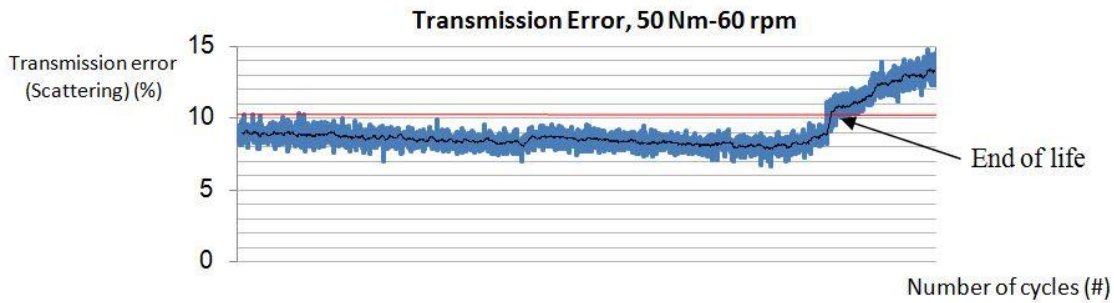


Figure 14. An example of a transmission error plot, where the average plot (black curve) is passing the maximum value of the error in the beginning of life, at this point the gear set is failed.

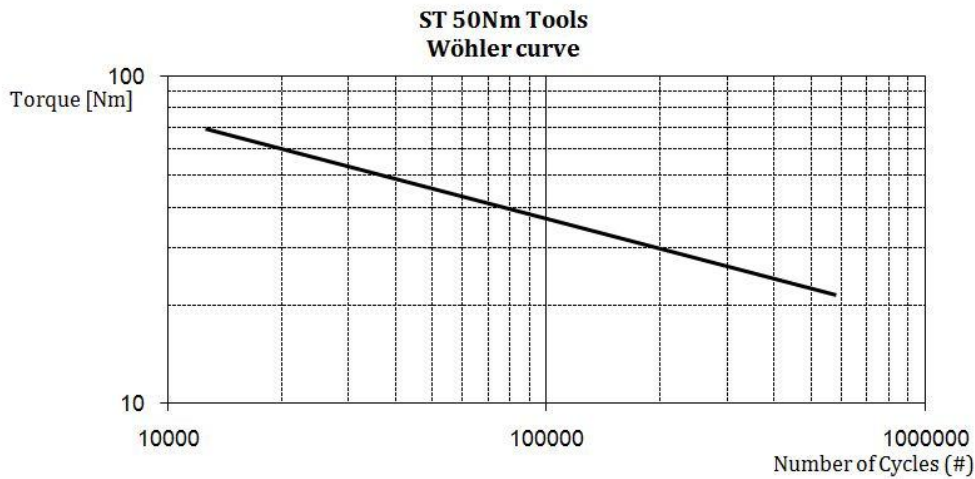


Figure 15. An example of a Wöhler curve

In addition, two running-in tests have been performed by AC Tools. Both tests had a torques of 50 Nm and a speed of 60 rpm and were performed with the purpose to investigate the effect of re-lubrication of the gears. These running-in tests showed that, depending on the running-in intervals, the results can vary between 1.5 to 8 times of Wöhler life. Figure 16 and Figure 17 show the results of two different running-in procedures, investigated by AC Tools. Comparing the life of the running-in tests and the Wöhler life of the gears (shown in Figure 15) verifies the effect of the running-in process on the gear life.

Using the Wöhler curve, it is possible to define a parameter for “Percent of Life” which is referred to as PoL and that shows the amount of life that has passed and it is calculated by the Palmgren-Miner rule. This rule helps to predict the life of components using the cumulative damage caused by different load types and levels.

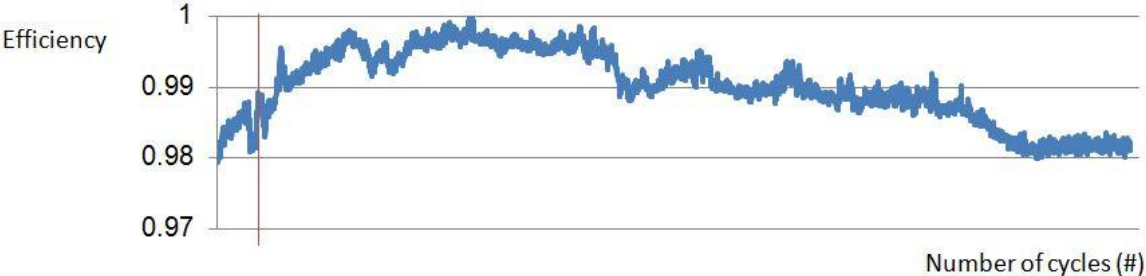


Figure 16. Efficiency curve for running-in procedure, one re-greasing after 10% of  $L_{50}$  life, the red line is showing the re-greasing time, which has shown a life six times longer than Wöhler life.

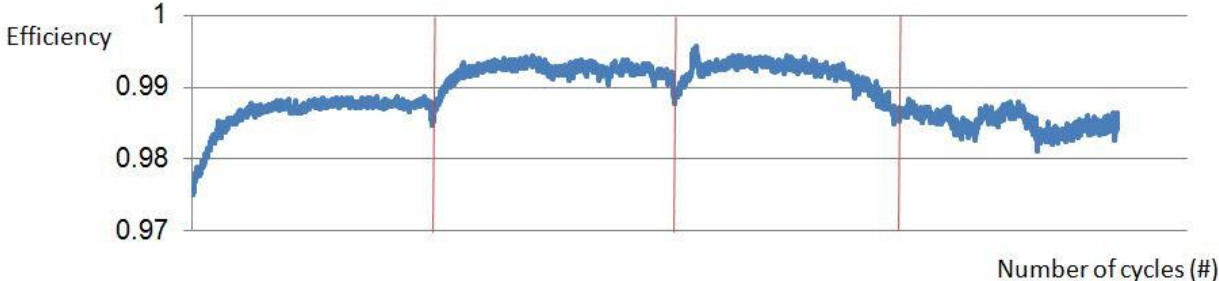


Figure 17. Efficiency curve for a running in process, three times re-greasing after every 10% of  $L_{50}$  life, the red line is showing the re-greasing time, which has shown a life as twice Wöhler life.

## 3 METHOD

*Experience has shown that running-in of gear surfaces can extend the life of gears. The question remains on the method, how to run-in the surfaces and the factors which affect the results of the running-in process.*

*A design of experiments was setup to determine the number of cycles, the loading and lubricant conditions, and speed during contact. After the test setup has been identified, for each test setup two repetitions have been performed.*

### 3.1 Instruments

#### 3.1.1 Test rig

A photo of the test rig is shown in Figure 18 and a schematic view in Figure 19. This test rig is coupled to software installed on a computer next to the rig. The counter, torque transducers, and the thermometers are transferring the signals to a power table. The power table is loading the data into the computer and controlling the data through software. This software interface is a LabVIEW program which can read the data from test rig and put constrains on it, e.g. the torque level, temperature level. In case the data does not match specific limitations, the software is capable to stop the test rig, for example if the torque is higher than a set value the computer system will shut the rig off.

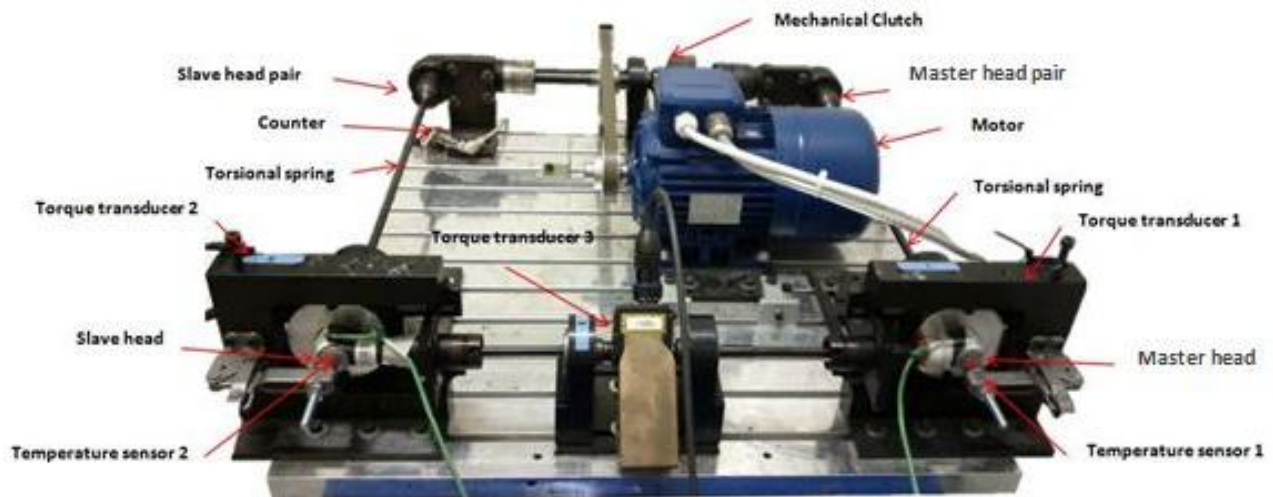


Figure 18. The angel head test rig, crucial components and sensors are identified with arrows.

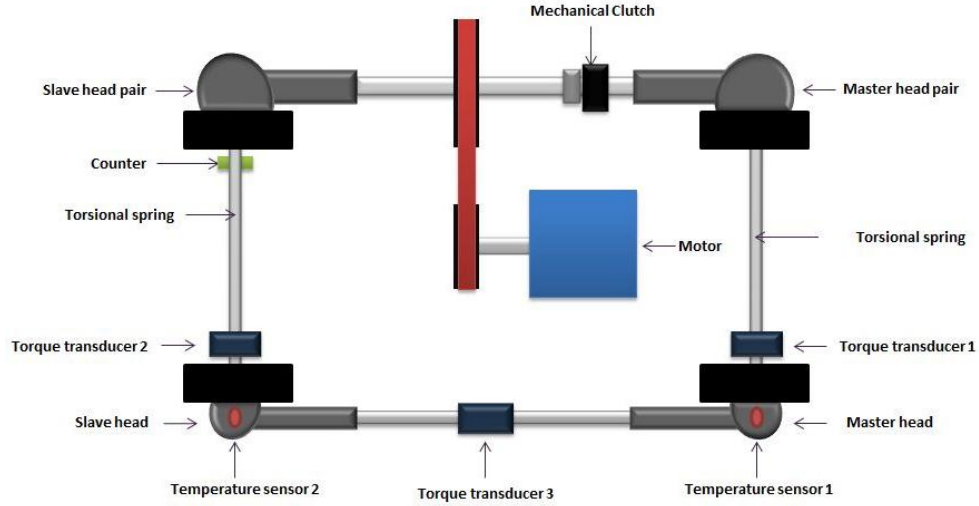


Figure 19. Schema of major parts of the test rig. Arrows show the crucial components as well as the test specimen (the master head), the slave head, the transmission, motor and sensors.

As shown in Figure 19, each test needs two gear pairs; one to use as a slave and one as the test specimen. Three torque transducers are used to check the applied torque with a sampling rate of 1600 Hz. There are two sensors attached to the slave and master heads to measure the temperatures of the bodies over time. This temperature for sure is not the tooth contact temperature but it can approximately show the lubricant bulk temperature. The three torque transducers are positioned: 1) on the gear side of the master head, 2) on the gear side of the slave head, and 3) on the pinion side in between the slave and master pinion. The master head needs to apply a clockwise torque on its gear side to fasten the nuts. This torque needs to be applied on the gear side (driven gear). To do so, there is a mechanical clutch to keep the pinion of the master head pair under loading torque, in this way a torque will be applied to the gear of the main head. It is possible to read this torque through torque transducer 1.

The motor is running the slave head pair and the motion is transferred to the slave head by a torsional spring (a bar). The torsional springs are subjected to the torsional torque applied from the mechanical clutch. An infrared sensor is counting the cycles which this torsional spring is passing. This number in the results and calculation part is named “number of cycles”. The master head pair will be driven by the gear of the master head which must have the same gear ratio as the slave. The speed parameter is controlled by the speed of the motor. Since the torque is applied mechanically by the clutch, it can decrease or increase due to the setup conditions. So it is possible to apply a maximum and minimum range of torque for each transducer to stop the test rig when the torque is out of range. But the main factor which is considered as failure of the test specimen is the scatter of the torque data (peak to peak transmission error), loaded from torque transducers. The calculated scattering error is shown in Equation 4.

$$\text{Scattering} = \text{Peak to Peak} \times \left( \frac{M_{out}}{M_{in}} \right) \times 100 \quad (6)$$

The peak to peak value is the difference of the maximum positive and the minimum negative peaks of the input signal.  $M_{out}$  and  $M_{in}$  are the input and output torque of the main test head respectively.

### 3.1.2 Surface measurement

2D surface measurements (2D) were done after each test cycle at AC Tools with a Mitutoyo tool (Figure 20). 3D surface measurements (3D) were made before and after completed all test cycles at KTH with a Taylor Hobson Form Talysurf PGI 800. Both measuring equipments use a standard stylus probe with tip radius of 2 micrometers.

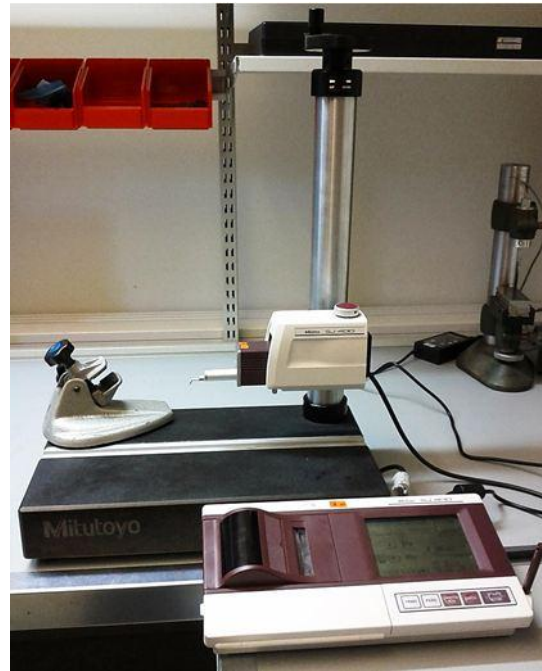


Figure 20. Mitutoyo surface measurement instrument, AC Tools

The advantage of using the Mitutoyo instrument is the probe design which is specially designed for measuring steep gear flanks (Figure 21). This special probe made it possible to measure the roughness from the root to the tip of the gear tooth. But this tool is not robust to environmental noises as machining vibrations and load sounds and since it has been installed in a room close to the workshop area, it is hard to measure the exact values and it has measurement errors of approximately  $\pm 0.2 \mu m$ . The 3D measurement tool at KTH is installed in an isolated room, however, the probe was not able to measure root to tip of the gear tooth flank.



Figure 21. The special Stylus probe for gear flank surface measurements

A microscope with a camera was used to observe the contact region after each step both to study the position of contact at each load and speed and the condition of the contact region after each running schedule (Figure 22). After making photos, a software was used to process and modify the photos according to the sharpness and zoom of the microscope. In addition, to hold the gears in special position during measurements and photographing, two holder parts have been designed, one for the pinion and one for the gear.

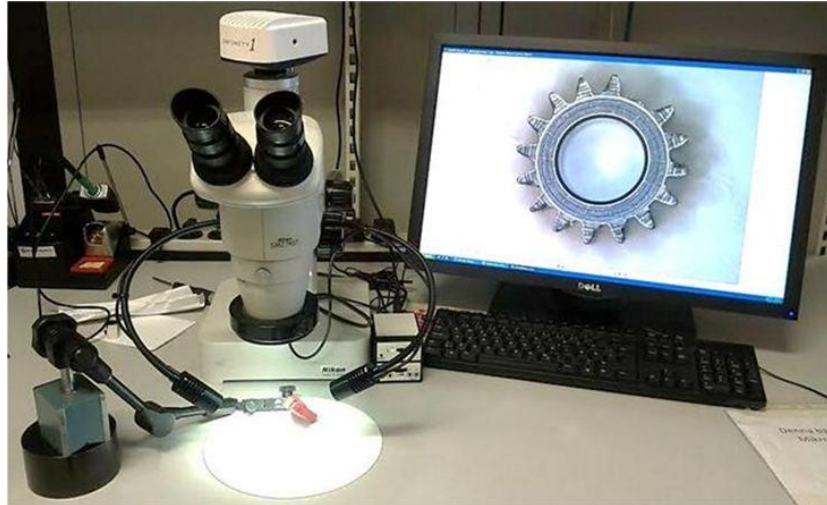


Figure 22. On the left the Nikon microscope, on the right the computer screen

## 3.2 Test procedure

To test one angle head, two gear pairs are needed, one as master and one as slave. For each test or at least for each step, the test rig can just be set to one torque value while speed can be changed during the test procedure. Temperature, speed, torque, scattering, number of cycles and time are loaded to a file and saved to the computer hard drive and it is possible to convert the log file to an Excel file.

The limits of accepted scattering value and torques are set manually in the software, as high and low limit of torque and high limit of scattering value for transducer 1-3. The test can be stopped manually or by the software.

### 3. 2.1 Following the same gear tooth

To be able to trace a gear tooth during measurements (i.e. reallocation), each gear (and pinion) has been named by numbers and three teeth on each gear have been chosen and marked. In this way it was possible to keep track of each gear tooth and the result comparison was easier, see Figure 23.

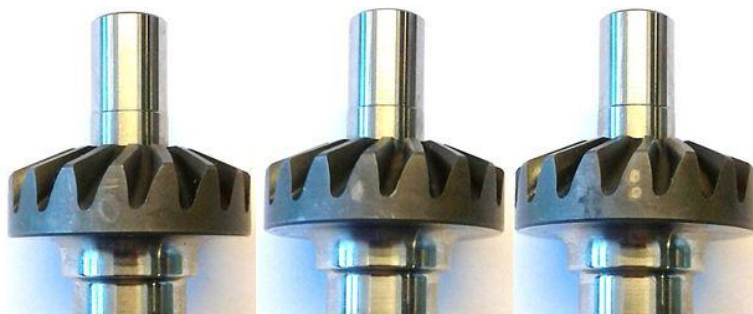


Figure 23. A picture of a coded gear and coded teeth: from left, gear number 30 tooth one, tooth two and tooth three, respectively.

### 3. 2.2 Measuring the gears during running-in procedure

After each test cycle three gear slots were cleaned in order to be able to measure the surface roughness (Figure 24). Only after the complete running-in procedure the whole gear could be cleaned in an ultrasonic bath using heptane followed by methanol. This was done before the 3D measurements.



Figure 24. A gear which is ready for 2D roughness measurement.

### 3. 2.3 Step by step measurements

Each test was repeated once. However, only for the first of two repetitions the surfaces were measured after each step of running-in. In order to measure the gear surface and to capture the contact region the master head was taken off from the test rig and only the gear (not the pinion) was disassembled from it. After the last step of the first repetitions of the test setups, 3D measurements was done on the gear tooth flank. In Figure 25 the side of the flank which was measured is shown.



Figure 25. Measured flanks are the on the convex gear flank

As shown in Figure 26, for the first test repetition, on each flank, three 2D measurements were done. This was repeated over three teeth after each step. The area of 3D measurements is also shown in Figure 26.



Figure 26. On the left the 3lines 2D measurement of the 1<sup>st</sup> repetitions, on the right the square area of 0.5x0.5 mm

For the second repetition of tests, 2D measurement was done only before and after the running-in procedure. Photos were taken after the running-in was finished. The roughness measurements for these tests were different (Figure 27). The measurements were not only on the heel side, but also in middle of the tooth and on the heel side.

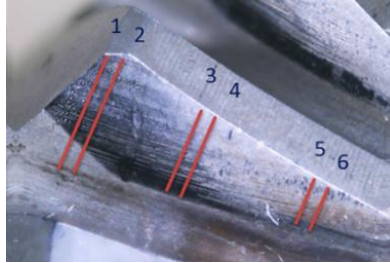


Figure 27. Six line measurements on the gear tooth flank

Keeping track of the pinion surface, it was necessary to disassemble the master head completely and re-assemble it to continue the test. This would cost more time and more noise (i.e. variation) to the results, which is the reason to skip the pinion teeth measurements.

When measuring the surface roughness a cut-off value of 0.7mm was used, however it is recommended by the ISO 1997 and DIN 4288 standards to use 0.8 mm as cut-off for grinded surfaces with  $R_a$  between 0.1 and 2  $\mu\text{m}$  with the maximum stylus tip radius of 2  $\mu\text{m}$ . This change was made due to the small size of the gears and the short tooth width of maximum 2.4 mm (in the heel cone). Hence the following settings, shown in Table 1, was used as evaluation length, cut-off and run-out for each line in three-line and six-line measurements.

Table 1. 2D measurement tool settings for 1<sup>st</sup> and 2<sup>nd</sup> repetitions

	Line Number	Cut-off (mm)	Evaluation length (mm)	Number of measured points	Run-out (mm)
3line	1, 2 and 3	0.7	2.1	4200	0.15
6line	1 and 2	0.7	2.1	4200	0.1
6line	3 and 4	0.7	1.4	2800	0.1
6line	5 and 6	0.7	0.7	1400	0.05

Other settings, such as cut-off wavelength of the low-pass filter ( $\lambda_s$ ) and the measuring point distance ( $\Delta x$ ) is set by standards from the tool manufacturer, where  $\lambda_s$  is 2.5  $\mu\text{m}$  and  $\Delta x$  0.5  $\mu\text{m}$ . The filter chosen was as Gaussian filter with R profile since the gears are face milled and the measurement lines are perpendicular to manufacturing marks.



### 3.3 Pretest

In order to develop a good test strategy, there was a need to study the parameters and the performance of the testing equipment. To study the level of each parameter and its effect on early wear, two pretest configurations were developed. The intention was to choose the best and the worst possible test cases which would lead to a choice of better parameter levels for the main Design of Experiment (DoE). These tests cover loading and speed effects, as shown in Table 2 and

Table 3. The results of these pretests were used to manage the main test plan and the DoE.

In pretest I, the load, speed, and number of cycles were set as constant. The main goal of this test was to observe the effect of high load (50 Nm) and low speed (30 rpm) for 13% of the gear life. This test is considered as the worst case. Pretest II is observing different loads and different speeds, just to compare with pretest one and previous studies performed by AC Tools.

Table 2. Pretest I, the worst case

Pretest I	Load (Nm)	Speed (rpm)	PoL (%)
Step 1	50	30	3.20
Step 2	50	30	3.20
Step 3	50	30	3.20
Step 4	50	30	3.20

Table 3. Pretest II, the best case

Pretest II	Load (Nm)	Speed (rpm)	PoL (%)
Step 1	10	90	0.001
Step 2	20	78	0.1
Step 3	30	66	0.48
Step 4	40	60	1.37

### 3.4 Design of experiment

To study the running-in effects on spiral bevel gears, a series of tests have been designed using full factorial design. It was decided to study the influence of three parameters; speed, change of lubricant, and percent of life (PoL). Load has been decided as the constant parameter which increases from 10 Nm to 50 Nm at five steps and the same for all test setups. For this experiment, which has three design parameters, a full factorial design was used. Each parameter has two levels, which according to DoE gives eight tests. The high and low level of parameters are shown in Table 4 to Table 6. Table 7 shows the full factorial design which has been used for the tests.

Table 4. Levels of PoL (Percent of life) as a design parameter

Level of PoL	PoL per load step				
	10 (Nm)	20(Nm)	30(Nm)	40(Nm)	50(Nm)
Low level (1%)	0.2	0.2	0.2	0.2	0.2
*High level (10%)	0.025	0.25	1.0	3.0	5.725

\*The second level of this parameter has been chosen later, after scrutinizing the test-rig results for the first level.

Table 5. Speed levels

High level (rpm)	120
Low level (rpm)	60

Table 6. Re-greasing levels

Low level	Grease is not changed during running-in procedure.
High level	Grease is changed after 0.1 PoL of 10 Nm load.

Table 7. Three factor full factorial design (design of experiment)

Design parameters				Responses									
Set	PoL	Speed	Grease	Total Life	EffS	EffR	EffL	$R_a$	$\sigma_R$	$R_q$	$R_p$	$R_v$	$R_z$
1	1	60	Un-changed										
2	1	60	Changed										
3	1	120	Un-changed										
4	1	120	Changed										
5	10	60	Un-changed										
6	10	60	Changed										
7	10	120	Un-changed										
8	10	120	Changed										

A discussion about each parameter (design factor) and measurable output parameter (response) is presented below. All the design parameters, responses, and constant parameters are explained in this chapter.

### 3. 4.1 Design parameters

#### *Load; the constant parameter*

The method which is widely used to run-in cylindrical gears is to run the gears at low torque, for example 20 % of the nominal load, at nominal speed for a certain number of cycles. This procedure will make the contact area smooth and adapted to contact condition and may result in an increased gear life.

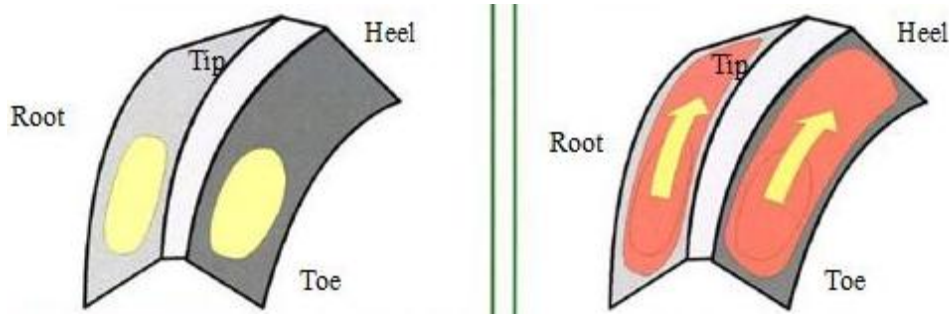


Figure 28. Shift of contact pattern due to increase in load (Klingelnberg, 2008)

In case of spiral bevel gears, the contact pattern is closer to toe at lower torque levels and moves towards the heel region at higher torques (Figure 28). Since the contact pattern is shifting, a range of torque has been chosen for the running-in of the gears. Since running-in needs to cover the entire contact pattern, the loading procedure, for all the gear sets, will cover, 20 % (10 Nm), 40 % (20 Nm), 60 % (30 Nm), 80 % (40 Nm) and 100 % (50 Nm) of the nominal load.

#### *Percent of life (PoL)*

Percent of life (PoL) is a design parameter, used by the author, which is defined as the number of cycles that the gear is subjected to at a specific torque level divided by the Wöhler life at the same torque level. This parameter is the same as the Palmgren-Miner cycle ratio ( $c$ ):

$$PoL = c = \sum \frac{n_i}{N_i} \quad (7)$$

where  $N_i$  is the Wöhler life of the gears at each torque level (Figure 15) and  $n_i$  is the number of cycles the gears are subjected to for each torque level. For instance if the gear is subjected to a 20 Nm torque for 4000 cycles it will have passed through 0.2 % of its life and it has the same impact on the life of the gear as if it was running at 30 Nm for 1000 cycles or at 10 Nm for 45000 cycles (Table 8).

Table 8. An example for PoL

Load (Nm)	Number of Cycles	Life (number of cycles)	PoL(%)
10	45000	22500000	0.2
20	4000	2000000	0.2
30	1000	500000	0.2

In this way, a good comparison can be done according to the impact of life for different torque levels. It can also show how a high load or low load changes the running-in effects. For example,

the gear age can pass 10% of its life by being loaded at 10 Nm for 2250000 cycles or 50 Nm for 7500 cycles. While in the second case, the chance of micro pitting is much higher.

### *Speed*

Running-in is related to the quality of the contact adaptation between the surfaces, and this process depends on the wear mechanism and the lubricant film thickness. Higher sliding velocity will result in higher wear where higher film thickness will be achieved by higher velocity. Thus speed has been chosen as a design parameter in the DoE.

### *Early re-lubrication*

During contacts in the boundary lubrication region and with plastic deformation of the asperities, the higher peaks will be removed or deformed in the few first cycles of life. Due to the fact that these solid particles can cause further damage to the surfaces by getting trapped between the contacting surfaces (Figure 29) or by acting as abrasive particles, an early change of grease is chosen as another running-in factor.

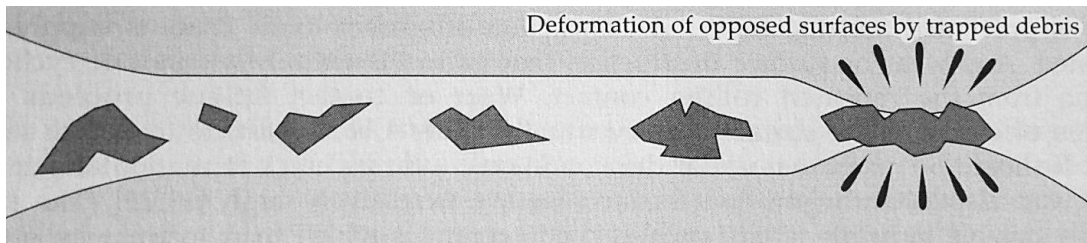


Figure 29. Solid particles in the lubricant (G.W. Stachowiak, 2001)

## 3. 4.2 Responses

### *Life ratio*

Life ratio is the main response which was studied in this DoE. This number is measured by counting the full number of cycles made by the gear till it breaks, divided by the Wöhler life of the gears ( $L_{50}$ ), defined by Equation 8. Actually it is almost the same as PoL and the only difference is the fact that Life ratio defines the end of life.

$$Life\ ratio = \frac{Life\ of\ the\ tested\ gear}{Wöhler\ life_{L_{50}}} \quad (8)$$

### *Surface topography*

Another definition of running-in is to reach the wear steady state. Since the wear process changes the surface topography, 2D measurements and 3D measurements was done for all tests. Due to the change in surface topography, parameters such as  $R_a$ , standard deviation of  $R_a$  ( $\sigma_{Ra}$ ),  $R_q$ ,  $R_p$ ,  $R_v$  and  $R_z$  have been chosen to study.

### *Efficiency*

Plastically deforming surfaces and wear transform energy and consequently decrease the efficiency level, which is also related to a reduction of friction. Thus one of the most important parameters to keep track of in the running-in process is the efficiency during running-in and the life of the gears. Hence three parameters have been defined to study as responses due to the

efficiency of the gear transmission; slope of increasing efficiency in the beginning of the life test (EffS), efficiency increase due to the running-in procedure (EffR), and efficiency increase over the life test process (EffL).

EffR is considered as the difference of the average efficiency for the first 20 cycles of running-in and the average of the last 20 cycles. EffL is calculated after the efficiency curve has reached steady state. It is equal to the difference of the average efficiency for the first 200 cycles of the life test and 200 cycles of the efficiency steady state. EffS is dependent on the EffL and the number of cycles that it takes the gears to reach steady state of efficiency and it is equal to arctangent of the EffL divided by the number of cycles. See Figure 30 and Figure 31.

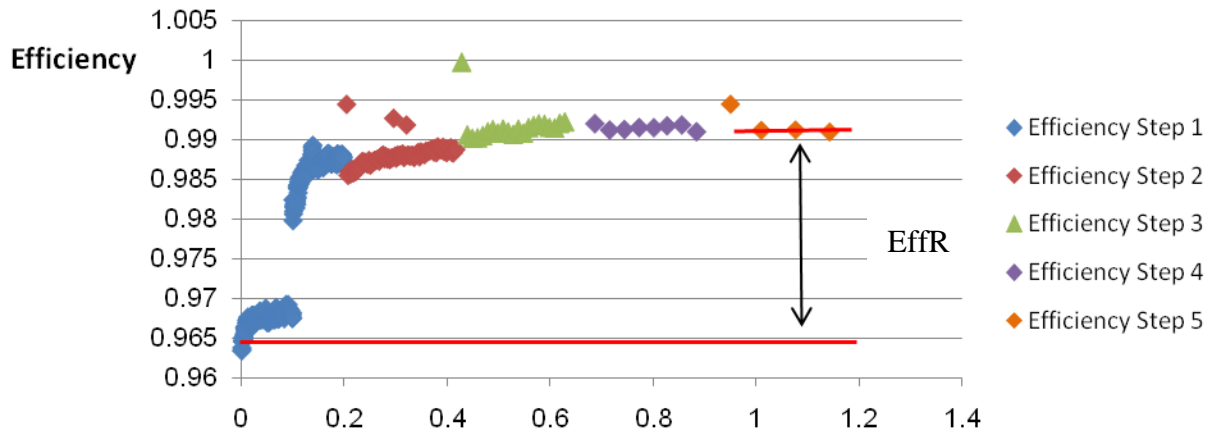


Figure 30. Definition of EffR. Percent of Life on the abscissa

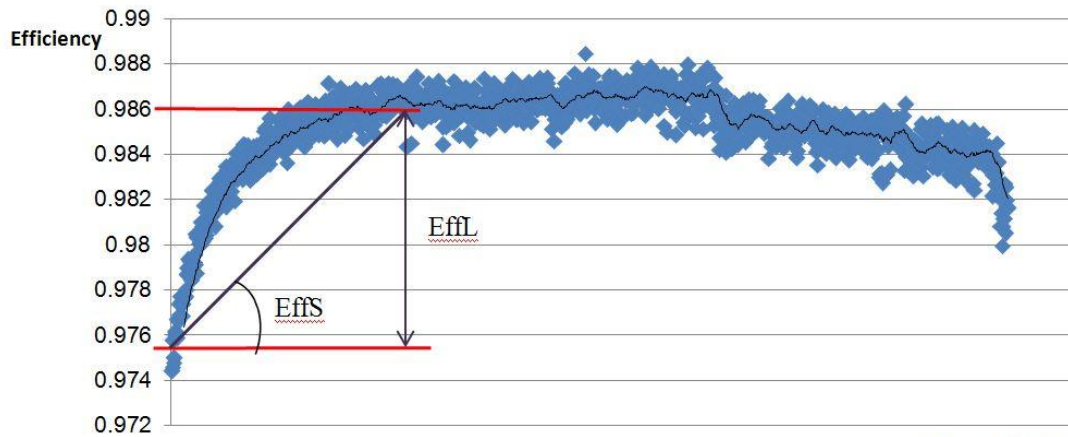


Figure 31. Definition of EffS and Eff. Percent of Life on the abscissa.

In Figure 32 a schema of the test procedure including the running-in and life test can be seen. Once a test has reached the end of the running-in process, regardless of re-lubrication factor, the lubricant (grease) is changed and the tool is left to run for life test.

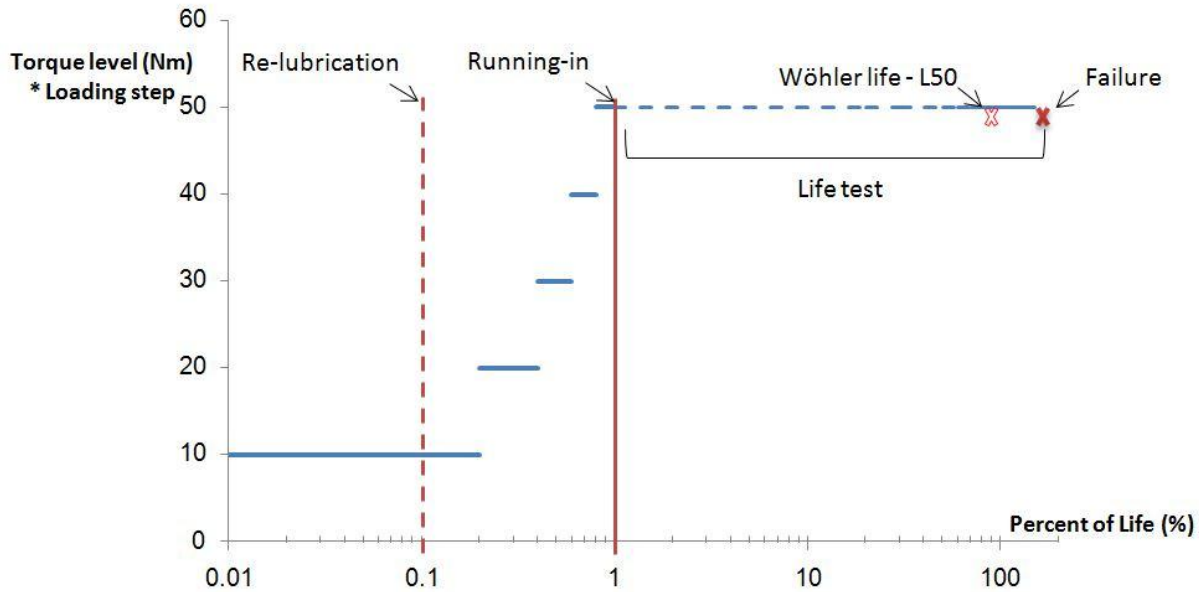


Figure 32. Schema of test procedure for running-in and life test

### 3.5 Analytical method

The lubricant which is used for these gears in the nut runner series ETV ST61-50-10 is a kind of grease with mineral oil and lithium soap and it contains EP additives plus solid lubricants ( $\text{MoS}_2$  1 to 10  $\mu\text{m}$  particles). Since no general film thickness calculation method exists for grease, a few assumptions have been made to simplify the calculations.

- To calculate the lubricant film thickness, as it has been discussed in Chapter 2.2.2, considering the grease as a solid lubricant, equations for hard EHD lubrication have been used and the properties of the lubricant have been assumed to be the same as for the base oil.
- Since the gears are spiral bevel gears and have non-rectangular contact in two directions, the equations for elliptical contact have been used.
- Simplifications will be used to translate the spiral bevel tooth to a spur gear according to M. Savage and P.C. Altidis, 1989, as previously explained in this chapter.
- Since these gears are face milled, the cutter radius has been used as the radius of the spiral curvature to model the conforming contact between the convex and concave side of the flanks.

All constants used for these calculations are presented in Appendix B.

The first step in the calculations is to define the elliptical contact of spiral bevel gears, which is the modeling of the contact region. In the projection of an elliptical contact the  $x$  and  $y$  can be shown by the radiuses of the ellipse, shown in Figure 33.

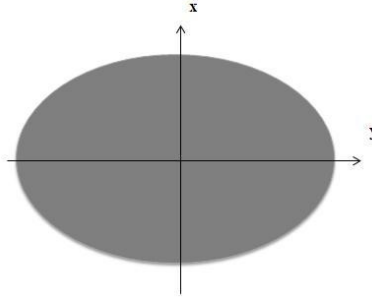


Figure 33.  $x$  and  $y$  direction for elliptical contact

The first step is to calculate the correct radius of the equivalent spur gear pitch radius, according to the mid-cone radius of the contacting gears. This procedure translates the mid-cone of the spiral bevel gear to the pitch cylinder of the spur gear tooth, as shown in Figure 34. Then it is needed to shift the coordinates to the cone tangent plane of the gear.

In Equation 18,  $R$  is the equivalent pitch radius,  $r$  is the mid-plane pitch radius of the spiral bevel gear and  $\Gamma$  is the mid cone angle.

$$R = \frac{r}{\cos \Gamma} \quad (9)$$

The next step is to calculate the pitch radius of the tooth in the tooth normal plane (normal to the spiral curve rather than normal to the cone tangent plane). This can be calculated using Equation 20 which results in the effective radius of the equivalent spur gear in the tooth normal plane,  $R_e$ .

$$R_e = \frac{R}{\cos^2 \beta} \quad (10)$$

where  $\beta$  is the mid spiral angle.

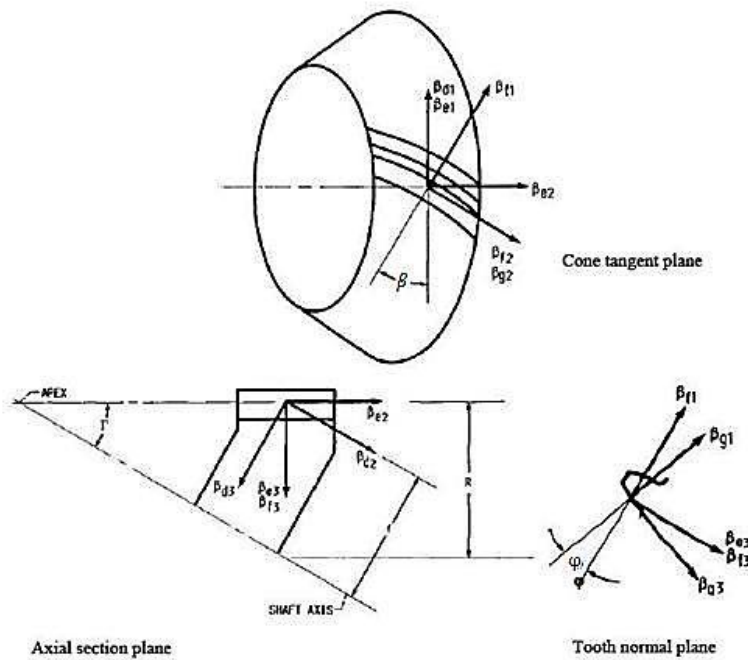


Figure 34. Spiral bevel gear tooth coordinates (M. Savage and P.C. Altidis, 1989)

The next step is to model the contact discs as shown in Figure 35.

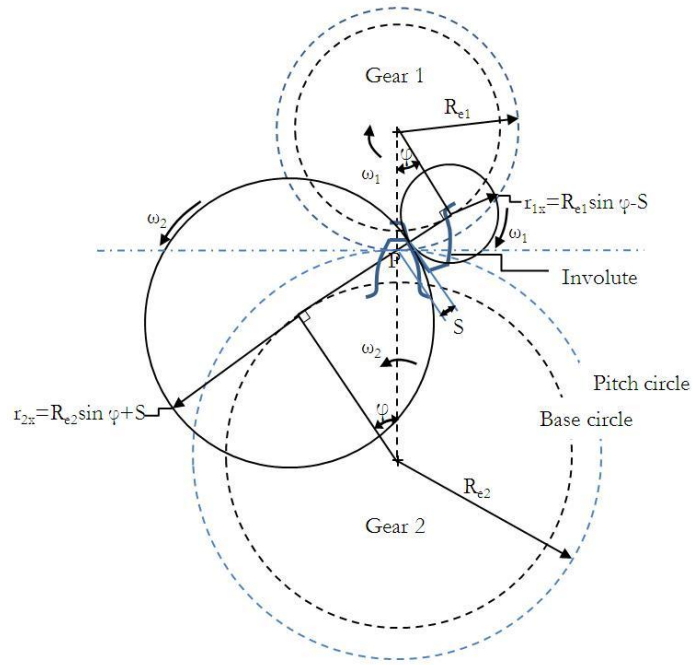


Figure 35. Contact disc generation, the  $x$  direction is parallel to the internal tangent line of the contact discs

$$\text{Gear ratio} = \frac{R_{e1}}{R_{e2}} = \frac{\omega_2}{\omega_1} \quad (11)$$

$$r_{1x} = R_{e1} \sin \varphi + s \quad (12)$$

$$r_{2x} = R_{e2} \sin \varphi - s \quad (13)$$

where  $\varphi$  is the pressure angle and  $S$  is the distance of the contact point from the pitch point on the line of action. In Figure 35, the  $x$  direction is parallel to the internal tangent line of the contacting discs.

Further, since there is a non-conformal contact between the discs, the effective radius in the  $x$  direction,  $R_x$ , is:

$$\frac{1}{R_x} = \frac{1}{r_{1x}} + \frac{1}{r_{2x}} \quad (14)$$

To calculate the effective radius in the  $y$  direction,  $R_y$ , the spiral contact between the concave flank of the pinion tooth and the convex flank of the gear tooth, which is a conformal contact, the following model is used, see Figure 36. In Figure 36 with two curved cylinders, it can be seen that each cylinder has the radius the contact disc in each contact point. The radius of the cylinder curvature has been considered as the cutter radius of the same flank. Since the contact in this direction is a conformal contact, the  $R_y$  value is calculated as follow:

$$\frac{1}{R_y} = \frac{1}{r_{1y}} - \frac{1}{r_{2y}} \quad (15)$$



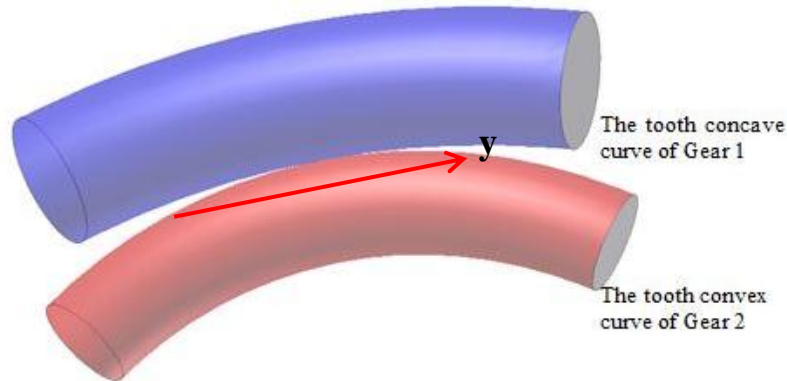


Figure 36. Model of the conforming contact of the pinion concave flank and the gear convex flank

The force calculation has been done by following the strategy of “Elements of metric gear technology “, Section 16 (SPD/SI, 2012).

### ***3.6 Simulation and finite element method***

To study the contact state such as forces, stress and deformations, a FE model of the studied spiral bevel gears, has been created with the Advanced Numerical Solution (ANSOL) HypoidK module. This software has different modules for different types of gear design.

Klingelnberg and Gleason are two different companies producing different gear manufacturing machineries. Therefore ANSOL use two different modules for each gear manufacturing setup. AC Tool uses Klingelnberg gears and software which makes it possible to import the gear geometry mesh directly to ANSOL. The ANSOL module used for these gears is named the HypoidK module which is adapted to hypoid and spiral gears designed and manufactured by Klingelnberg software and machines. After importing the gear mesh files to HypoidK and setting up the system details, the gears have been simulated under life test situation, 50 Nm torque and 60 rpm speed.



The following chapter presents the test results as well as a result analysis. The comments on the test results made in this chapter are used in the discussion and conclusions chapter.

## 4.1 Pretests

To study the effect of each factor on running-in process, two pretests have been done following the Table 2 and

Table 3.

Pretest I has been decided as the worst case, with low speed and high torque. The result of low speed is a thin lubricant film layer in the contact and a high applied torque affects both the minimum film thickness and the contact pressure, as shown in Figure 37 and Figure 38. Pretest II was defined as the mildest case with low torque and high speed.

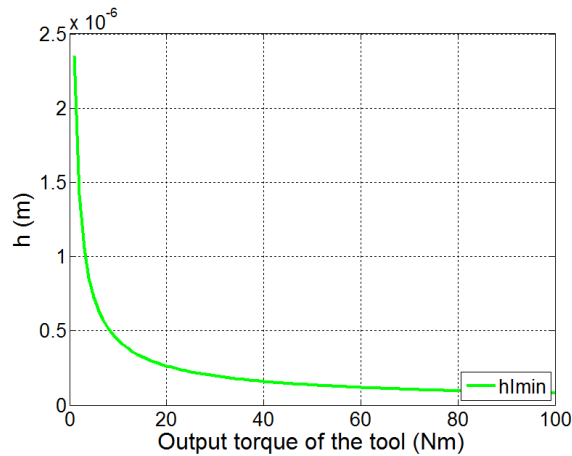


Figure 37. Effect of applied torque on minimum fluid film thickness (for the studied AC gears)

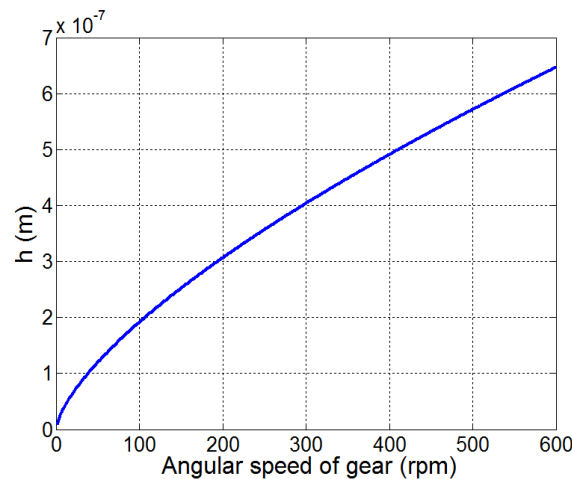


Figure 38. Effect of angular speed on minimum fluid film thickness (for the studied AC gears)

### 4.1.1 Pretest I

After first step of Pretest I (3% PoL at 50 Nm torque and 30 rpm speed) the test was stopped due to high damage of the gear tooth. Although there are signs of scuffing and lubricant burns, the test rig did not show any error when stopping the test. The only parameter which was exceeding its limit was the temperature in a way that it could be noticed by touching the housing body. The following tables and pictures contain the main results of Pretest I.

After the first step of Pretest I, The following pictures (Figure 39 and Figure 40) were made. On both the gear and the pinion, signs of contact failure can be seen. On the gear tooth, Figure 39, the area marked as 1 on the gear tooth, shows wear marks in dedendum, and area 2 shows burn marks of lubricant, and area 3 shows the marks made during the deburring process in the manufacturing line.

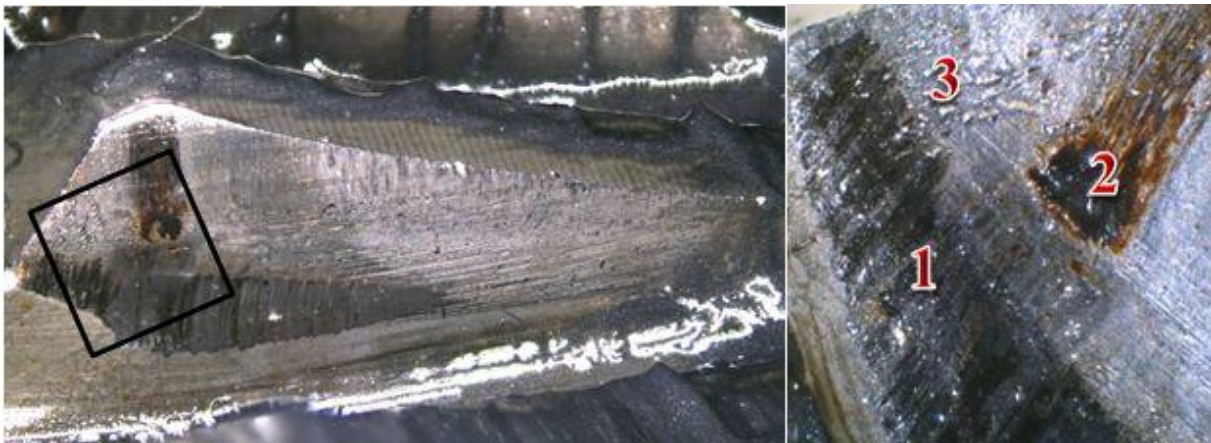


Figure 39. Gear tooth after first step of *Pretest I* (3 PoL, 50 Nm and 30 rpm)

In Figure 40, the pinion tooth is shown after Pretest I. The same burn marks can be seen on the contact area (2) and on the tip of the tooth (shown as 1), and wear signs can be seen (the tip is in contact with the dedendum of the gear tooth). Number 2 in Figure 40 shows a deep wear mark.

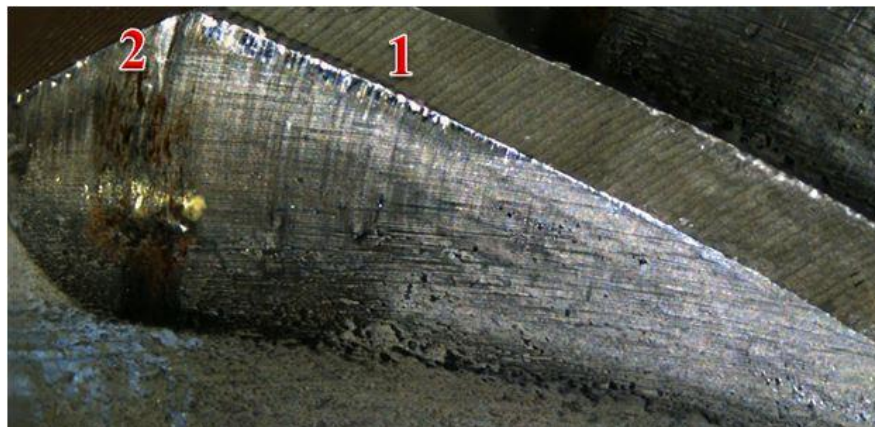


Figure 40. Pinion tooth after first step of *Pretest I*. (3 PoL, 50 Nm and 30 rpm)

Figure 41 shows the surface measurements of the convex flank of the gear. The measurements of the concave flank of the pinion can be seen in Figure 42, which shows that the pinion is rougher

after running-in. These results can be also found in Appendix B. This is due to the deep wear mark shown as 3 in Figure 40. It can be seen that for the gear flank the average reduction in peak height is 3  $\mu\text{m}$  as well as there is a reduction of 0.5  $\mu\text{m}$  for  $R_a$  and  $R_q$ , which is equal to a 50% reduction of the surface roughness value,  $R_a$ .



Figure 41. Roughness values on gear tooth, *pretest 1*. Horizontal axis is presenting the position of 2D measurement on the gear flank and vertical axis is presenting  $R_a$ ,  $R_q$  and  $R_p$  values in  $\mu\text{m}$ .

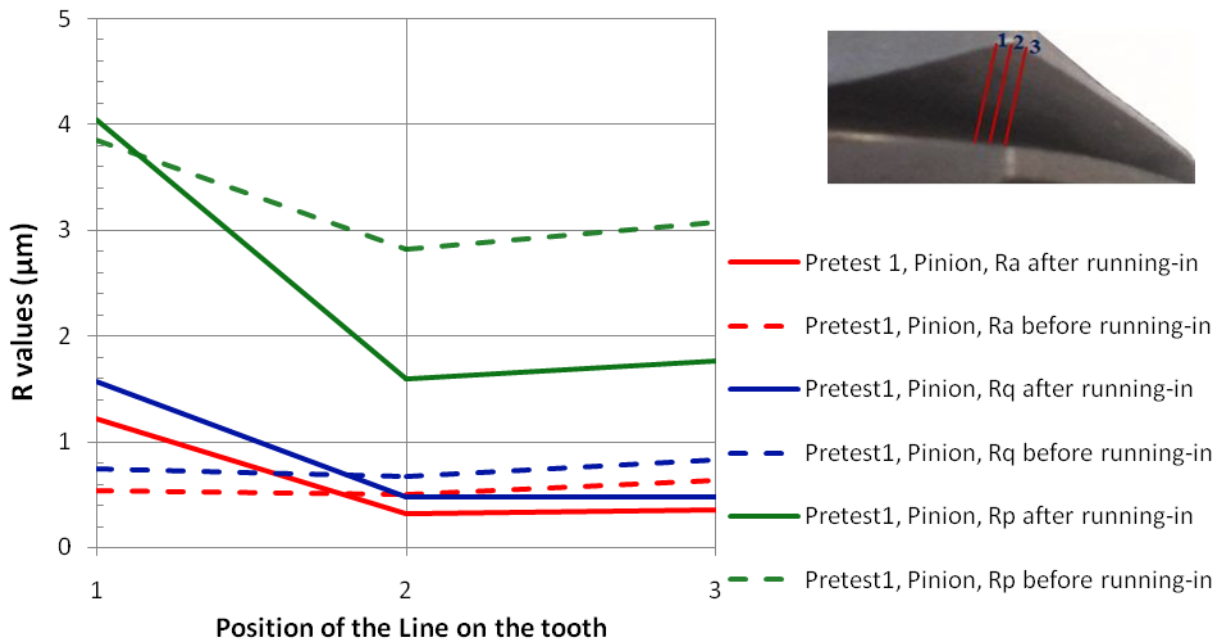


Figure 42. Roughness values of the pinion tooth, *Pretest 1*. The horizontal axis is presenting the position of the 2D measurement line on the pinion flank and the vertical axis is presenting  $R_a$ ,  $R_q$  and  $R_p$  values in  $\mu\text{m}$ .

One of the most important data from the test rig is the efficiency over PoL, which for Pretest I is shown in Figure 43.

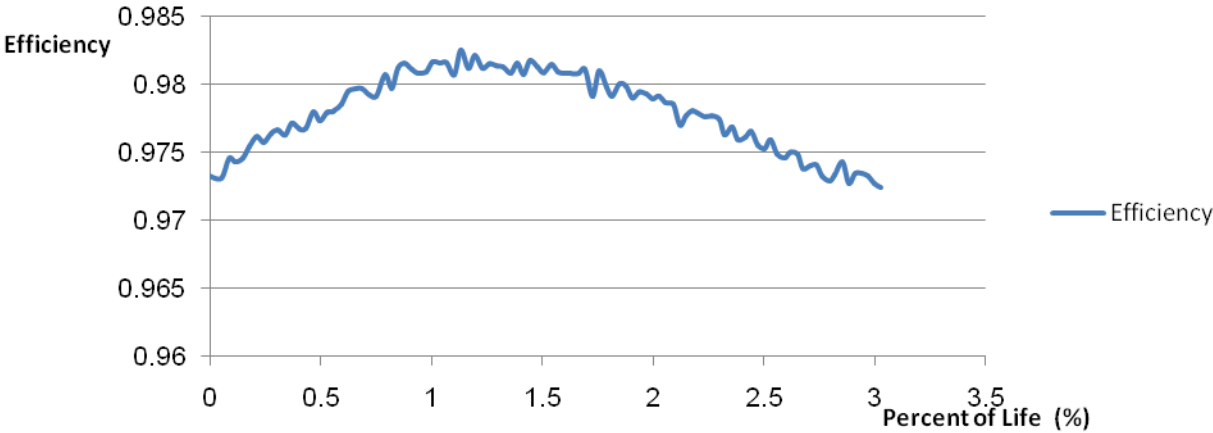


Figure 43. Efficiency curve for *Pretest I* in the first 3 PoL of the gear set, 50 Nm and 30 rpm. The horizontal axis is presenting the PoL and the vertical axis is presenting the efficiency of the gear set.

To show how the efficiency diagram looks in the first 3% PoL and to compare with the results of Pretest I, the test results from AC Tools are presented in Figure 44. The test parameters of the AC Tools experiments are 50Nm torque and 60 rpm speed.

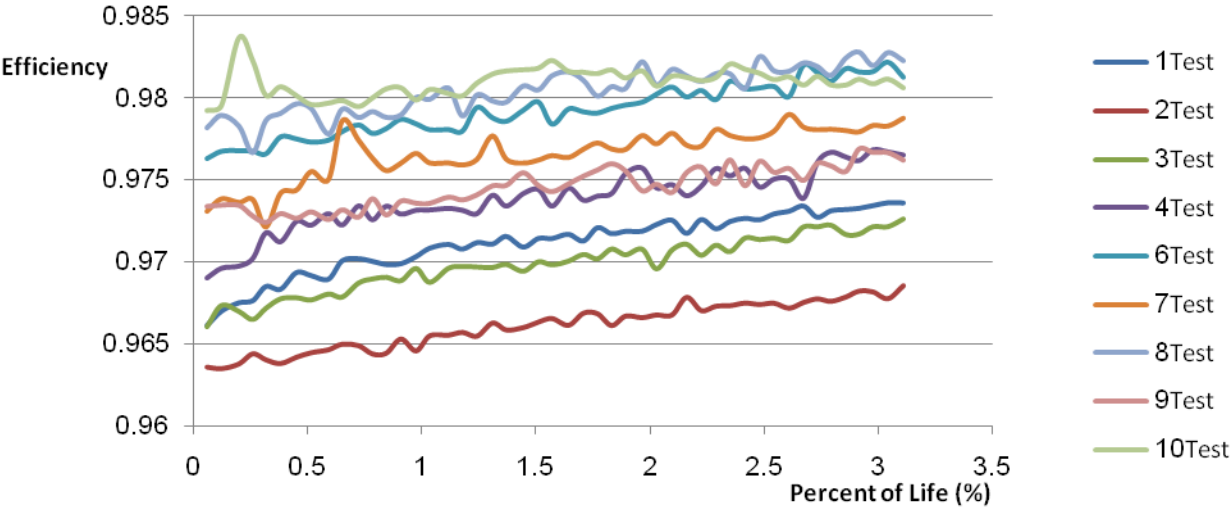


Figure 44. Efficiency curve of ten tests performed by AC Tools. The first 3 PoL of the gears, 50 Nm and 60 rpm . The horizontal axis is presenting the PoL and the vertical axis is presenting the efficiency of the gear set.

The AC Tools tests show a difference in the level of the efficiency value, but as it is shown in Figure 44, they are all following the same positive slop comparing to Figure 43 which shows a fast raise and then a drop of efficiency after 1 PoL. This fact can be due to the damage from tip contact of the pinion and failure of the lubricant layer which could be seen from the burn marks on the gear flank. To show the increasing temperature, Figure 45 presents the stable torque scattering diagram.

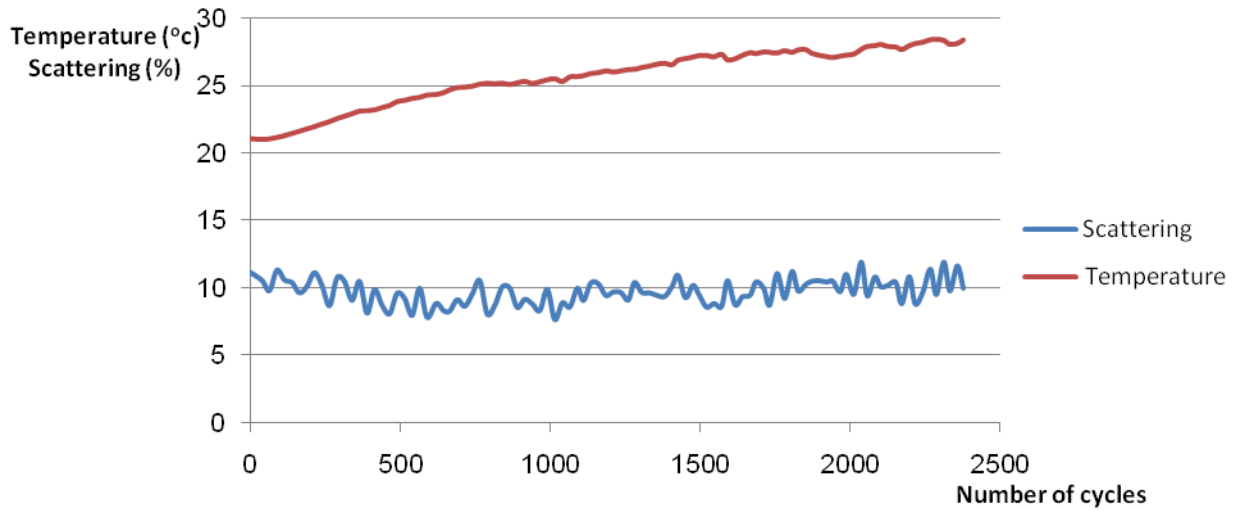


Figure 45. Grease bulk temperature and scattering of transmitted torque (transmission error)

Due to the results of Pretest I, the low level of speed parameter, which was supposed to be 30 rpm, was changed to 60 rpm for the main test plan.

#### 4.1.2 Pretest II

Figure 46 shows the tooth and the contact region of the gear tooth flank in Pretest II. Comparing this picture with Figure 39 there is no deep wear marks and no burn mark left from lubricant failure. The gear in Figure 46 has been running for all the steps shown in

Table 3. The torque has been gradually increased during the process, starting at 10 Nm and continuing at 20, 30 and 40 Nm. All the torque steps had an equal number of cycles (not equal PoL), but different speed. In Figure 46 still some scuffing marks can be seen on the dedendum area (shown as number 1 in the picture) which is not as deep as the ones in Pretest I. In Figure 47 the pinion tooth is shown.

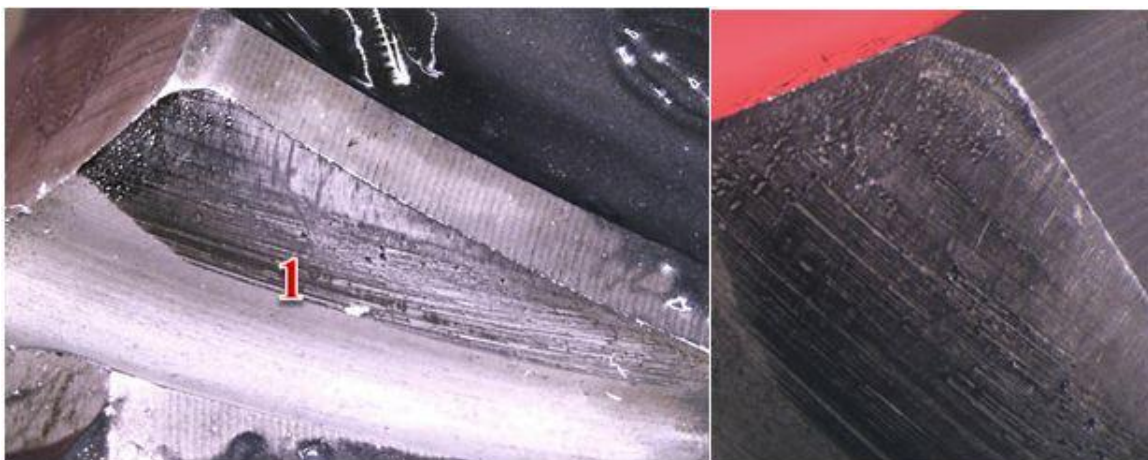


Figure 46. Pretest II, gear flank after the full running-in procedure of 11 PoL Step loading and step speed

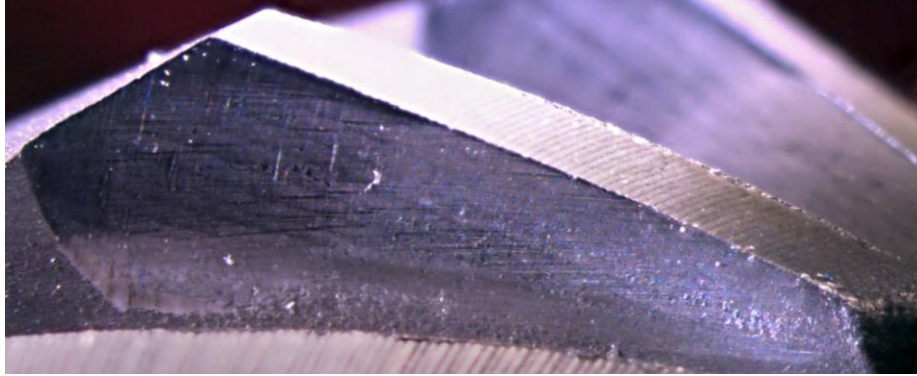


Figure 47. Pinion tooth after first step of *Pretest II*. (11 PoL, step loading, step speed)

The surface roughness values for the gear and the pinion before and after running-in are presented in Figure 48 and Figure 49, respectively. These figures show how the  $R$  values are changing in the contact region, note that the high pressure contact region is on the heel area of the gear tooth and similarly at the heel area of the pinion tooth. Comparing Figure 41 and Figure 48 for the gear tooth  $R$  values, and Figure 42 and Figure 49 for the pinion tooth  $R$  values, it is noticeable that  $R_a$ ,  $R_q$  and  $R_p$  values are more even at different positions on the contacting area. These results can be also found in Appendix B.

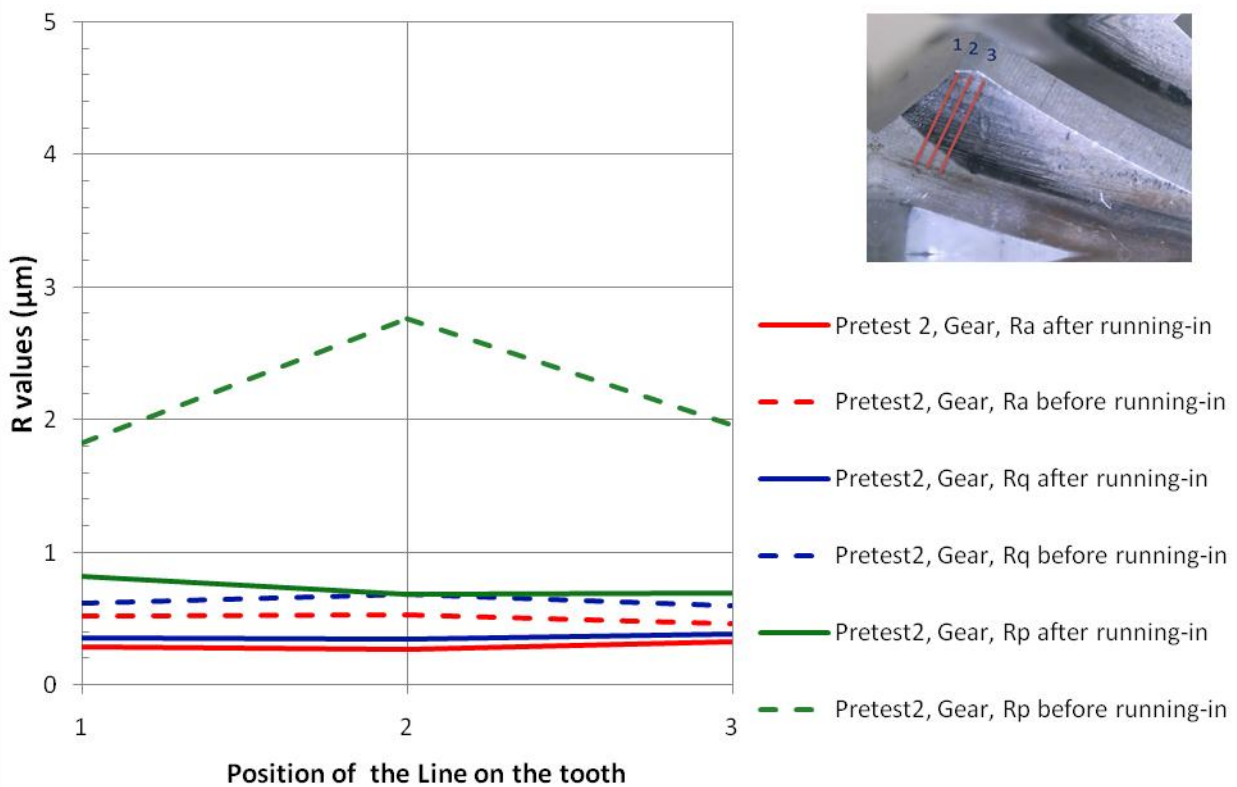


Figure 48. Roughness values on the gear tooth, *Pretest II*. The horizontal axis is presenting the position of 2D measurement on the gear tooth flank and the vertical axis is presenting  $R_a$ ,  $R_q$  and  $R_p$  values in  $\mu\text{m}$ .



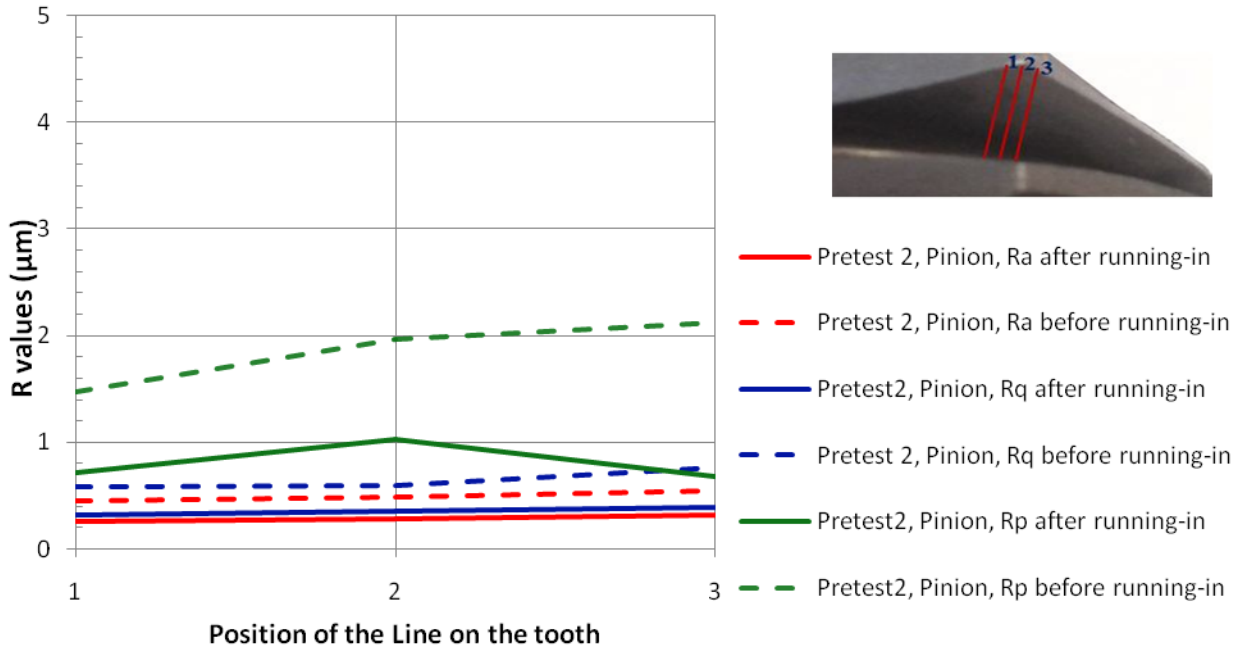


Figure 49. Roughness values on pinion tooth, *Pretest II*. The horizontal axis is presenting the position of 2D measurement on the pinion tooth flank and the vertical axis is presenting  $R_a$ ,  $R_q$  and  $R_p$  values in  $\mu\text{m}$ .

The test rig data for pretest II is presented in the Figure 50. An increase in the level of efficiency can be seen between step one and step two of the running-in process. This change in level of the efficiency happens in all the tests which are followed by different torque (loading) steps, regardless of the speed parameter. As shown in Figure 51, as the torque level is changed from 10 to 20 Nm, the efficiency increases and the torque deviation is reduced. From Figure 50 it can be seen that there is no efficiency level change between step two and step three which have been loaded by a torque of 20 Nm and 30 Nm, respectively. From step three to step four, or 30 Nm to 40 Nm, a reduction in efficiency level occurs, which can be due to the shifting of contact region on the gear tooth from toe to heel for higher torques.

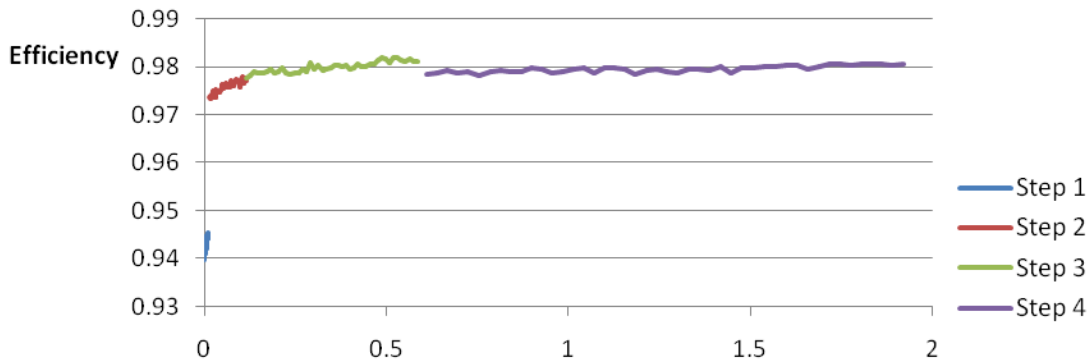


Figure 50. Efficiency curve for *Pretest II* equal number of cycles in each load step (10 Nm and 90 rpm, 20 Nm and 78 rpm, 30 Nm and 66 rpm, 40 Nm and 60 rpm) resulting in different PoL for each load step. The horizontal axis is presenting PoL and the vertical axis is presenting the efficiency of the gear set.

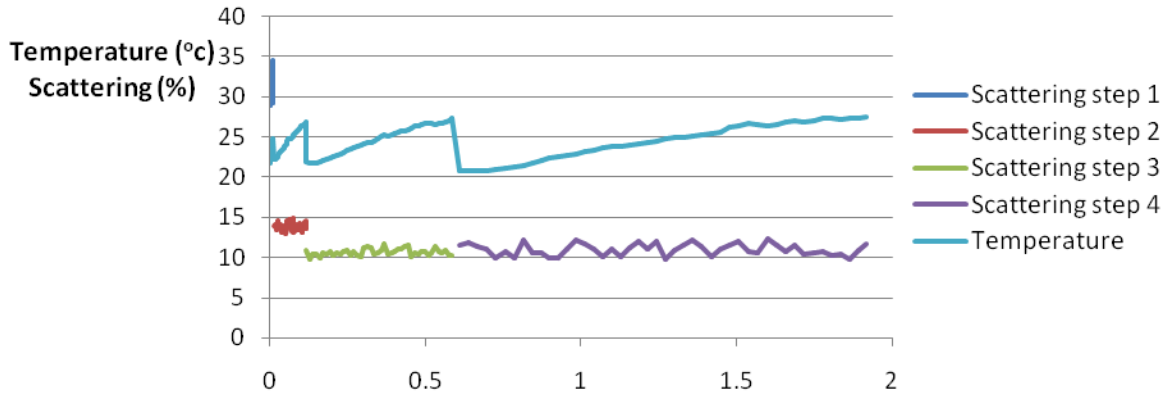


Figure 51. Deviation of the transmitted torque (transmission error) and temperature, PoL on the abscissa

## 4.2 Main tests

After the pretests and analyses of the data and learning the capabilities of the test rig, the full factorial design was decided, as presented in Table 7, with three parameters; PoL, speed, and early re-lubrication in the first few cycles. But later on, due to the time limits and some test rig problems, the test schedule was reduced to a two-factor full factorial design with the design factors speed and early re-lubrication with a low and a high level for each parameter, hence the PoL factor has been chosen as a constant parameter of 1% for all five loading steps as presented in the following expression. The performed experiment is presented in Table 9.

Loading procedure during all test-setups=

$$\text{load step 1} + \text{load step 2} + \text{load step 3} + \text{load step 4} + \text{load step 5} \quad (16)$$

Table 9. Two factor full factorial design

Test Setup	Design parameters			Responses			
	PoL (%)	Speed (rpm)	Re-lubrication	Life ratio	$R_a(\sigma_a)$	$R_q$	$R_p$
1	1	60	Un-changed				
2	1	60	Changed				
3	1	120	Un-changed				
4	1	120	Changed				

For each test setup, two repetitions have been performed. The test schedule has been followed by

one test of each test setup (first repetition) and then the second repetition have been done. In the gap between the first repetition and the second repetition, the test rig has been through an accident which made the torque transducers to lose their calibration. Once the re-calibration was done and the test rig came to work, the run-in gears were tested for life. Studying the data from life tests has shown that more calibration of the test rig is necessary. The life test data has been modified according to the test rig calibration coefficients.

After the first repetitions of the test setups, the second repetition was started. Based on an analysis of the data and photos from the first repetition, the testing process was changed as:

1. Due to time limits, surface measurements and photos after each load step and 3D measurements were skipped. After finishing the running-in process, 2D measurements were performed and the contact region was captured by the microscope.
2. Because the contact area is mostly concentrated to the heel region, six line roughness measurements (Figure 27) were used to determine which of the running-in setups that can shift the contact area towards the toe region.
3. As a result of the test rig accident and recalibration of the torque transducers, the value of the efficiency was not comparable to the ones before the accident. So it was decided to study the slope of efficiency increase, i.e., the trend, rather than the efficiency value.
4. Since for the first repetitions in the life test the torque transducers were out of calibration, the actual torque which were applied for the life test was 54 Nm instead of 50 Nm. This has changed the life of the gears so another parameter was used instead, which is referred to as “Life Ratio” in Table 9. This factor is simply the life of the gears divided by the Wöhler life for the same torque value ( $L_{50}$ ).

The torque (load) steps to be followed were decided as shown in Table 10. As mentioned before, all the test specimens have passed all the loading steps (one to five). After completion of step five, a final re-greasing was done, which is defined as the running-in process.

Table 10. Loading steps and the number of cycles

	Step 1	Step 2	Step 3	Step 4	Step 5
Load (Nm)	10	20	30	40	50
PoL (%)	0.2	0.2	0.2	0.2	0.2

#### 4.2.1 Results of 1<sup>st</sup> repetitions

In Table 11, pictures from the first repetition of each test setup are shown for comparison. The pictures were taken after each loading step (during the running-in process). These pictures indicate how the contact area shifts in position according to load and/or rotational speed. Test-set 3 and test-set 4 are the ones subjected to re-lubrication after the first half of the first load step was passed (0.1% of life in 10Nm). In Table 11 “step” stands for loading step.

Table 11. Photos after each loading step , comparison of different test setups , repetition 1

	Test-set 1 (60 rpm)	Test-set 2 (120 rpm)	Test-set 3 (60 rpm)	Test-set 4 (120 rpm)
Step 1 (10 Nm)				
Step 2 (20 Nm)				
Step 3 (30 Nm)				
Step 4 (40 Nm)				
Step 5 (50 Nm)				

\*The deep marks on the heel area are marks from deburring process during manufacturing

Comparing the loading steps, it can be observed that when increasing the load from 10-50 Nm, the contact region moves from the root towards the tip of the tooth. At a speed increase the gear contact pattern is shifting towards the heel tip. It should be noted that ANSOL does not show any change in the contact pattern due to a change in speed.

As each test specimen was subjected to a 2D surface roughness study, the comparison of the results are presented as follows by comparing the new gear  $R$  values and the gear  $R$  values after each loading step. As said before, the  $R$  values have been measured after each step of loading and following the 3 Line measurements for the first repetitions. (Figure 52 to Figure 55)

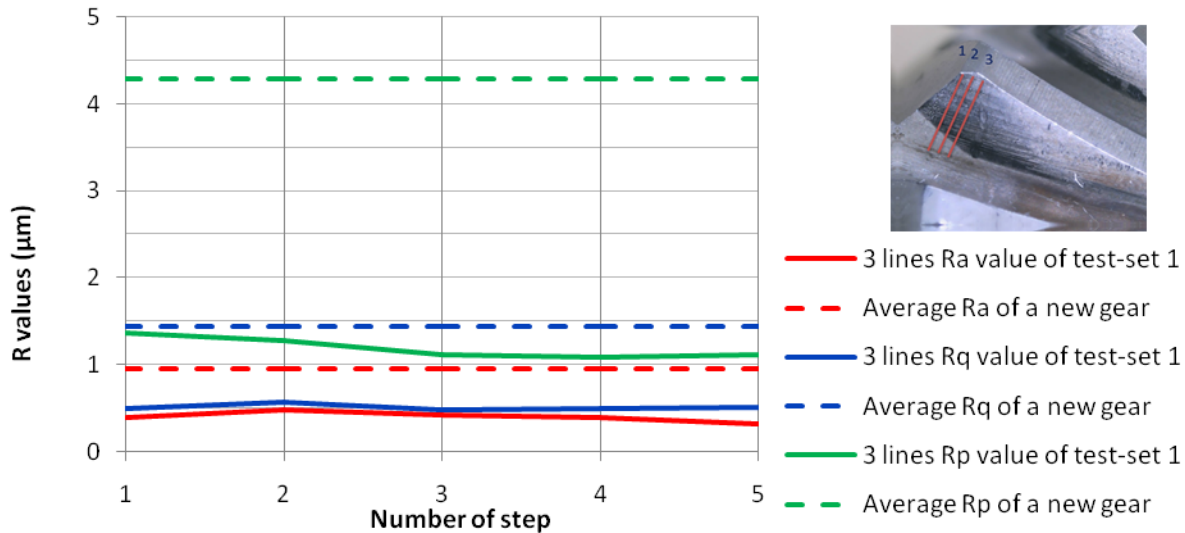


Figure 52. 3 Line  $R$  values of the gear flank in test-set 1, repetition 1 versus load step number

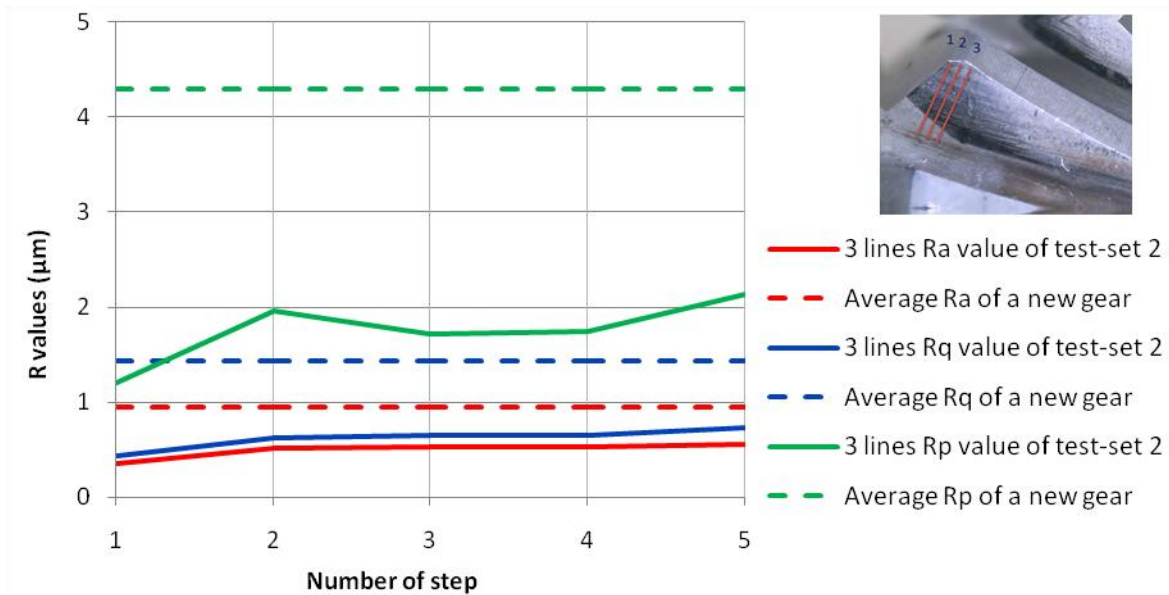


Figure 53. 3 Line  $R$  values of the gear flank in test-set 2, repetition 1 versus load step number

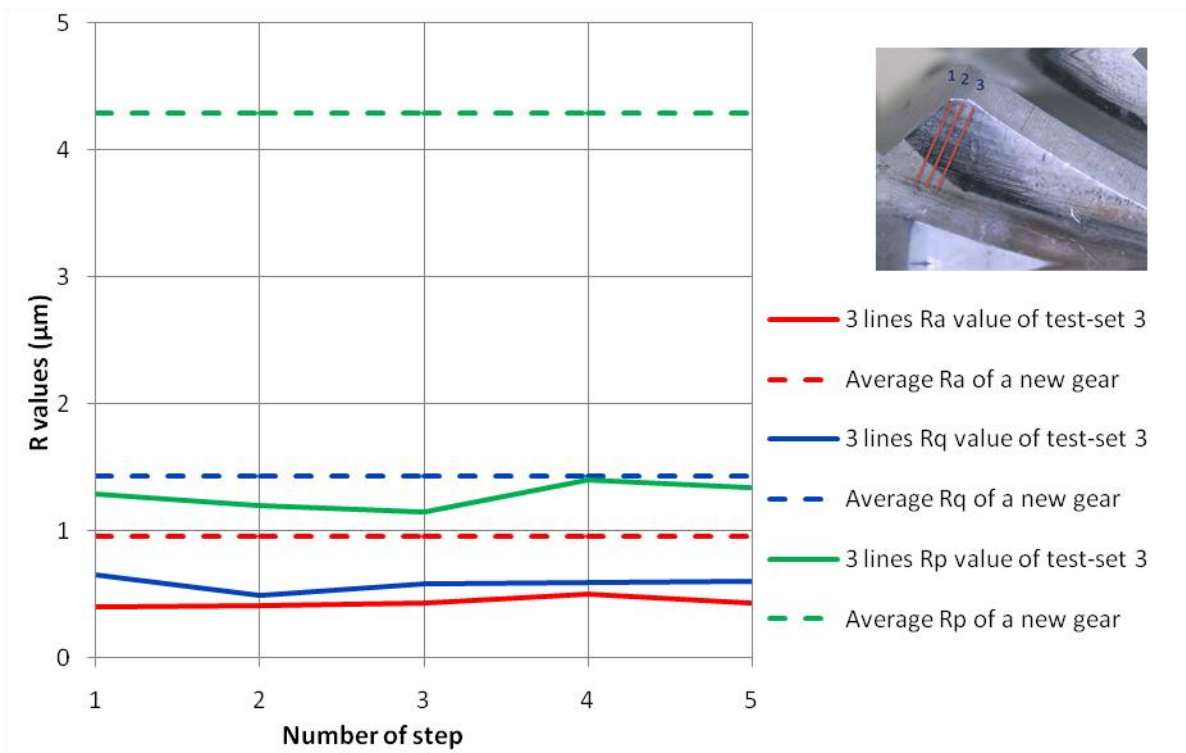


Figure 54. 3 Line  $R$  values of the gear flank in test-set 3, repetition 1 versus load step number

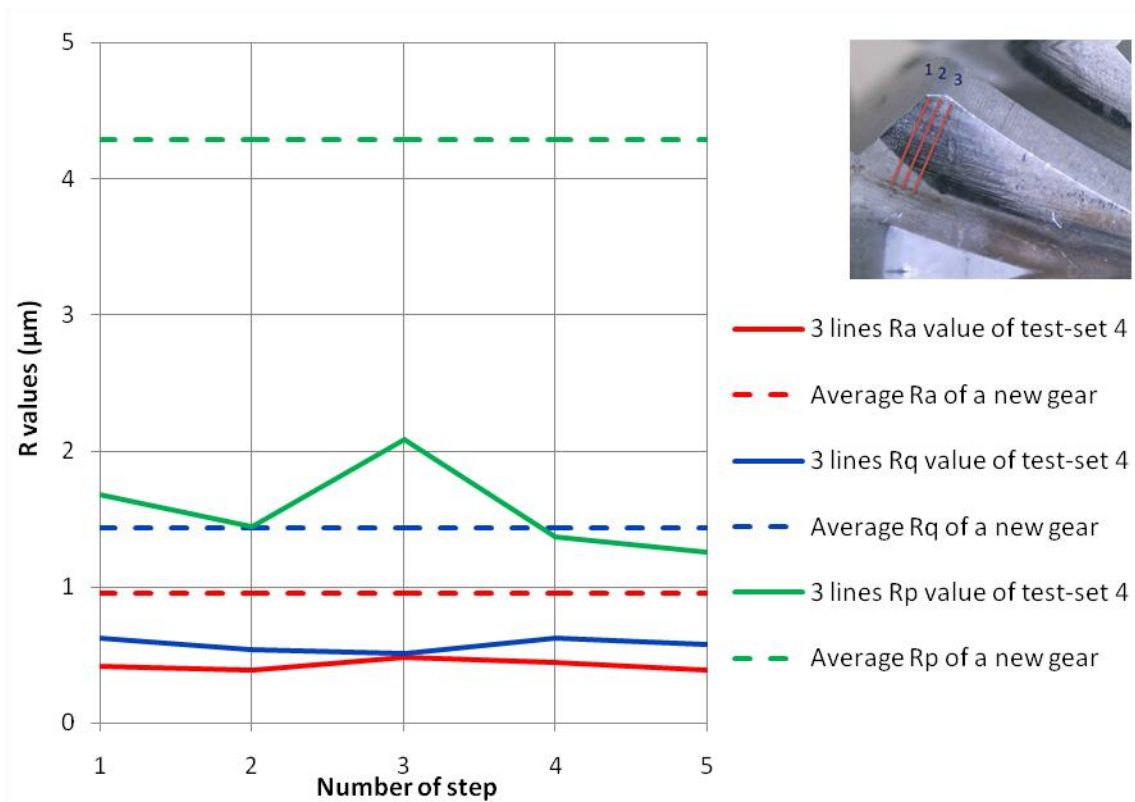


Figure 55. 3 Line  $R$  values of the gear flank in test-set 4, repetition 1 versus load step number

According to Figure 52 to Figure 55 after step 1, the roughness value,  $R_a$ , was reduced to more than 50% of the roughness of the new gear surface and by looking at  $R_q$  values, it can be said that test 1 has a more evenly distributed surface roughness. For test 1 and test3,  $R_p$  values of the new gear flank have been reduced by 50 to 70% which can result in a better lubrication condition.

For the presented measurements, the ISO 1997 standard was used for the R profile with a Gaussian filter and a cut-off parameter of 0.8 mm.

On the 3D measurements, it should be noted that, as shown in Figure 26, the measured area is too small ( $0.5 \times 0.5 \text{ mm}^2$ ). Although the gears are not identical, the first few measured teeth have shown that for new gears, the data is the same with a high accuracy. Knowing this, just one of the gears was chosen to be measured (on three teeth) while the gear was still new, and the data is used as reference data for a new gear tooth. Moreover, a model of the teeth has been made using replica technique and it has been kept to be used in case of any future needs.

The goal during the measurements was to capture the same area for the gears and the teeth. The same setting was used during measurements according to the EUR15178N report, Flatness parameters ISO 12781, Gaussian filter cutoff 0.8mm and order 12 of the polynomial was used for form removal. The measurement results and the new gear surface measurements are shown in Figure 56 to Figure 60.

According to the 3D measurement results, test 4 has the smallest surface roughness, the  $S_a$  value, but Figure 60 shows the sliding marks left from running-in procedure (sliding and milling directions are shown in the pictures). An abrasive scratch mark can be seen in Figure 58 where no early re-lubrication was done. The measurement results are presented as numbers and values in Appendix C.3.

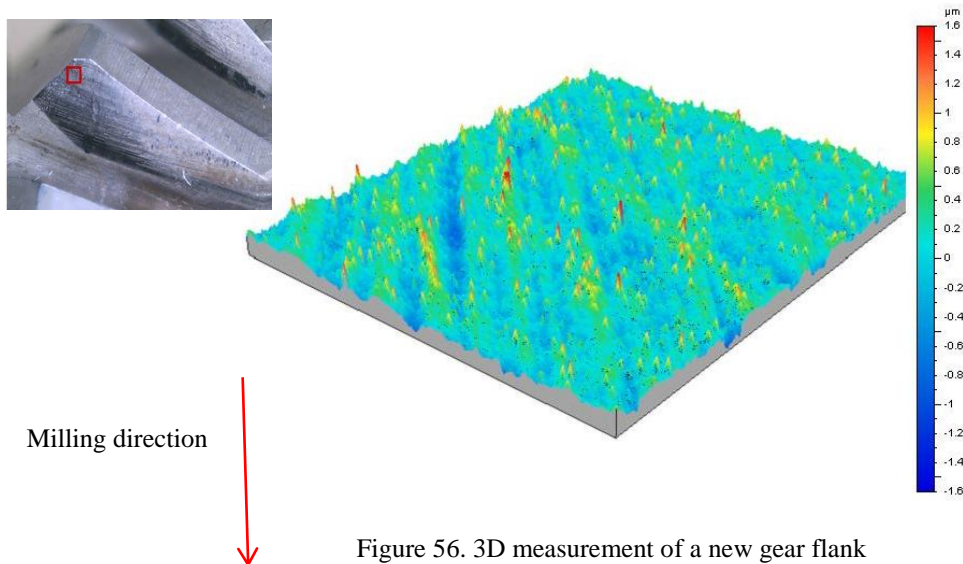


Figure 56. 3D measurement of a new gear flank

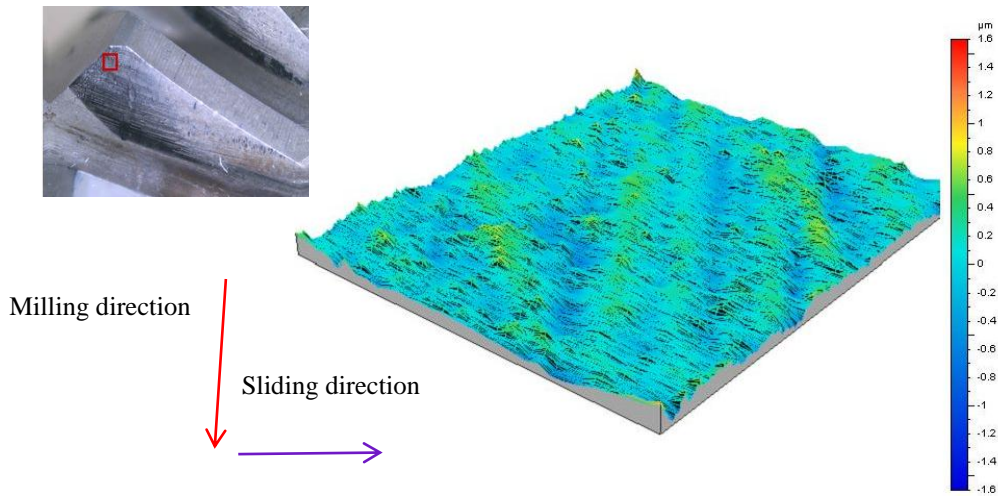


Figure 57. 3D measurements of the gear flank after running-in test-set 1

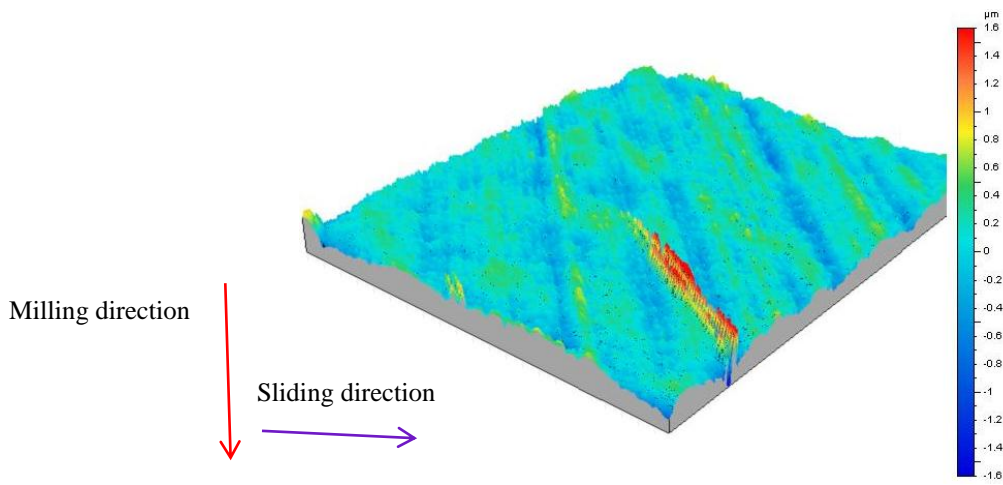


Figure 58. 3D measurements of the gear flank after running-in test-set 2

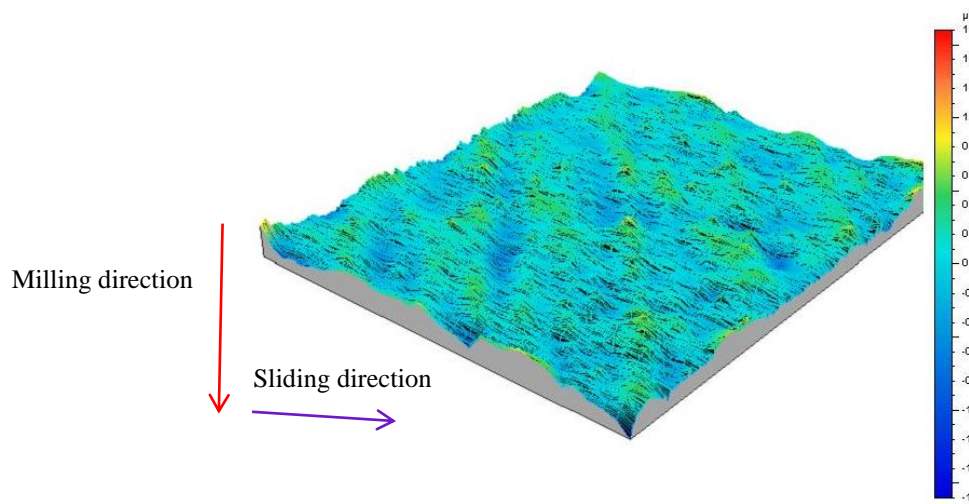


Figure 59. 3D measurements of the gear flank after running-in test-set 3



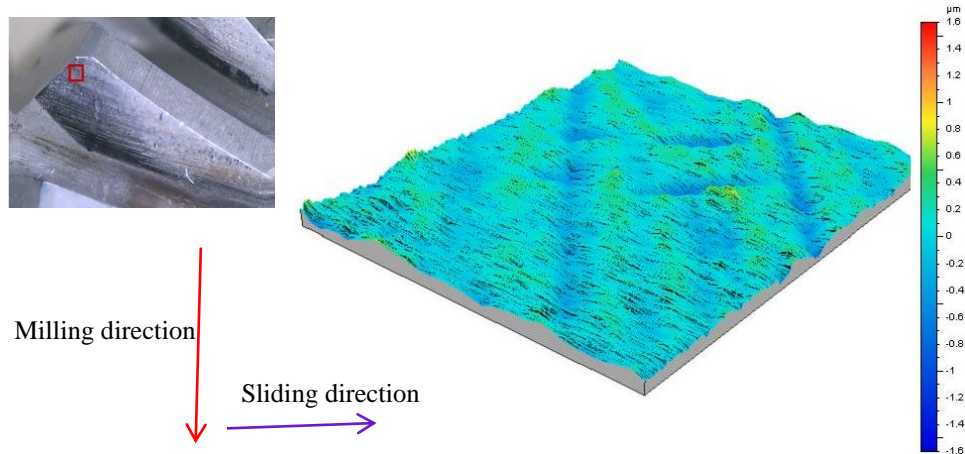


Figure 60. 3D measurements of the gear flank after running-in test-set 4

Since all the efficiency curves and all of the curves for the deviation of the transferred torque are following the same path and form, they are not presented in Appendix D. Table 12 and Table 13 present the results of the running-in procedure and the life test. Table 12 presents the EffR (the efficiency increase due to the running-in process), EffL (efficiency increase over the life test process), and EffS (the slope of increasing efficiency in the beginning of the life test). In Table 13 the life ratio of the tested gears can be seen.

As shown in Table 13, the life ratio of test-sets 2 and 4, with a high speed factor of 120 rpm, show a high life ratio, and the two other tests, with low speed factors, both show a low life ratio. Later these results are compared with results of the 2<sup>nd</sup> repetitions. For test 3, the failure mode according to AC Tools was different, the failure for AC Tools is a surface failure of the tooth flank, but the gear tested in test 3 has failed due to brakeage of the tooth tip.

Table 12. Efficiency increase during running-in, 1<sup>st</sup> repetitions

Test-set (Repetition)	EffR(%)	EffL(%)	EffS (°)
1 (1 <sup>st</sup> )	2.11	0.72	0.0165
2 (1 <sup>st</sup> )	2.16	0.86	0.0198
3 (1 <sup>st</sup> )	0.81	1.04	0.0297
4 (1 <sup>st</sup> )	0.45	0.68	0.0196

Table 13. Life ratio of the 1<sup>st</sup> repetitions


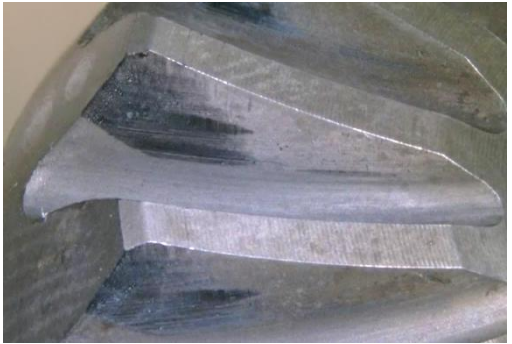


Test-set (Repetition)	Torque used for life test (Nm)	Life Ratio
1 (1 <sup>st</sup> )	54	1.18
2 (1 <sup>st</sup> )	54	1.67
3 (1 <sup>st</sup> )	54	1.19
4 (1 <sup>st</sup> )	54	1.72

## 4.2.2 Results of 2<sup>nd</sup> repetitions

The 2<sup>nd</sup> repetition of the tests was performed after re-calibration of the torque transducers, so the results from the test rig differ from the 1<sup>st</sup> repetitions due to the errors and change of calibration.

For the 2<sup>nd</sup> repetition of the test setups, photos, as shown in Table 14, were taken only after the fifth loading step (after the running-in had finished).

Table 14. Photos after the fifth loading step, comparison of different test setups, 2<sup>nd</sup> repetitions

	60 rpm	120 rpm
No re-lubrication	 <p>Figure 61. Test-set 1, 2<sup>nd</sup> repetition</p>	 <p>Figure 62. Test-set 2, 2<sup>nd</sup> repetition</p>
Re-lubricated	 <p>Figure 63. Test-set 3, 2<sup>nd</sup> repetition</p>	 <p>Figure 64. Test-set 4, 2<sup>nd</sup> repetition</p>

As can be seen in the pictures from tests 1 and 4, a contact mark can be seen close to the root in the toe region. In Figure 62, test 2, some sliding marks can be seen on the pitch line. Such marks were not observed in the other tests, during the 1<sup>st</sup> and 2<sup>nd</sup> repetitions

It was explained above that no contact or low contact on the toe area was observed during the 1<sup>st</sup> repetitions, and hence the 2D measurement strategy was changed from 3Line measurements to 6Line (explained in Chapter 3.1.1.2). The results are presented in Figure 65 to Figure 68.

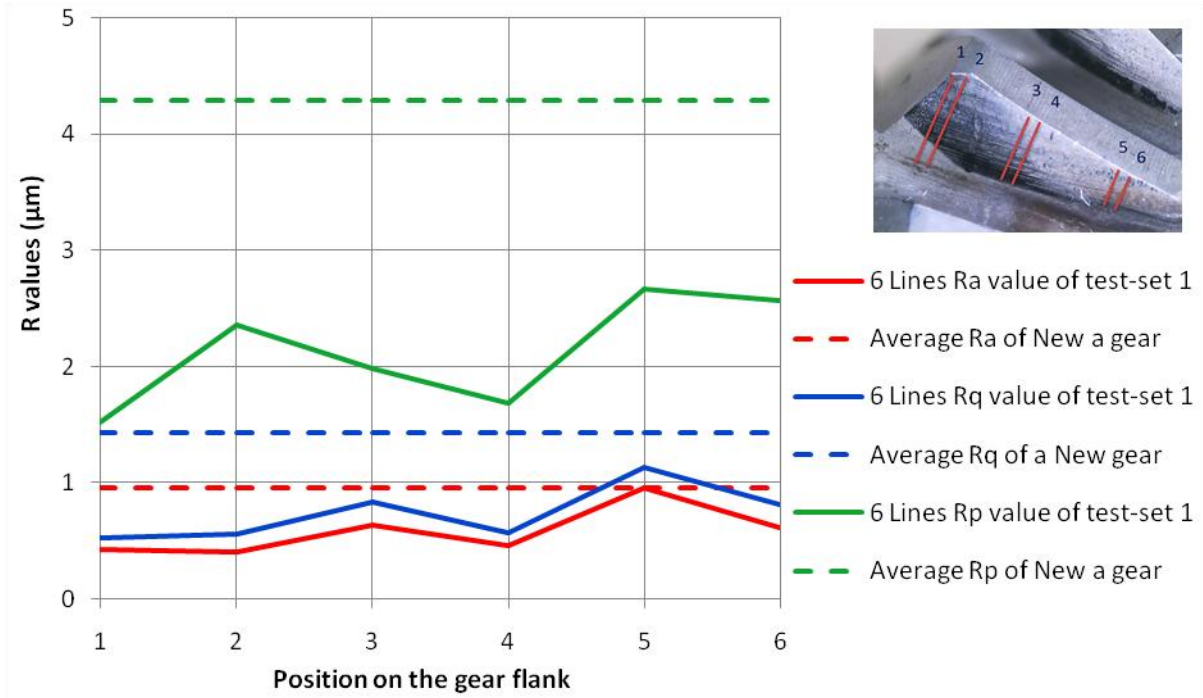


Figure 65. 6 Line  $R$  values of the gear flank in test-set 1, repetition 2, along the gear tooth flank (heel to toe)

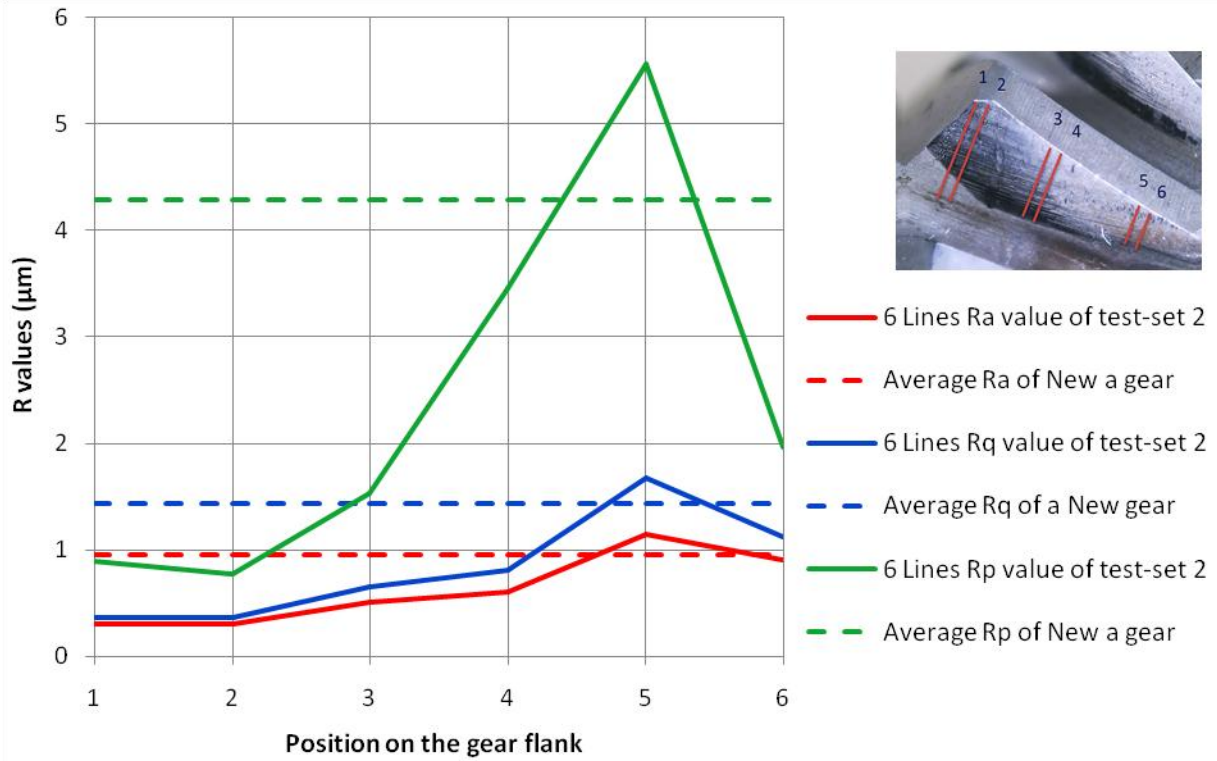


Figure 66. 6 Line  $R$  values of the gear flank in test-set 2, repetition 2, along the gear tooth flank (heel to toe)

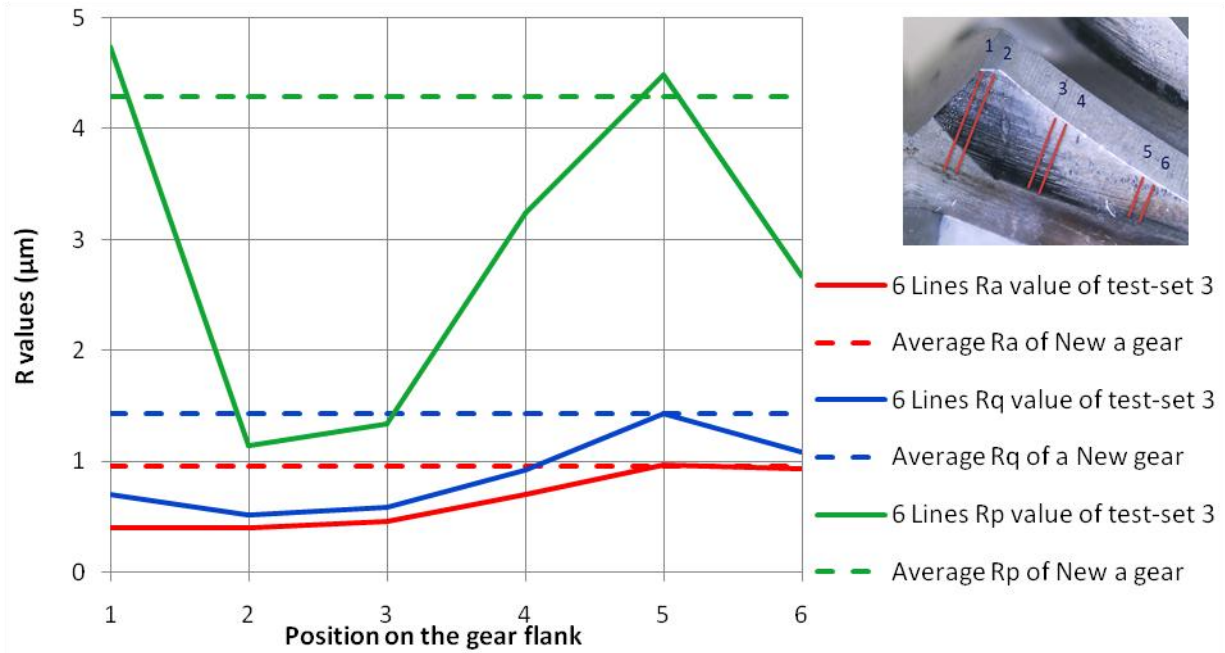


Figure 67. 6 Line  $R$  values of the gear flank in test-set 3, repetition 2, along the gear tooth flank (heel to toe)

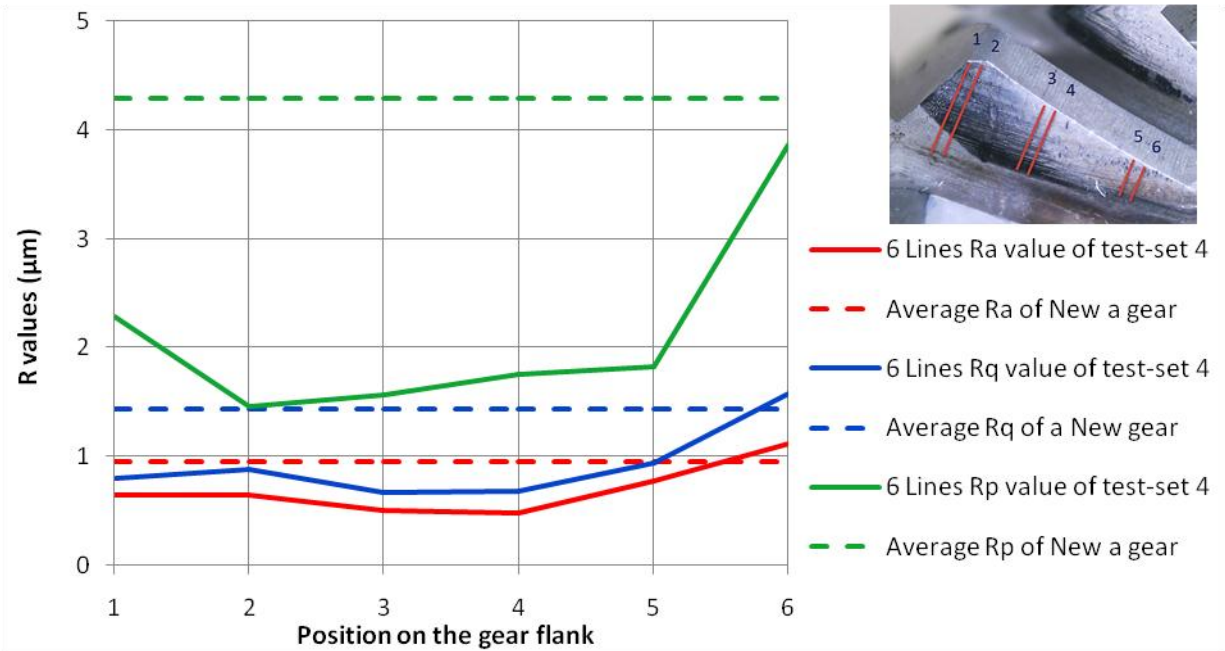


Figure 68. 6 Line  $R$  values of the gear flank in test-set 4, repetition 2, along the gear tooth flank (heel to toe)

According to the figures above for test 2 and test 3, the maximum peak value does not show any reduction. For test 4, the peak value has been reduced up to line 5 and line 6, i.e. the line closest to the toe, has kept its maximum pick value, while for test 1 a reduction in the peak value can be seen for all the measured lines as for line 5 and line 6. Test set 1 was done at 60 rpm and with no re-lubricating, while test set 4 was done with 120 rpm speed and re-lubrication.

Table 15 and Table 16 present test rig results of the running-in procedure and the life test.

Table 15. Efficiency increase during running-in, 2<sup>nd</sup> repetition

Test-set (Repetition)	EffR (%)	EffL (%)	EffS (°)
1 (2 <sup>nd</sup> )	0.18	0.59	0.0170
2 (2 <sup>nd</sup> )	2.78	0.91	0.0209
3 (2 <sup>nd</sup> )	2.48	0.65	0.0313
4 (2 <sup>nd</sup> )	2.35	0.67	0.0322

Table 16. Life ratio of the 2<sup>nd</sup> repetitions

Test-set (Repetition)	Torque used for life test (Nm)	Life Ratio
1 (2 <sup>nd</sup> )	50	1.75
2 (2 <sup>nd</sup> )	50	1.30
3 (2 <sup>nd</sup> )	50	1.44
4 (2 <sup>nd</sup> )	50	1.31

For the 2<sup>nd</sup> repetition of the tests, the best life ratio was found for the test 1 and test 3, which both had a running-in procedure with a speed of 60 rpm. It should be noted, that test 2 was stopped before reaching the life test by definition of AC Tools, and it should be noted that during the running-in procedure, in first step of loading, this specimen showed some errors regarding torque deviation.

#### 4.2.3 Optimization of design parameters versus life ratio

As the main result of this work, relations between design parameters and life ratio is presented in Table 17, Table 18 and Figure 69. Instead of number of cycles during the life test, life ratio has been studied due to miss-calibration of the test rig. The so called miss-calibration of the test rig caused the torque transducers to show lower torque values (50 Nm) than the actually applied torque (54 Nm). Test-sets 2 and 4 are both show a high life ratio for the first repetitions that were subjected to 54 Nm torque during the life test.

In Table 17, the loading torque of the life test and the resultant life ratio are shown for each test set and its repetitions. In addition, the mean ( $m$ ) and standard deviation ( $\sigma$ ) of the life ratio and alsoof the calculated signal-to-noise ratio (SNR) are presented.

To calculate the signal-to-noise ratio for a higher response (mean value) and smaller noise effect (standard deviation) a strategy shown in Equation 17 was used.

$$SNR = 20\log\left(\frac{m}{\sigma}\right) \quad (17)$$

According to the results presented in Table 17, Test set 3 is the most robust test set, although considering the optimization facts, test set 2 is the more optimal and robust one with the second best SNR and the best mean value for the life ratio.

Table 17. Life ratio for each test-set and the design parameters

			Load	LR	m	$\sigma$	SNR
Set 1	60rpm & No re-lubrication	R1	54	1.18	1.46	0.40	11.23
		R2	50	1.75			
Set 2	120rpm & No re-lubrication	R1	54	1.67	1.48	0.26	15.02
		R2	50	1.30			
Set 3	60rpm--& Re-lubricated	R1	54	1.19	1.32	0.18	17.28
		R2	50	1.44			
Set 4	120rpm-& Re-lubricated	R1	54	1.72	1.52	0.27	14.39
		R2	50	1.31			

Table 18. Mean and standard deviation of life ratio according to the design parameters

	Speed			Re-lubrication			Interaction factor Speed*Re-lubrication		
	Test sets	m	$\sigma$	Test sets	m	$\sigma$	Test sets	m	$\sigma$
Low Level	Test 1 &3	1.39	0.27	Test 1 &2	1.48	0.28	Test 2 &2	1.40	0.21
High Level	Test 2 &4	1.50	0.23	Test 3&4	1.42	0.23	Test 1 &4	1.49	0.29
Effect		0.11			-0.06			0.09	

The table above, Table 18, presents the effect of each design parameter, by comparing the high and low level response of each parameter and the result of the interaction of the design parameters.

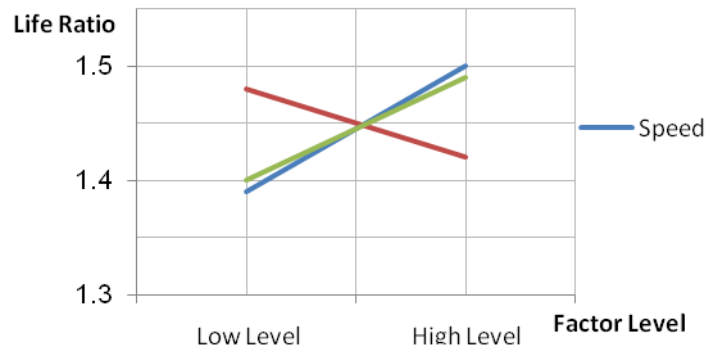


Figure 69. Effects of design parameters on life ratio

According to Table 18, the speed factor has the most statistically significant effect on the test results, which means changing the speed will affect the test results more than grease and the interaction factor.

#### 4.2.5 Study the effect of efficiency increase on life ratio

As mentioned before, the increase of efficiency during running-in and life test and the slope of the efficiency increase are parts of the studied responses.

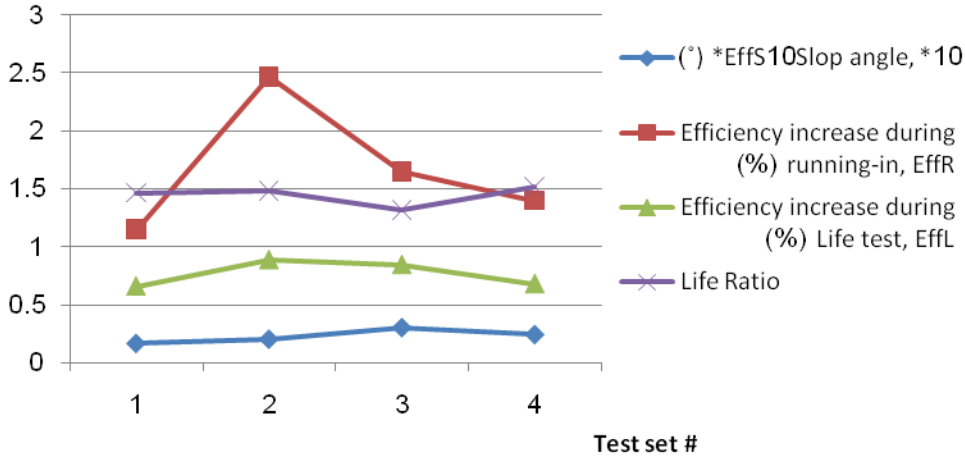


Figure 70 shows the average EffR, EffL and EffS and also the life ratio of the tested gears.

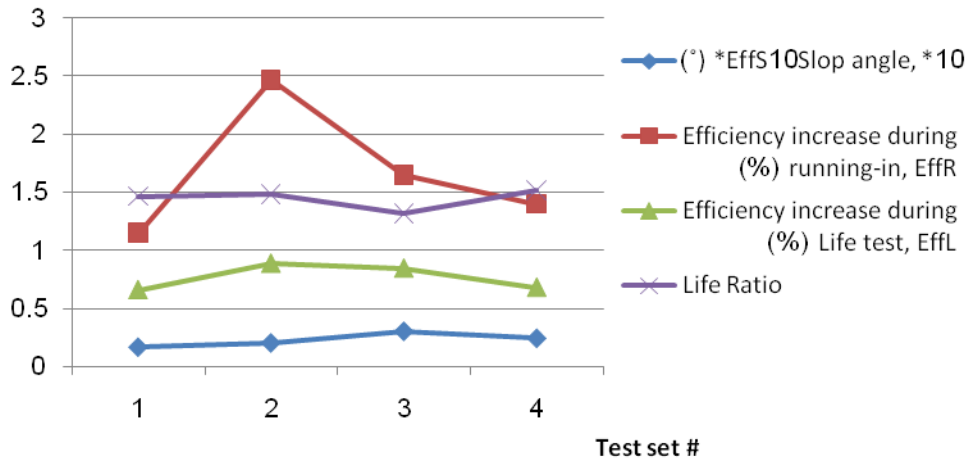


Figure 70. Comparing the average life ratio for each test setup with EffR, EffL and EffS

The diagram shows, that the life ratio (purple curve) has an inverse relation to EffS (blue curve) which actually presents the increasing rate of efficiency during the life test. This correlates to the fact that the slower the efficiency increases, the longer the gear will last. In other words, the slower the wear rate, the longer the part will last.

#### 4.2.6 Speed factor and contact region

Comparing the photos (Table 11) with the speed factor it can be noticed that for 120 rpm the contact region is shifting towards the tooth tip. A sketch has been made to compare the effect of the speed on shifting of contact region (Figure 71).

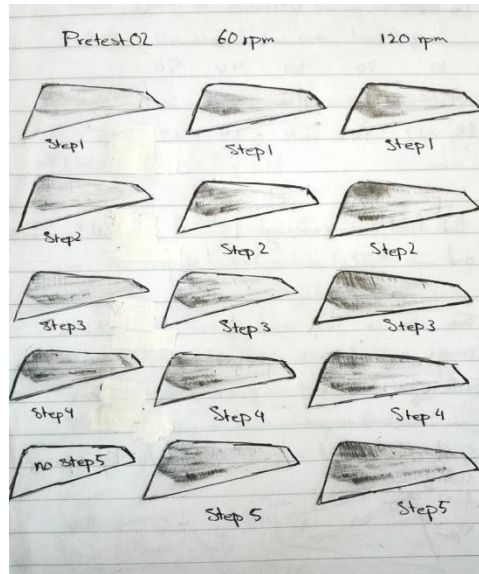


Figure 71. Sketch to compare the effect of high and low speed level

Figure 71 shows that for step one, two, and three in the 60 rpm tests, the contact region did not reach the tip of the tooth, but for tests with 120 rpm the contact region is more close to the tip.

### 4.3 Calculation

The results for the calculated parameters are presented in Figure 72, where ‘ $S$ ’ defines the distance between the meshing point and pitch point (shown in Figure 35). The  $\Lambda$  value for a new gear at the pitch point is 0.0723 and for the gear after running-in it is 0.1265. In Figure 72, the negative  $S$  values show that the calculation has been done for the heel area. from the tip of the gear tooth to the root of the pinion tooth.

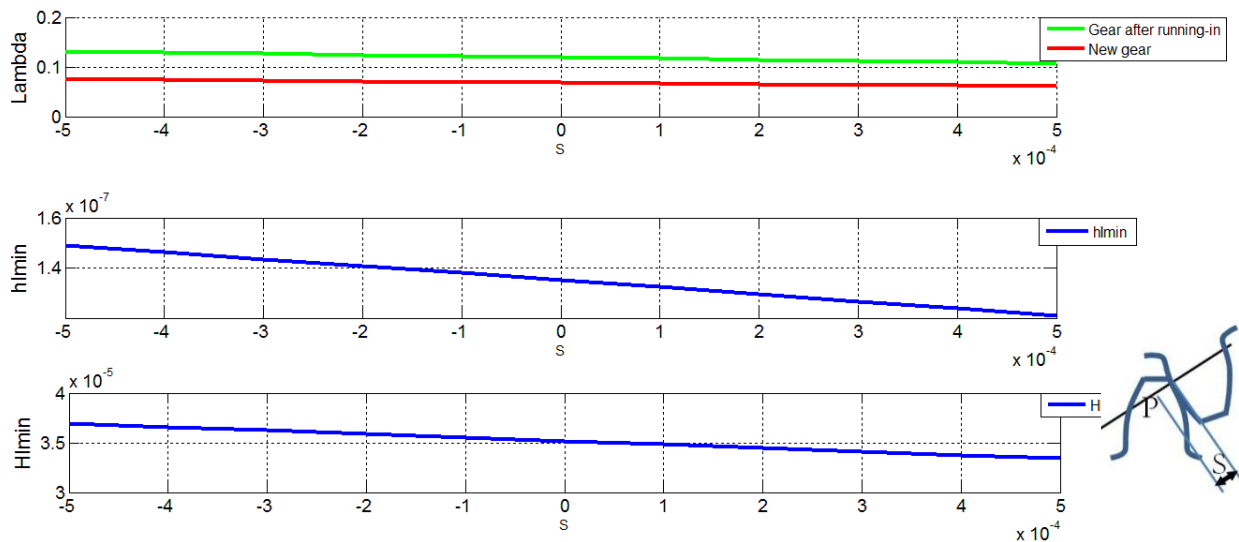


Figure 72.  $H$  (m),  $h$  (m) and  $\Lambda$  value versus  $S$  (m) which is the distance from pitch point (P) on the gear tooth flank to the contact point. The horizontal axes is presenting  $S$ , -0.5 to +0.5 mm of the pitch point.



Knowing the roughness values at the pitch line (for the gear flank before and after running-in), the result can be compared to the diagrams in Figure 11. According to Figure 11, a surface with 0.9  $\mu\text{m}$  roughness ( $R_a$ ) and minimum EHD film thickness of 0.12  $\mu\text{m}$ , is on the border of boundary lubrication and the transition zone to the mix lubrication region. After the running-in procedure, the lubrication region changes towards the mixed lubrication regime; Table 19 defines the lubrication zone for each test setup.

Table 19. Lubrication zone for each test setup according to surface roughness and calculated minimum EHD film thickness

	<i>Roughness (<math>\mu\text{m}</math>)</i>	<i>Lubrication zone</i>
Test set 1	0.4-0.5	Border of transition to the mixed lubrication regime
Test set 2	0.3	Mixed lubrication regime
Test set 3	0.4	Border of transition to the mixed lubrication regime
Test set 4	0.7-0.5	Transition zone between boundary lubrication and mixed lubrication regime

These results match the optimization results as test 2 has the best lubrication condition and it is also the most optimized running-in procedure according to Chapter 4.2.3.

## 4.4 Modeling

The ANSOL HypoidK software was used to study the contact pattern and contact pressure distribution. The gear geometry was made in the Klingelnberg software in the .msh format which can be imported directly to the HypoidK module.

Figure 73 and Figure 74 show the high contact pressure and the contacting area located in the heel region. The maximum contact pressure calculated by HypoidK module is 4.5 GPa which is almost double the capacity of this gear surface/material with a Vickers Hardness (HV) of 700 (equal to a tensile strength of 2.3 GPa), see Figure 75.

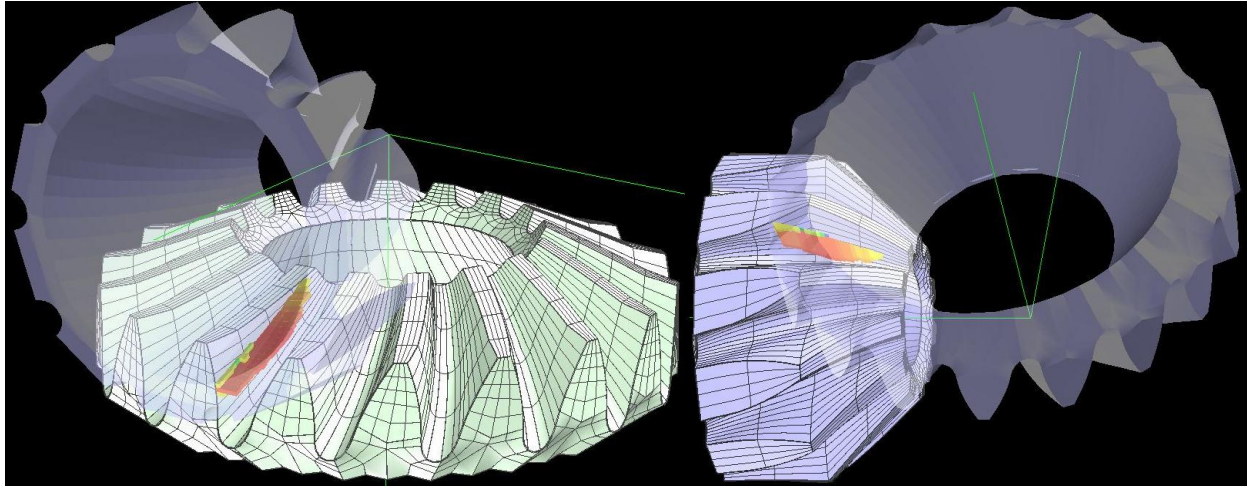


Figure 73. Contact pressure calculation from ANSOL, one tooth in mesh. The contact pressure is fairly distributed but a high contact pressure on the heel edge of the tooth can be seen.

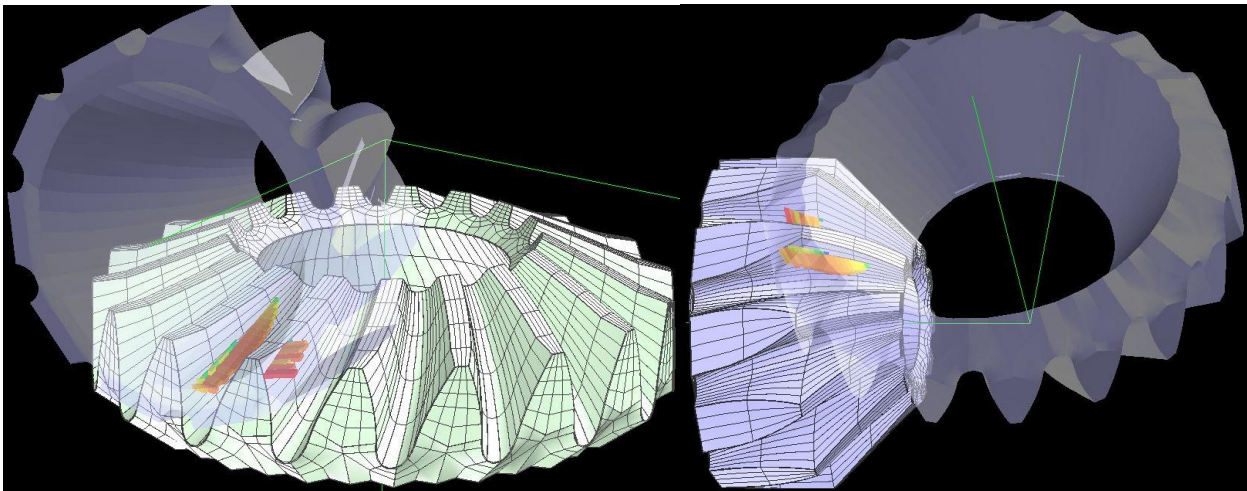


Figure 74. Contact pressure calculation from ANSOL, Edge contact can be seen on the tooth flank. The maximum pressure on the gear tooth flank which is in the beginning of the meshing cycle is on the edge of it and is contacting the dedendum area of the pinion tooth flank.

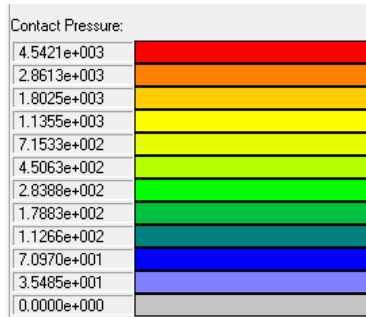


Figure 75. The contact pressure map in  $\text{N/mm}^2$  for Figure 73 and Figure 74, the maximum pressure value is 4.5 GPa

Table 20. the gear geometry model versus the real gear geometry (model simplifications)

	Gear tooth	Pinion tooth
Atlas Copco gear tooth		
The possible mesh file by Klingelberg		

The mesh used for modeling did not have the exact geometry of the gears used by AC Tools but it was the closest to what the Klingelberg software could export as a CAD file. The differences are shown in Table 20. Furthermore, the effects from rim, shaft, and bearings were not modeled.

In Figure 74, the edge contact between the pinion tooth and the gear tooth can be seen. This effect can also be seen in the contact pictures (Table 11 and Table 14), which is caused by a bad edge design of the gear tooth. The model shows that the load is concentrated to the heel area but the torque is carried by a larger area of the gear tooth which does not match with observations made with the microscope. To some extent, this deviation can be explained by the differences between the FE model and the actual gears. In addition, some assembly errors, shaft, bearing, and housing deflections can have important effects on the results.



## 5 DISCUSSION AND CONCLUSIONS

*In this chapter the most important and significant points are noted and discussed.*

### 5.1 Discussion

During the life test of the 1<sup>st</sup> repetitions, it was noted that tests with the high speed level (120 rpm) show a higher life ratio than the low speed level. Comparing results for high and low speed levels, using the same torque, the high speed level shifts the contact more close to the tip of the tooth, due to bending giving a tip contact that has negative effects. But the same effect can be used to manage the running-in process with a lower torque and a higher speed. This shift of the contact zone towards the tip explains the higher life ratio in the 1<sup>st</sup> repetitions for test-set 2 and test-set 4. In test-set 2 and test-set 4, the gears were run-in with the same torque ( maximum 50 Nm) as in test-set 1 and test-set 3 but with a higher speed level. During the life test, the specimens were tested with 54 Nm, hence the specimens which passed running-in with higher speed, showed longer life for higher speed levels.

This can occur due to deflections and bending effects of the rim, shaft, bearings, or the tool housing. The ANSOL software does not show any changes in the contact region due to speed variation of a perfectly assembled gear pair, since the dynamic effects are neglected (only static loading is permitted). This fact alone can show the need for a tolerance stack-up analysis (analyzing the effects of tolerance in assembly) of these tools.

The heel contact pressure on the gear tooth flank is too high which is the reason for the observed edge contact marks on the gear tooth. The simulation in ANSOL (Advanced Numerical SOLution software) shows that the maximum contact pressure in the pinion and gear teeth takes place on the heel (edge of the teeth). In other words it looks like that the gear and pinion teeth are cut in the heel area, right in the contact region where we find the maximum contact pressure, see Figure 76. It should also be noted that the maximum contact pressure is as high as 4.5 GPa.

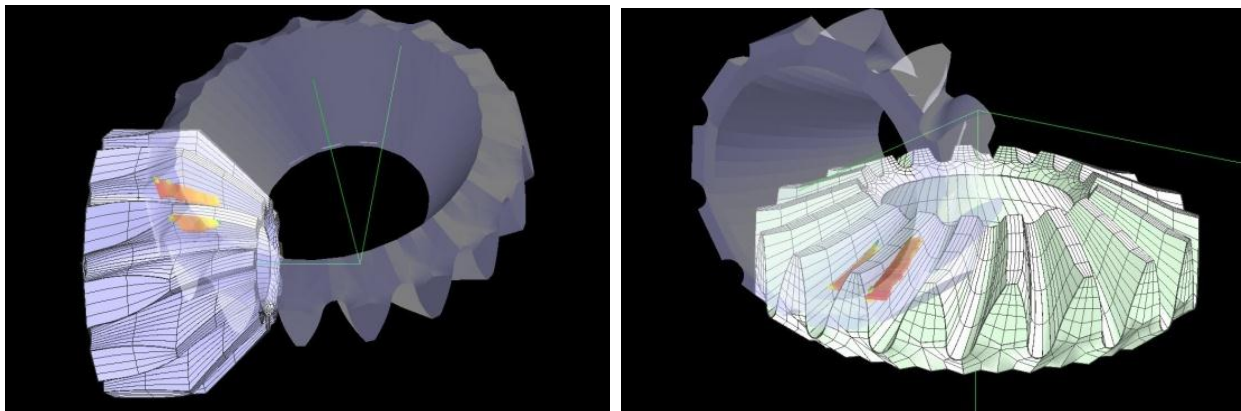


Figure 76. On the left pinion tooth to gear tip contact and the effect of gear heel edge contact on the pinion, and on the right the effect of pinion tooth tip contact and the high contact pressure caused by the gear edge contact, are shown.

Figure 76 can explain the failure type of these gears (Figure 77) which happens in the same area

as the deformation of teeth in Pretests I (Figure 39 and Figure 40), presented in the following figures.

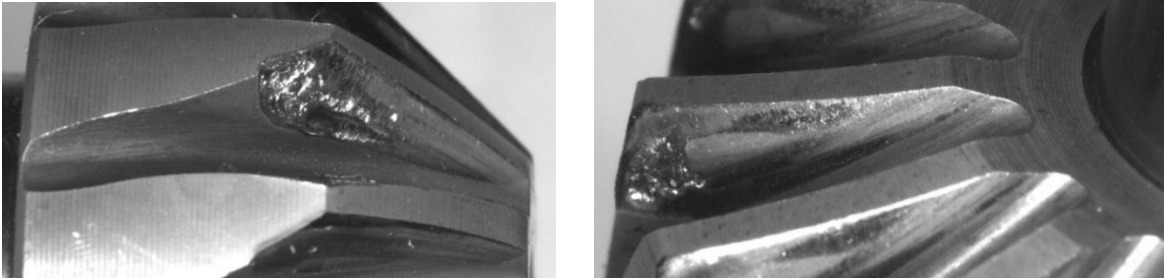


Figure 77. On the left, a pinion tooth which has been running for a while after failure, deformations on tip and heel edge, and scuffing marks in dedendum can be seen. On the right a failed gear tooth with deformations of the tooth edge and pitting in dedendum of the heel region.

The surface roughness of gear tooth flanks have been measured and analyzed. The results showed that the roughness value would remain constant for an increased torque level, but it should also be considered that the gears have been running with the low load for a longer time. So, it has been observed in this study, that a longer time of running with a low torque has larger effects than short running with a high torque.

According to  $R_q$  and  $R_p$  values for test-set 1 and test-set 4 in the 2<sup>nd</sup> repetitions, the contact region is more close to the toe than in test 2 and test 3. These two test-sets are the ones which either both had the high level for both re-lubrication and speed, or the low level of both parameters. These tests have one of the highest life ratio and the least sensitive results. It should also be considered that each test only has two repetitions, which means more investigations are needed to get more reliable results.

Although the  $\Lambda$  value is smaller than the value indicating boundary lubrication (1), a study of the surface roughness and the minimum film thickness predicts a better lubrication condition. The calculations and the study show that with a running-in procedure which reduces the  $R_a$  value by 50%, the lubrication regime will shift to mixed lubrication that will help to extend the gear life, see Figure 11.

During the tests at the highest possible torque and speed the test specimen broke and caused a high shock load to the torque transducers and other elements of the test rig. Due to the failure and problems caused by this accident the efficiency level, results are not comparable for the tests before and after that accident. Re-calibration of the test rig elements has been done but even after re-calibration the calculated efficiency is higher than 100%, an error that is caused by the low accuracy of the torque transducers.

All the running-in tests extended the gear life, but due to time limits different levels of percent of life could not be tested. But, as said before the most optimal and robust test setup is test set 2, with a high speed and no early re-lubrication. This test set up is the one which after analysis of the influence from the roughness in the contact region, showed the best lubrication mode among the whole test setups.

## **5.2 Conclusions**

Studying running-in of a new spiral bevel gear increased the gear life regardless of the running-in method used in this study.

According to the performed tests, an optimized running-in procedure is suggested. The gears which were run by higher speed during running-in tend to last longer. This may be due to a better lubrication mode and/or a more favourable deformation of the contact region.

The lubricant film thickness factor,  $\Lambda$ , is small compared to the surface roughness value ( $R_a$ ). However by comparing the minimum elastohydrodynamic lubrication film thickness and the surface roughness values ( $R_a$ ), the lubrication region is in a fairly good condition for gear contacts. For gears after running-in, the lubrication mode is mostly in the transition regime between boundary and mixed lubrication, and it can reach to a state of mixed lubrication.

The subtask of modeling the gear contact with a commercial gear contact simulation software was initiated and the simulated contact state of the gears was studied and reported. The finite element model shows a more evenly distributed load on the gear and pinion tooth rather than what is observed in the real world. Since the finite element model is a perfectly aligned assembly with extremely smooth surfaces, it should be said that these gears are designed in a way that with a better assembly or manufacturing process they can result in a more favourable contact pattern which may increase the gear life.

It was also been shown that the gears have tip and edge contact that cause wear and pitting in the dedendum of the gear and pinion teeth which indicates a need for redesigning the gears.

Even though for spiral bevel gears, the contact pattern changes for different torques, but as shown in this study, the largest change in surface roughness takes place in the very first running-in step. To get a better knowledge of the shifts due to speed levels at different torques, more investigations are needed.





## 6 RECOMMENDATIONS AND FUTURE WORK

---

### 6.1 Future work

Since there was not time enough to test the specimens for a high PoL factor (longer running-in with more cycles), the test schedule can be continued with a high PoL factor.

A more precise model of the studied gears can be made with ANSOL HypoidK. This model should have a better representation of the gears and cover the rim, the shaft, bearings, and the housing. In this way a thorough assembly analysis can be done to find more robust assembly tolerance limits.

A better calculation model of grease can help to choose a more appropriate lubricant. Even testing different lubricants can help to reach a better lubrication mode.

Since the best contacting profile is the worn profile, measuring the worn profile of the tooth after the most optimal running-in procedure can help to study the deformation of the gear flank due to the detailed contact mechanisms and pressure distributions. This can help to study the effect of running-in and to answer the question of “Is the reduction of roughness improving gear life or is it the deformation caused by the contact pressure that is improving life?”.

Testing the gear sets at lower torques and at higher angular speeds which change the contact pattern, can give insights on how to tune the torque and speed levels.

It has been decided to study the worn profile of the best test setup gears, by measuring the tooth profiles before and after running-in, and also after the life test to measure the deformations of the tooth profile, which will lead to interesting results. This could not be done due to time limitations.

### 6.2 Recommendations

The followings are the recommendations for AC Tools:

- To be able to reduce the errors in the measured efficiency and torque level, the test rig needs to be equipped with better or more precise torque transducers.
- To solve the tip and edge contact problem with high contact pressures, a redesign of the gears is needed. This is also supported by the static simulations.
- Performing tolerance stack up analysis of the assembly is needed.
- By the definition of life at AC Tools, the gear surface fails when the average of the transmission error during some cycles, reaches the maximum allowable transmission error of the gear during its life. This definition can be changed to the first sharp change in the rolling average of the transmission error (over a specific number of cycles). In this way, the test can be stopped when the failure is initiated, and the actual failure mode and be studied more carefully.



## 7 REFERENCES

---

### **BOOKS, ARTICLES, LECTURES AND PRINTOUTS:**

- Beek A., “*Advance engineering design*”, 2009( [www.engineerinf-abc.com](http://www.engineerinf-abc.com))
- Dizdar S., “*Boundary lubrication : a literary survey*”, 1995
- Dizdar S. and Andersson S., “*Formation and failure of boundary layers in mixed and boundary lubricated sliding contacts*”, 1997
- Hamrock B.J., ” *Fundamental of fluid film lubrication*”, Marcel Dekker, second edition, 2004
- Hardy W. and Doubleday I., “*Boundary lubrication – The paraffin Series*”, Proceedings of the Royal Society of London. Series A, Vol. 100, No. 707, 1922
- Klingelberg, “*Spiral bevel and Hypoid gear cutting system*”, Klingelberg AG, Training center, 2008
- Litvin F. L. and Fuentes A., “*Design, manufacture, stress analysis, and experimental tests of low-noise high endurance spiral bevel gears*”, Mechanism and Machine Theory 41, 2006
- Litvin F.L. and Wang A.G., ” *Computerized generation and simulation of meshing and contact of spiral bevel gears with improved geometry*”, University of Chicago 1997
- Martines R., “*Industrial lubrication and tribology*”, Volume 63, November1, 2011
- Pirro D.M., “*Lubrication Fundamentals*”, Marcel-Dekker,2001
- Savage M. and Altidis P.C., “*Tooth contact shift in loaded spiral bevel gears*”, Fifth International Power Transmission and Gearing Conference sponsored by the American Society of Mechanical Engineers Chicago, Illinois, April 25-27, 1989
- Sjöberg S., “*On the running-in of gears*”, Licentiate thesis, Department of Machine Design-Royal Institute of Technology, 2010
- Stachowiak G. W.,”*Engineering Tribology*”, Butterworth-Heinemann, second edition, 2001
- Stolariski T. A., “*Rolling contacts*”, Professional Engineering Publishing, 2000
- Townsend D. P., “ *Dudley’s gear handbook*”, McGraw-Hill, second edition, 1992

## **ONLINE SOURCES:**

ANSOL, <http://ansol.us/Products/>, manuals and software from 2011

[www.AtlasCopco.se](http://www.AtlasCopco.se), picture taken in January 2012

<http://www.brenaclemente.com>, picture taken in February 2012

"Elements of metric gear technology", SPD/SI (<http://www.sdp-si.com/D805/D805cat.htm#tech>)  
retrieved in April 2012

MATLAB, <http://www.mathworks.se/products/matlab/>, version R2011b

<http://en.wikipedia.org/wiki/Gear>, accessed in February 2012

## APPENDIX A

---

*In this Appendix the details about the Hamrock-Dawson equation, which has been used for calculations, is presented. These equations are applicable to elliptical contacts and hard EHD lubrication conditions.*

### **Hamrock-Dawson equation**

The Hamrock-Dawson (B.J. Hamrock, 2004) formula for elliptical prediction was used for calculating the minimum film thickness due to the contact pattern form of the spiral bevel gears, Equation A.1.

$$H = 3.63U^{0.68}G^{0.49}W^{-0.073}(1 - e^{-0.68k}) \quad (\text{A.1})$$

where  $U$  is a dimensionless speed factor,  $G$  a dimensionless materials parameter,  $W$  is a dimensionless load factor, and  $k$  is the ellipticity parameter. From this equation it can be said that the minimum EHD film thickness is more dependent on the speed factor than on the load factor.

To calculate  $H$ , dimensionless speed factor,  $U$ , is calculated as:

$$U = \frac{\eta_0 V}{E' R_x} \quad (\text{A.2})$$

where  $V$  is the linear velocity, meaning the resultant of the rolling and the sliding velocity :

$$V = \sqrt{\bar{u}^2 + \bar{v}^2} \quad (\text{A.3})$$

$\bar{u}$  represents the rolling velocity for each point (Equation A.4) and  $\bar{v}$  is the sliding velocity while  $E'$  is the effective elastic module for the gear and pinion with the same material (Equation A.5).

$$\bar{u} = \frac{\omega_b r_b \sin \varphi + \omega_a r_a \sin \varphi}{2} \quad (\text{A.4})$$

$$E' = \frac{E}{1-\nu^2} \quad (\text{A.5})$$

Where  $\varphi$  is the pressure angle,  $\omega_a$  is the angular velocity of the gear,  $r_a$  is the involute radius of the contact point of the gear and  $\omega_b$  and  $r_b$  show the same values for the pinion.  $E$  is the Young's modulus and  $\nu$  is the Poisson ratio.

The dimensionless material parameter,  $G$ , is calculated as:

$$G = E\alpha \quad (\text{A.6})$$

where  $\alpha$  is the pressure viscosity factor of the lubricant.

The dimensionless load factor,  $W$ , is:

$$W = w_z / E' R_x^2 \quad (\text{A.7})$$

where  $w_z$  is standing for the normal load and  $R_x$  is the radius of contact curvature in the  $x$  direction.

The ellipticity parameter,  $k$ , is:

$$k = \alpha_r^{2/\pi} = \left(\frac{R_y}{R_x}\right)^{2/\pi} \quad (\text{A.8})$$

where  $R_y$  is the radius curvature in the  $y$  direction.  $R_y$  is calculated with respect to the nature of the contact, for example in the case of contact between two cylinders,  $R_y$  is considered as infinity. The directions of  $x$  and  $y$  are dependent on the calculated curvature radiuses in these directions and the following relation should always be true:

$$\frac{1}{R_x} > \frac{1}{R_y} \quad (\text{A.9})$$

Thus the minimum film thickness,  $h$ , is achieved as:

$$h = HR_x \quad (\text{A.10})$$

where  $H$  is the dimensionless film thickness and  $R_x$  is the effective radius of the contact in the  $x$  direction.

The dimensionless film parameter,  $\Lambda$ , for an ideally smooth surface run in the EHD regime is as follow:

$$\Lambda = \frac{h}{(R_{q,1}^2 + R_{q,2}^2)^{1/2}} \quad (\text{A.11})$$

Where  $h$  is the minimum film thickness and  $R_{q1}$  and  $R_{q2}$  are the RMS roughness values of the two surfaces in contact.

## APPENDIX B

---

*Appendix B presents the constants that have been used to calculate the basic geometric model of the gears and their contact for the film thickness calculation and the properties of the lubricant.*

### **Constants used in calculations**

<b>Constant</b>	<b>Value</b>
Absolute viscosity (cp)	158.61090
Pressure-viscosity coefficient (mm <sup>2</sup> /N)	0.0134
Youngs modulus (GPa)	270
Poissons ratio	0.3
Number of pinion teeth	11
Number of gear teeth	17
$\Gamma_1$ , Pitch cone angle of pinion (°)	32.9
$\Gamma_2$ , Pitch cone angle of gear (°)	24.9
$\varphi$ , Pressure angle (°)	32
$\beta$ , Mean spiral angle (°)	15
$r_1$ , Mean pitch cone diameter of the pinion (mm)	16.11
$r_2$ , Mean pitch cone diameter of the gear (mm)	24.90
Curvature radius on drive flank of pinion (mm)	32.54
Curvature radius on drive flank of gear (mm)	31.33
$\omega_2$ , Gear rotational speed (rpm)	60
$T_2$ , Output torque of the gear box (Nm)	50

## APPENDIX C

Appendix C presents the surface roughness values for each loading step in the pre-tests.

### C.1 2D measurement results of pretest I

Table C.1. The results of 2D surface measurements *pretest I* on gear flank

Surface roughness parameters ( $\mu\text{m}$ )	Gear before Running-in			Gear after Running-in		
	Line 1	Line 2	Line 3	Line 1	Line 2	Line 3
$R_a$ ( $\sigma_{Ra}$ )	0.78(0.82)	0.73(0.74)	1.21(1.36)	0.45(0.26)	0.38(0.58)	0.52(0.40)
Ra average ( $\sigma_{Ra}$ )	0.91 ( 1.04)			0.45 (0.44)		
$R_q$	1.11	1.04	1.82	0.53	0.69	0.67
$R_p$	4.49	4.94	6.68	0.91	3.69	1.75
$R_v$	-1.31	-1.40	-2.70	-1.05	-1.10	-1.25
$R_z$	5.80	6.34	9.38	1.96	4.79	3.00
$R_p$ average	5.37			2.12		
$R_v$ average	-1.81			-1.13		
$R_z$ average	7.17			3.26		

Table C.2. The results of 2D surface measurements *pretest I* on the pinion flank

Surface roughness parameters ( $\mu\text{m}$ )	Pinion before Running-in			Pinion after Running-in		
	Line 1	Line 2	Line 3	Line 1	Line 2	Line 3
$R_a$ ( $\sigma_{Ra}$ )	0.54(0.52)	0.50(0.44)	0.64(0.53)	1.21(0.98)	0.32(0.35)	0.35(0.31)
Ra average ( $\sigma_{Ra}$ )	0.56(0.50)			0.63(0.75)		
$R_q$	0.75	0.67	0.83	1.56	0.48	0.48
$R_p$	3.86	2.83	3.08	4.04	1.59	1.77
$R_v$	-1.37	-1.58	-1.48	-3.05	-1.42	-1.54
$R_z$	5.22	4.41	4.56	7.09	3.01	3.31
$R_p$ average	3.25			2.47		
$R_v$ average	-1.488			-2.00		
$R_z$ average	4.73			4.47		



## C.2 2D measurement results of pretest II

Table C.3. The results of 2D surface measurements *pretest II* on the gear flank

Surface roughness parameters ( $\mu\text{m}$ )	Gear after running-in			Gear before Running-in		
	Line 1	Line 2	Line 3	Line 1	Line 2	Line 3
$R_a$ ( $\sigma_{Ra}$ )	0.29(0.20)	0.27(0.22)	0.32(0.20)	0.52(0.33)	0.53(0.43)	0.46(0.37)
Ra average ( $\sigma_{Ra}$ )	0.29(0.21)			0.50(0.38)		
$R_q$	0.35	0.35	0.38	0.61	0.68	0.59
$R_p$	0.82	0.68	0.69	1.82	2.77	1.97
$R_v$	-0.78	-1.04	-1.17	-1.20	-1.68	-1.65
$R_z$	1.60	1.72	1.86	3.02	4.45	3.62
$R_p$ average	0.73			2.19		
$R_v$ average	-0.99			-1.51		
$R_z$ average	1.73			3.70		

Table 21. The results of 2D surface measurements *pretest II* on the pinion flank

Surface roughness parameters ( $\mu\text{m}$ )	Pinion after running-in			Pinion before Running-in		
	Line 1	Line 2	Line 3	Line 1	Line 2	Line 3
$R_a$ ( $\sigma_{Ra}$ )	0.26(0.17)	0.29(0.20)	0.31(0.24)	0.45(0.36)	0.48(0.35)	0.55(0.53)
Ra average ( $\sigma_{Ra}$ )	0.29(0.21)			0.50(0.42)		
$R_q$	0.31	0.35	0.39	0.58	0.60	0.76
$R_p$	0.72	1.02	0.68	1.48	1.97	2.13
$R_v$	-1.13	-1.00	-1.48	-1.69	-1.20	-3.27
$R_z$	1.85	2.01	2.16	3.16	3.17	5.40
$R_p$ average	0.81			1.86		
$R_v$ average	-1.20			-2.05		
$R_z$ average	2.01			3.91		

### C.3 3D measurement results of main tests

Table C.5. Results of the 3D surface measurements, all the numbers are in  $\mu\text{m}$

	$S_a$	$S_q$	$S_p$
New gear	0.197	0.255	1.89
Test 1	0.185	0.234	1.32
Test 2	0.19	0.258	3.92
Test 3	0.182	0.232	1.12
Test 4	0.161	0.206	0.877

# APPENDIX D

This appendix covers the row data from the running-in procedure, such as efficiency, deviation of the transmitted torque.

## D.1 Efficiency and torque deviation diagrams; 1<sup>st</sup> repetitions

### D.1.1 Test-set 1

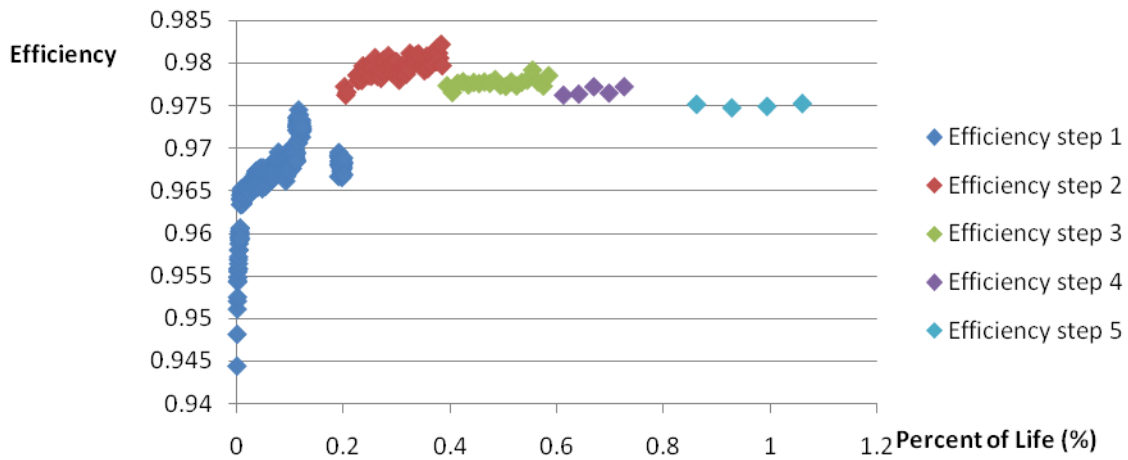
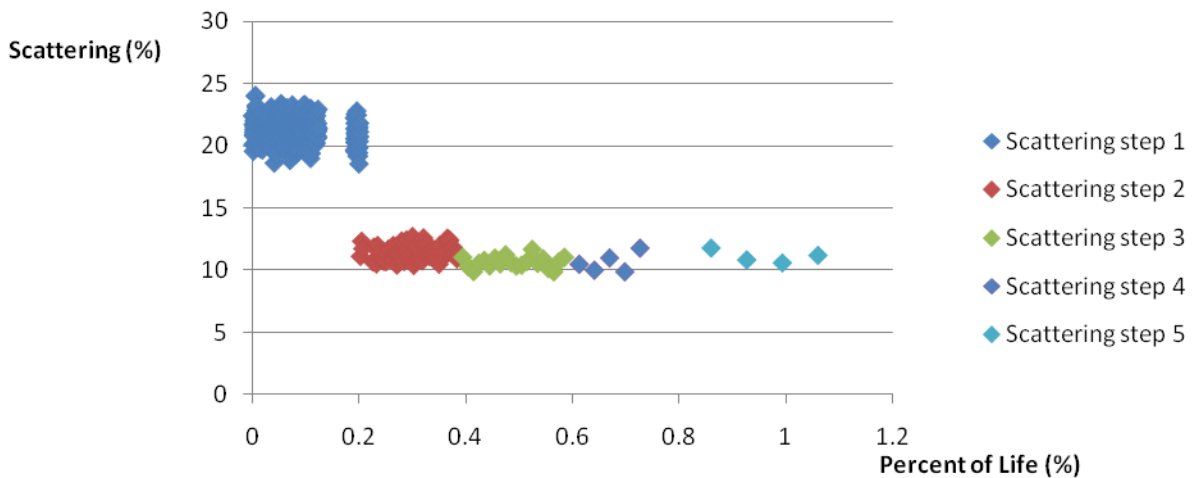


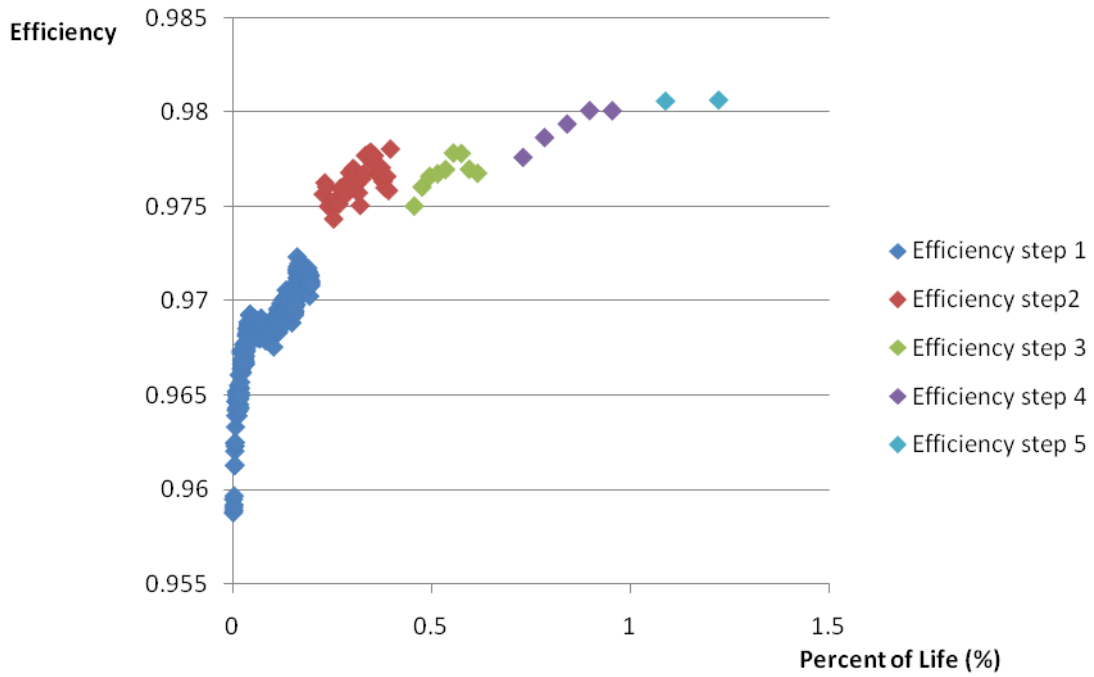
Figure D.1. Efficiency versus Percent of Life, test-set 1, 1<sup>st</sup> repetition



FigureD.2. Scattering of transmission error versus Percent of Life, test-set 1, 1<sup>st</sup> repetition

In Figure . and Figure D.2 a part of data is missing due to software errors and control system overloading.

## D.1.2 Test-set 2



### D. 1.3 Test-set 3

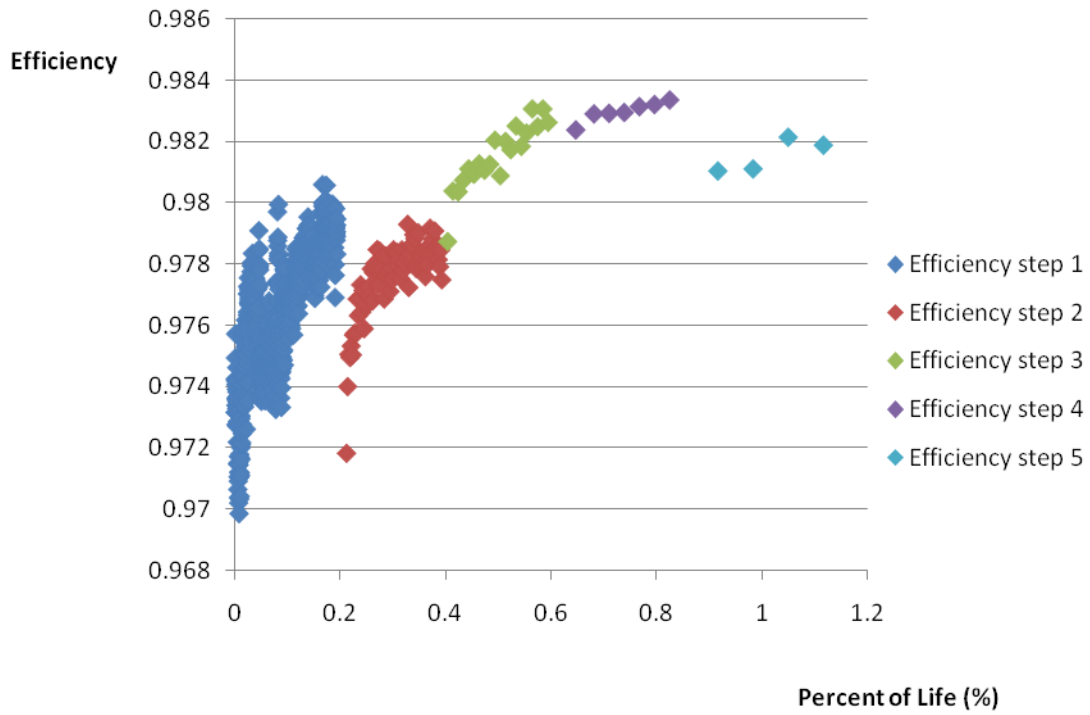


Figure D.5. Efficiency versus Percent of Life, test-set 3, 1<sup>st</sup> repetition

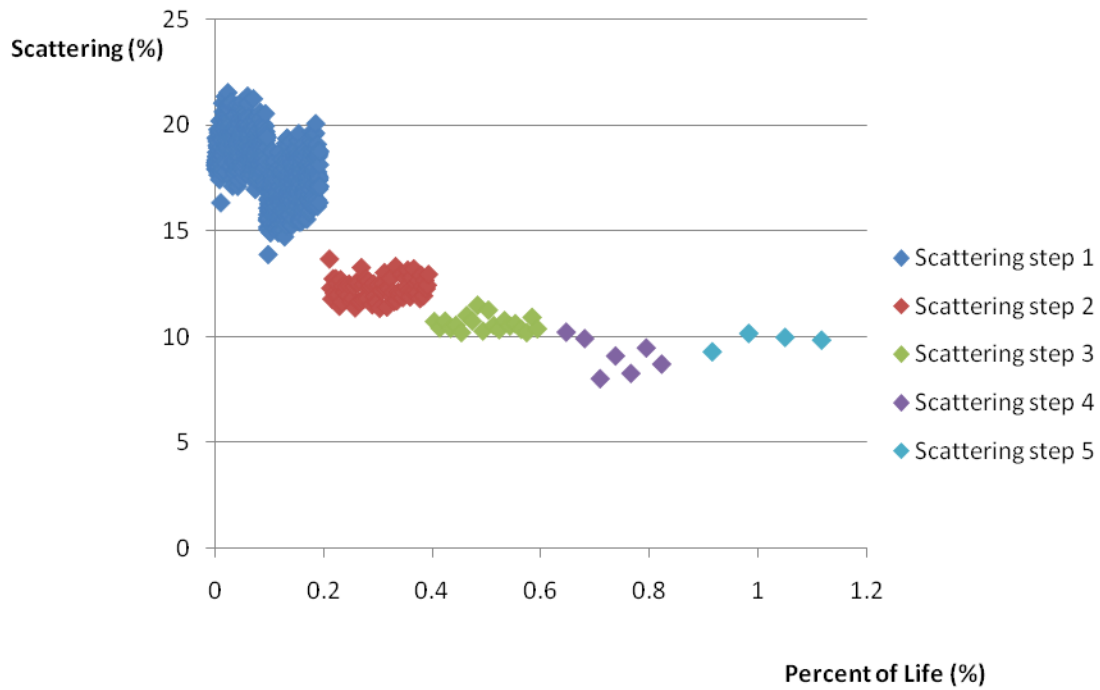


Figure D.6. Scattering of transmission error versus Percent of Life, test-set 3, 1<sup>st</sup> repetition

### D.1.4 Test-set 4

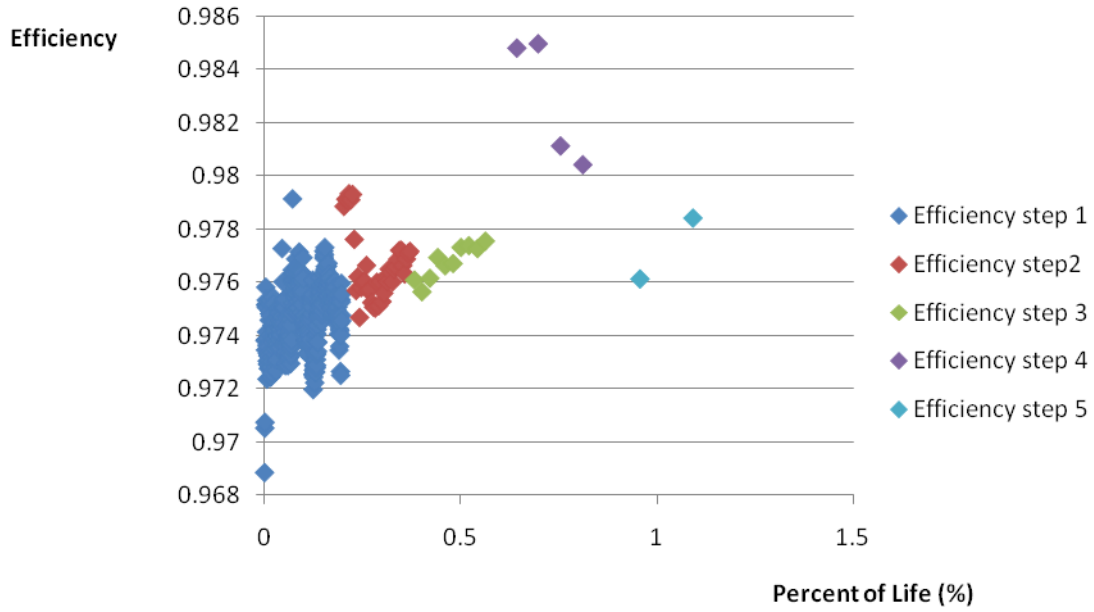


Figure D.7. Efficiency versus Percent of Life, test-set 4, 1<sup>st</sup> repetition

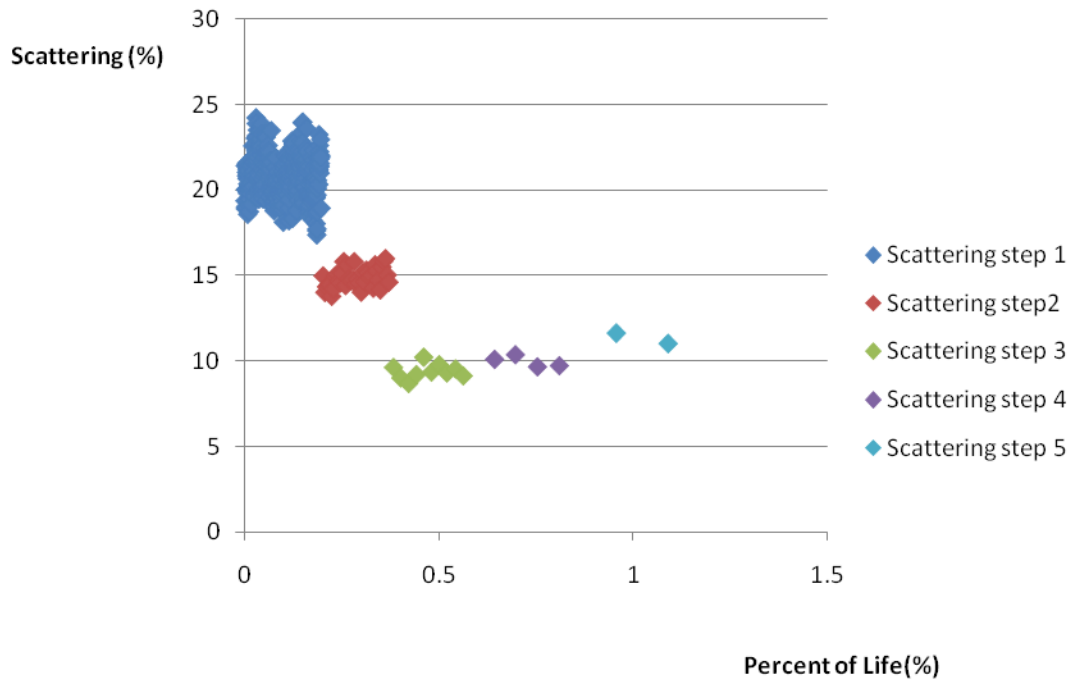


Figure D.8. Scattering of transmission error versus Percent of Life, test-set 4, 1<sup>st</sup> repetition

# D.2 Efficiency and torque deviation diagrams; 2<sup>nd</sup> repetitions

## D.2.1 Test-set 1

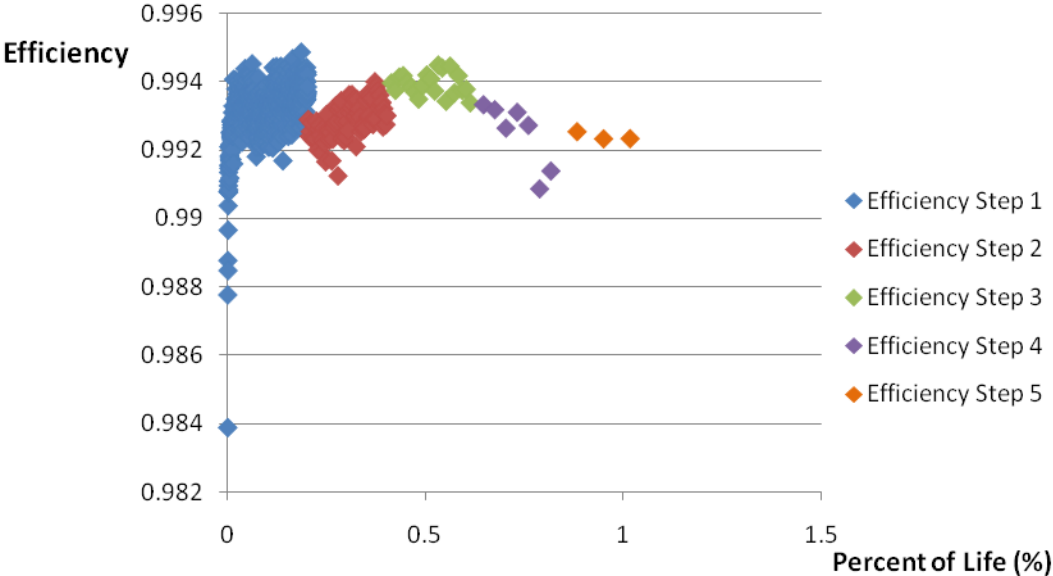


Figure D.9. Efficiency versus Percent of Life, test-set 1, 2<sup>nd</sup> repetition

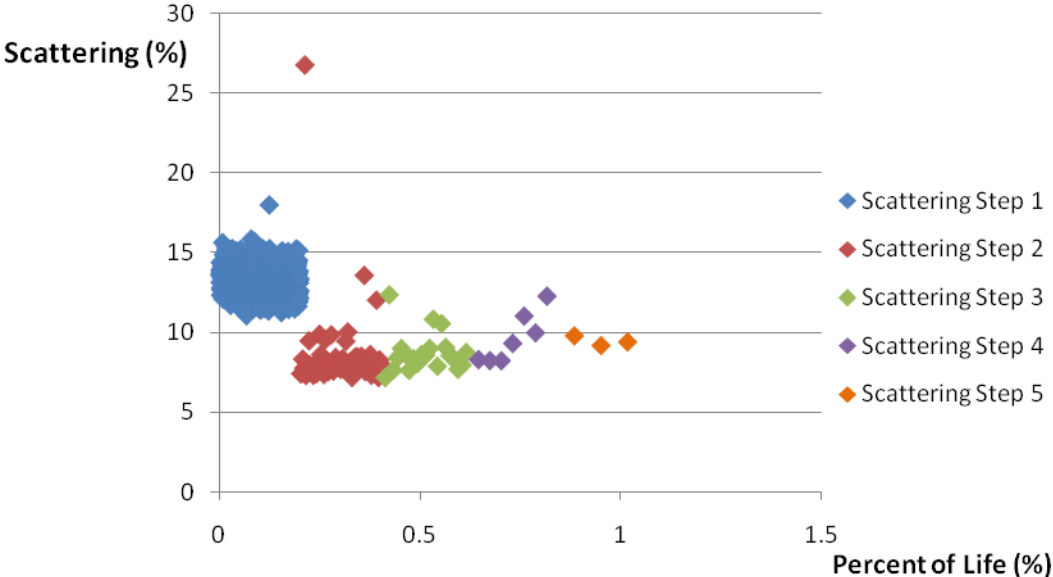


Figure D.10. Scattering of transmission error versus Percent of Life, test-set 1, 2<sup>nd</sup> repetition

## D.2.2 Test-set 2

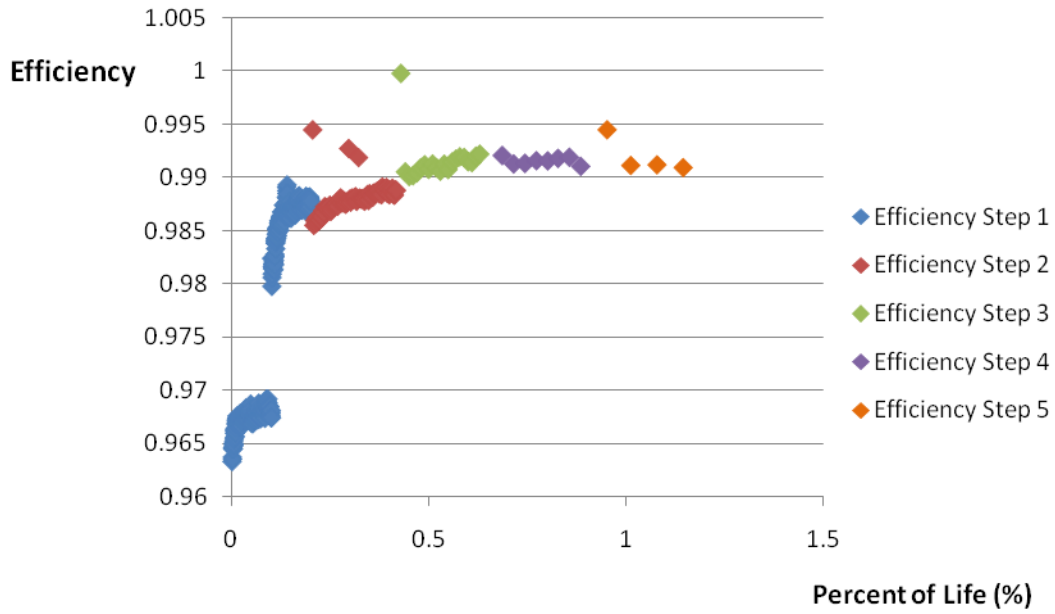


Figure D.11. Efficiency versus Percent of Life, test-set 2, 2<sup>nd</sup> repetition

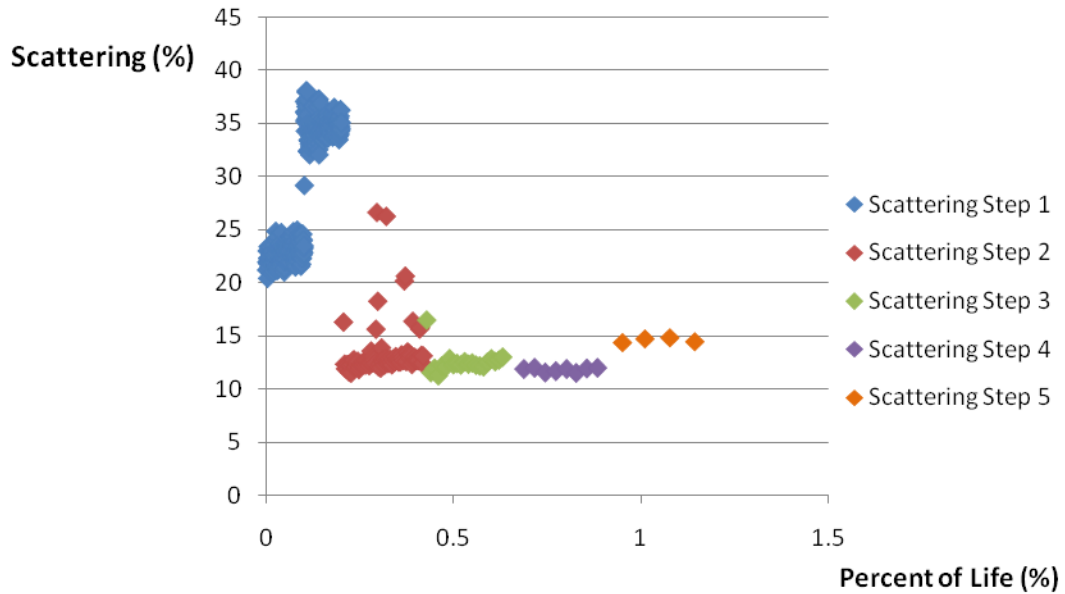


Figure D.12. Scattering of transmission error versus Percent of Life, test-set 2, 2<sup>nd</sup> repetition



### D.2.3 Test-set 3

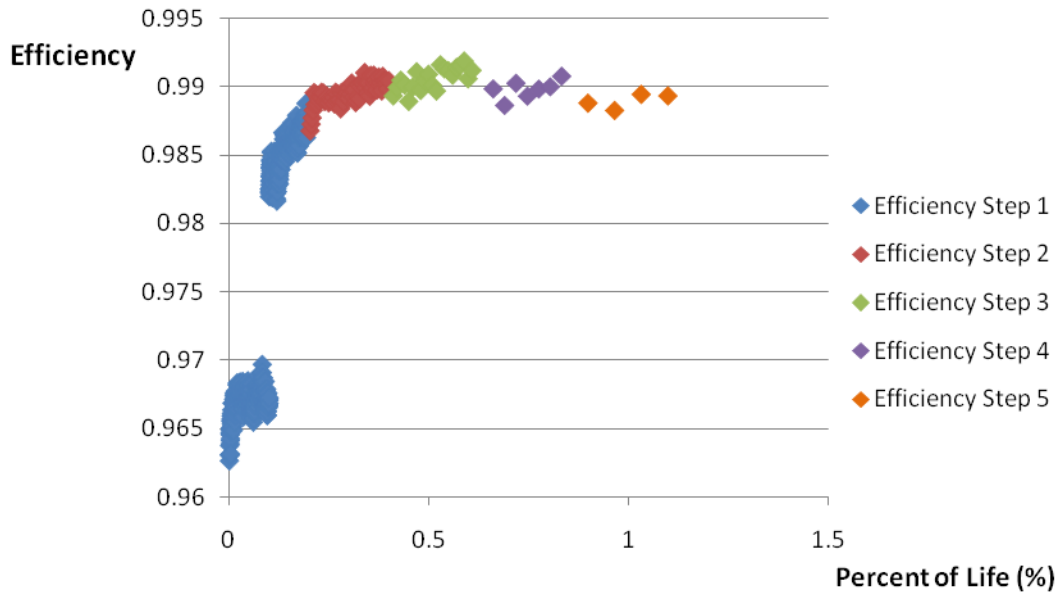


Figure D.13. Efficiency versus Percent of Life, test-set 3, 2<sup>nd</sup> repetition

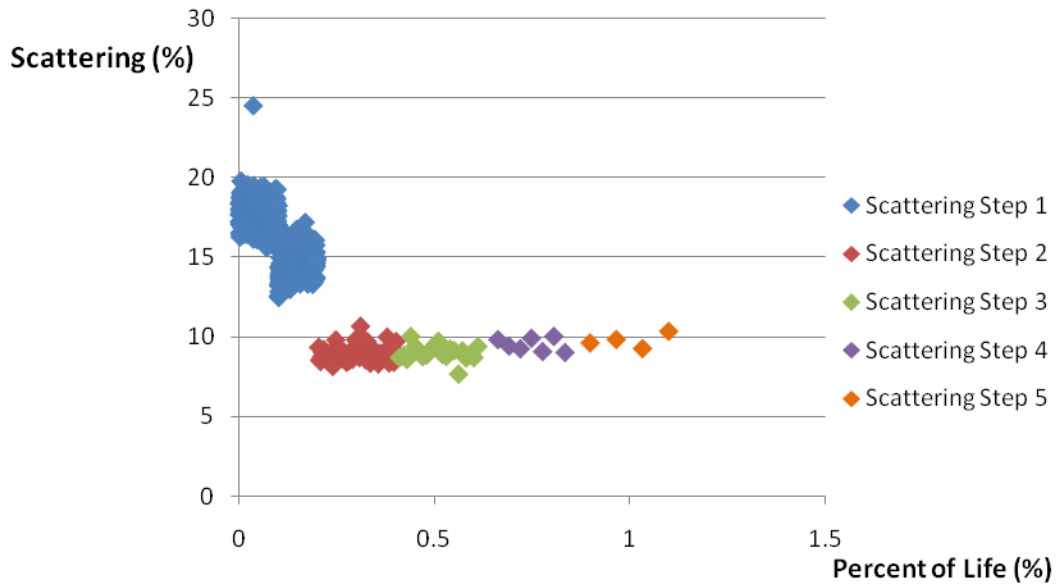


Figure D.14. Scattering of transmission error versus Percent of Life, test-set 3, 2<sup>nd</sup> repetition

## D.2.4 Test-set 4

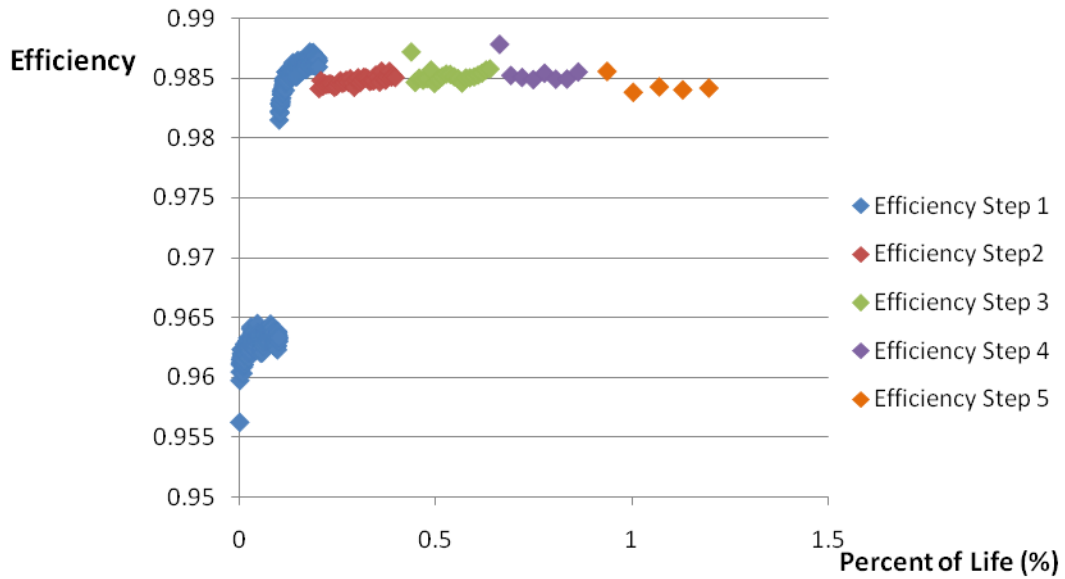


Figure D.15. Efficiency versus Percent of Life, test-set 4, 2<sup>nd</sup> repetition

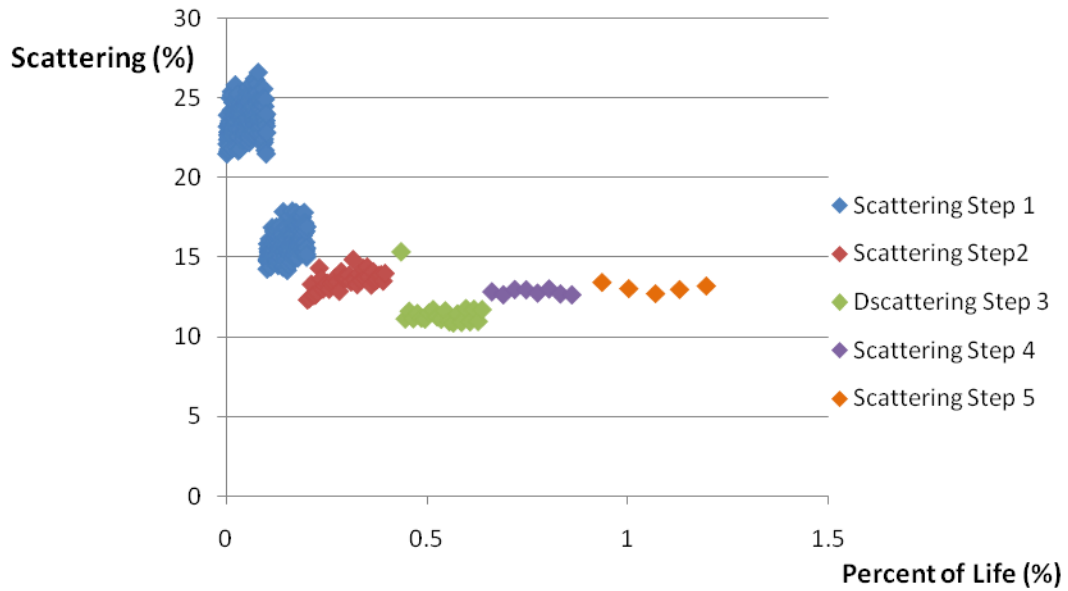


Figure D.16. Scattering of transmission error versus Percent of Life, test-set 4, 2<sup>nd</sup> repetition